The background features a light blue grid with a network diagram overlaid. The diagram consists of a grid of nodes connected by lines, with some nodes highlighted in a darker blue. The overall aesthetic is technical and modern.

Network Coding: Exploiting Broadcast and Superposition in Wireless Networks

Jasper Goseling

Network Coding: Exploiting Broadcast and Superposition in Wireless Networks

Proefschrift

ter verkrijging van de graad van doctor
aan de Technische Universiteit Delft, op gezag van
de Rector Magnificus prof. ir. K.Ch.A.M. Luyben,
voorzitter van het College voor Promoties,
in het openbaar te verdedigen op
donderdag 4 november 2010 om 15:00 uur door

Jasper GOSELING,

elektrotechnisch ingenieur,
geboren te Enschede.

Dit proefschrift is goedgekeurd door de promotor:

Prof. dr. ir. S.M. Heemstra de Groot

Samenstelling promotiecommissie:

Rector Magnificus,

Prof. dr. ir. S.M. Heemstra de Groot,

Dr. ir. J.H. Weber,

Prof. dr. R.J. Boucherie,

Prof. dr. M.C. Gastpar,

Prof. dr. ir. R.L. Lagendijk,

Prof. dr. Ø. Ytrehus,

Dr. ir. F.M.J. Willems,

voorzitter

Technische Universiteit Delft,

promotor

Technische Universiteit Delft,

copromotor

Universiteit Twente

Technische Universiteit Delft

en University of California, Berkeley

Technische Universiteit Delft

University of Bergen

Technische Universiteit Eindhoven

ISBN 978-94-6113-027-3

All rights reserved. No part of the material protected by this copyright notice may be reproduced or utilized in any form or by any means, electronic or mechanical, including photocopying, recording or by any information storage and retrieval system, without the prior permission of the author.

Copyright © 2010 by J. Goseling

Cover design: J. Goseling and W. van den Worm

Printed by Wöhrmann Print Service, Zutphen

Acknowledgements

There are a number of people that have played, in various ways, an important role in the realization of this thesis. First of all I would like to thank Suhas Diggavi and Christina Fragouli for a very pleasant and inspiring time at EPFL. Their guidance has been invaluable in my development as a researcher. I would also like to thank my promotor Sonia Heemstra de Groot for the important role she has played in enabling me to perform the research that has led to this thesis. In this respect, many thanks, as well, to John de Waal and Richard Boucherie.

It has been a true pleasure to have had Jos Weber as my copromotor. Working together with Jos has been a wonderful experience. His keen eye, creativity and perseverance have been a true inspiration. I would like to thank him for his ongoing support throughout the process of writing this thesis.

Part of the research that is represented in this thesis is the result of collaboration with Michael Gastpar. Working with Michael has been a very valuable and wonderful experience.

Finally, I would like to thank all my friends and colleagues at EPFL, TU Delft, TI-WMC and the University of Twente. Thanks to them, writing this thesis has been a pleasure.

Jasper Goseling
Enschede, October 2010.

Contents

1	Introduction	1
1.1	Challenges in Wireless Communications	1
1.2	Abstractions of the Wireless Medium	2
1.3	Beyond Network Flows	3
1.4	Network Coding	5
1.5	Code Design for Multiple Multicast Sessions	10
1.6	Exploiting Broadcast	13
1.7	Exploiting Superposition	15
1.8	Summary of Results and Organization of the Thesis	16
2	Network Coding for Undirected Information Exchange	21
2.1	Introduction	21
2.2	Model	22
2.3	Example	23
2.4	Rate Region	25
2.5	Preserving Coding Points	27
2.6	Preserving Local Coding Vectors	31
2.7	Discussion	32
3	Multi-Rate Network Coding	33
3.1	Introduction	33
3.2	Model	37
3.3	Network Coding at Minimum Cost	39
3.4	Multi-rate Network Coding	40
3.5	Discussion	45

4	The Energy Benefit of Network Coding	47
4.1	Introduction	47
4.2	Model and Problem Statement	50
4.3	Results	52
4.4	An Efficient Code on the Hexagonal Lattice	57
4.5	An Efficient Code on the Rectangular Lattice	65
4.6	Extended Energy Consumption Model	76
4.7	Discussion	87
5	The Transport Capacity of Line and Lattice Networks	89
5.1	Introduction	89
5.2	Computation Coding	92
5.3	Model and Notation	93
5.4	Main Results	97
5.5	Upper Bounds	103
5.6	Achievable Schemes	123
5.7	Extension to Gaussian Models	136
5.8	Discussion	138
5.A	Proof of Lemma 5.28	139
6	Outlook	149
	Bibliography	153
	Summary	163
	Samenvatting	165
	Curriculum Vitae	167

Chapter 1

Introduction

Contents

1.1	Challenges in Wireless Communications	1
1.2	Abstractions of the Wireless Medium	2
1.3	Beyond Network Flows	3
1.4	Network Coding	5
1.5	Code Design for Multiple Multicast Sessions	10
1.6	Exploiting Broadcast	13
1.7	Exploiting Superposition	15
1.8	Summary of Results and Organization of the Thesis	16

1.1 Challenges in Wireless Communications

Emerging applications of wireless networks put an ever increasing demand on the inherently limited resources that are available. These applications range from wireless broadband internet access for home use, putting constraints on the available bandwidth — to deployment of sensor networks for environment monitoring in rural areas, in which case battery lifetime is the critical factor, directly influencing network lifetime. The available bandwidth is limited and hence appropriate measures have to be taken to make more efficient use of bandwidth. The problem concerning energy consumption is that

improvements in battery technology are not keeping up with the increased demand from emerging applications. Therefore, in order to maintain reasonable battery lifetime it is imperative to decrease the energy consumption of wireless devices.

Of course, improving efficiency in wireless networks has been the topic of many studies. Some of the improvements that have been suggested in literature are cross-layer optimization [32, 55], power control [43, 68, 72], improved routing [8, 9, 69] and the use of cognitive radio [37, 71]. However, all these methods are based on a common set of basic operating principles. In this thesis we investigate fundamentally different methods to improve efficiency. In the next two sections 1.2 and 1.3 we will introduce these methods and see how they are different from the operating principles that are used in state-of-the-art technology and the literature mentioned above.

1.2 Abstractions of the Wireless Medium

The overwhelming complexity of designing a communication system asks for a divide-and-conquer approach. A method that has proven to be very successful is to use a layered overall system architecture, with the ubiquitous OSI model as a resulting standard [89]. One of the challenges in a communication system is to deal with noise and errors. The task of the physical layer, the lowest layer in the OSI model, is to provide a means of reliably transmitting information between neighbouring devices. The result is a network of reliable links between devices. In a sense, the physical layer provides an abstraction of the transmission medium.

In state-of-the-art technology, the abstraction provided by the physical layer is that of reliable point-to-point links. This means that messages originating from one device are received by at most one other device. Moreover, each device receives at most one message. The abstraction to reliable point-to-point links, together with the layered system architecture has enabled enormous advances in technology. In particular, it has enabled development and wide deployment of wireless networks, like IEEE 802.11 based networks.

However, for *wireless networks* the abstraction to point-to-point links is not always the most suitable one, since it is ignoring the most important characteristics of the wireless medium, *broadcast* and *superposition*. Broadcast

implies that all devices in a certain neighbourhood of a transmitter are receiving its signal. Superposition implies that the signal received by a device is the sum of the signals transmitted by all devices in its neighbourhood. The traditional means of dealing with superposition, as is being done in most state-of-the-art technology, is to try and decode only one of the signals and treat the interfering signal as noise. There are many results that suggest that there are other ways of dealing with superposition, see, for instance [14]. In particular, it is possible to decode each of the individual messages.

More recently it has been observed [64] that one is not necessarily interested in decoding each of the individual messages. In particular, it might be useful to decode only a sum of these messages. The advantage is that this can be done at a higher rate than decoding individual messages. Note that the abstraction of the transmission medium resulting from these methods of dealing with superposition is no longer a network of point-to-point links.

Results from [14,17,35,50,66,82] suggest that by allowing broadcast and interference to be exploited at the physical layer can greatly improve efficiency. In a part of this thesis we consider the abstraction of the transmission medium resulting from exploiting superposition by decoding sums of messages. By taking also broadcast into account we obtain an abstraction of the wireless medium in which nodes can transmit a common messages over their outgoing links (broadcast) and receive a sum of the messages transmitted over their incoming links (superposition).

1.3 Beyond Network Flows

The physical layer provides reliable communication between neighbouring nodes. Of course, in most networks there are many nodes, most of which can not communicate directly to all other nodes in the network. Hence, data will need to be carried across several links in order to arrive at the intended destination. Higher layers in the OSI model provide a means of routing/relaying information through the network.

A very useful idea is to reduce the routing problem to the problem of establishing a *network flow* in a graph, where the edges in the graph represent reliable links between nodes provided by the physical layer. The reduction of routing to a network flow problem has enabled enormous advances in theory

and corresponding technology. In particular, it has enabled development of large-scale wired networks, like the Internet. Some of the theory that has been developed consists of a characterization of network capacity in terms of a min-cut condition, decentralized algorithms for route discovery, etc. See, for instance, [12] for an introduction to the wealth of theory that has been developed on network flow problems and references to other literature.

Despite the fact that it has enabled great advances, the concept of network flow inherently fails to capture some of the properties of information being transmitted over a network. Note, that in a network flow problem nodes are allowed to generate, forward and store data. However, merging and copying data are not possible. This implies that data from different connections is kept independent. The important thing to note is that in principle nodes can also process data before retransmitting it in the network. Obviously, the physical layer already processes data by using forward error correcting codes to battle noise. It was first observed in [2, 86] that (even in networks of reliable links) it can be beneficial to allow nodes in the network to process data before retransmitting it. The corresponding abstraction is that of *network information flow*. The processing performed by nodes has been termed *network coding*. In a network information flow setting information from different connections is no longer kept independent, but mixed together. Network information flow should be put in contrast to traditional network flow problems in which data is treated as a commodity, like water flowing through pipes, items being transported or cars on a road. However, bits are not cars [20]. In particular, information can be processed, *i.e.*, computations can be performed.

We will see in this thesis that the use of abstractions of the physical layer, exploiting broadcast and superposition, together with network coding offers great opportunities for improving efficiency, both in terms of bandwidth and energy consumption. There are, however, many challenges. Part of these challenges come from the fact that it is not clear how the more complex abstractions of the physical layer can be translated into practical systems. Also, for network flow many practical algorithms have been developed. Counterparts of these algorithms for the information flow setting will have to be developed. Some of these aspects will be covered in this thesis. Most likely, the increased complexity will lead to some overhead in practical systems. Therefore, it is

of importance to know exactly how much the use of a different physical layer abstraction and network coding can gain us. Therefore, we will also develop bounds on the gains that can be obtained.

The remainder of this chapter is organized as follows. In Section 1.4 we will give a more detailed introduction in the field of network coding (network information flow). In Section 1.5 we discuss network coding for multiple multicast sessions. In Section 1.6 we discuss the combination of using network coding and exploiting broadcast. In Section 1.7 we discuss how to exploit interference by allowing sums of messages to be decoded by devices. Finally, in Section 1.8 we provide an overview of the results presented in this thesis and an outline of the other chapters.

1.4 Network Coding

The network information flow problem and the term network coding were introduced in [2]. In the past ten years the topic has received much attention, resulting in many research papers (cf. [1]) and a number of monographs [24, 25, 38, 84] dedicated to network coding. An introduction to the theory of network coding is provided in [25]. A more detailed treatment of some aspects of the theory is provided in [84] and [38]. An overview of potential applications is provided in [24]. After introducing the basic idea of network coding, we provide a review of some of the applications of network coding later in this section.

We illustrate the concept of network coding based on a widely-used model that was introduced in [49]. The network is modelled as an acyclic directed graph in which the edges can carry symbols from a finite field \mathbb{F}_q . If $q = 2$ the symbols are bits and addition and subtraction of symbols corresponds to the exclusive or operation. The (acyclic) network is assumed to be delay-free, *i.e.*, symbols ripple through the network in zero time. While this is a substantially idealized model of a communication network it has allowed the development of many results in network coding theory. The traffic pattern that we consider is multicast, *i.e.*, all symbols transmitted by the (single) source need to be received by all destinations.

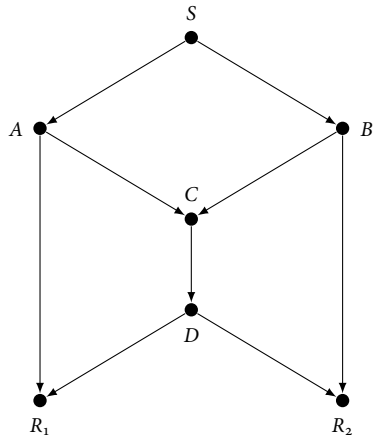


Figure 1.1: Multicast configuration with source S_1 and receivers R_1 and R_2 .

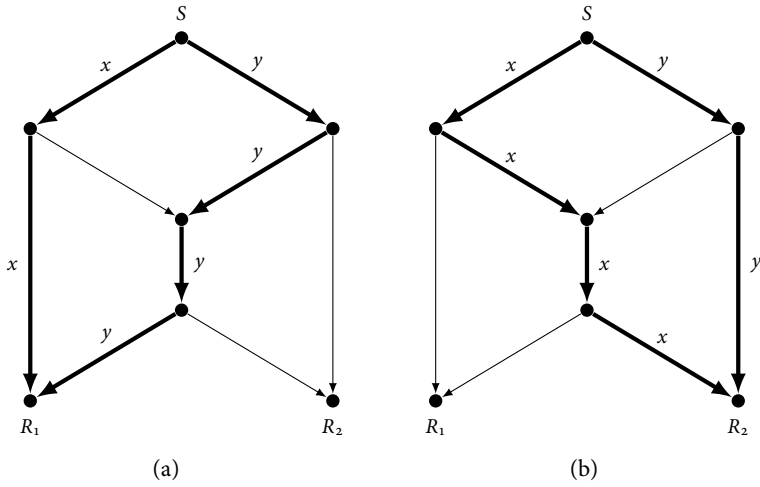


Figure 1.2: Routing at rate 2 to receivers R_1 and R_2 in (a) and (b) respectively.

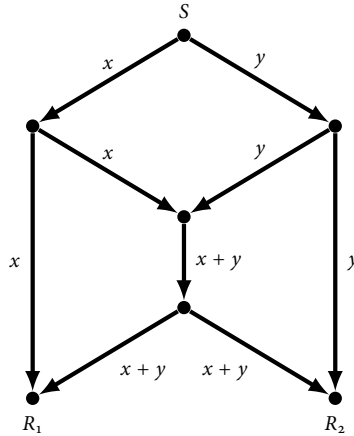


Figure 1.4: Network coding solution on the butterfly.

obtained a network information flow of size 2, as illustrated in Figure 1.4. The result obtained in [2] is that the maximum size of a network information flow for multicast on a directed graph equals the minimum of the min-cut to a destination, where the minimum is over all destinations.

The above example demonstrates that network coding has the potential to increase the throughput in multicast configurations that can be modelled by a directed graph. We will see in Section 1.6 and in the remainder of this thesis that there is also great potential in reducing cost. We will be mostly interested in the energy consumption in wireless networks as a cost metric. In the large body of literature on network coding many other potential benefits of network coding have been identified, an overview of results up to 2007 can be found in [24]. Here, we briefly mention some of the potential applications. In the presence of stochastic arrivals and packet erasures network coding could reduce delay and queue sizes [75]. Also, robustness against link failures can be obtained using less resources [73, 85]. Also, since not the data itself, but only evidence of the information is transmitted, it is possible to obtain security against eavesdroppers [7, 21]. It possible to perform network coding in such a way that, if an eavesdropper obtains only partial information, this information is useless. Network coding ideas have also been applied in peer-to-peer

applications for content distribution. An application has been developed that does not suffer from the low data rates experienced at the start and end of, for instance, Bittorrent sessions [29]. Finally, we mention the use of network coding for distributed storage [15]. Network coding can significantly reduce the overhead required to perform distributed storage in, for instance, sensor networks.

Some of the key results in network coding have been established in [2, 39, 40, 49, 52]. In the above example we chose a linear function of x and y to be transmitted. In [52] it was shown that for multicast problems linear operations are always sufficient. The functions reduce to linear combinations over finite fields. Based on linear coding, the problem of network information flow reduces to finding weighting coefficients for the linear combinations, a problem denoted as *code design*. A polynomial-time algorithm for code design for multicast was presented in [40]. The problem with this algorithm is that it requires knowledge of the complete graph, *i.e.*, it is a centralized algorithm. More recently it has been demonstrated that it is also possible to choose the coding coefficients randomly [39]. Of course, this might lead to occasional errors when not all receivers can decode, but by making by the field size sufficiently large, the error probability can be made arbitrarily small.

Unfortunately, for the case of multiple sessions very little is known. In directed graphs one can construct examples that demonstrate that network coding can significantly improve throughput [54]. For undirected networks, however, a long-standing conjecture is that network coding can not improve the throughput [54] for multiple unicast sessions. The problem is hard, since it has been shown in [16] that in the case of multiple sessions it is no longer sufficient to consider linear coding operations. Despite the lack of a general theory of network coding for multiple sessions, there exists important practical work demonstrating the power of network coding for multiple sessions. A complete integration of network coding ideas in a state-of-the-art wireless networking protocol stack, including measurements from a testbed, was presented in [46]. The system of [46] shows better performance in terms of throughput than traditional systems that do not utilize network coding.

At various points in this thesis we will compare our solutions to the type of codes that were introduced in [46]. Therefore, we introduce these codes in a bit more detail. The codes introduced in [46] operate according to a prin-

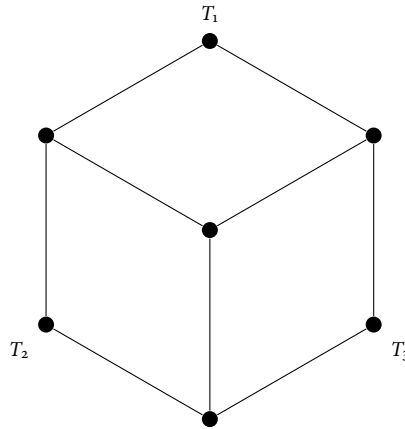


Figure 1.5: Information exchange between terminals T_1 , T_2 and T_3 on the undirected butterfly network.

ciple that we will refer to in the remainder as *decode-and-recombine*. These codes satisfy the constraint that each symbol in each linear combination that is transmitted is explicitly known by the node transmitting that linear combination. Note, that this is a restriction from the general linear coding strategy, in which linear combinations of coded messages can be retransmitted. The motivation behind using decode-and-recombine codes is that it prevents information from spreading too much in the network, away from the path between source and destination, a heuristic introduced by Katti et al. [46]. Hence, the use of a decode-and-recombine strategy results in reduced complexity.

1.5 Code Design for Multiple Multicast Sessions

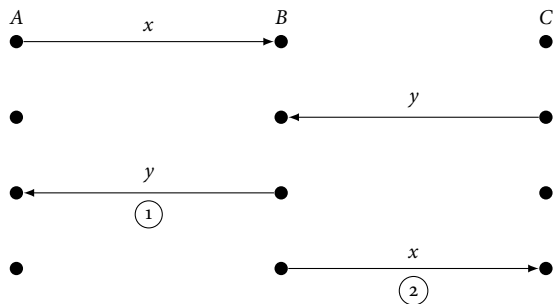
We have seen in the previous section that, in general, very little is known for network coding for multiple sessions. In this thesis we consider two special cases of multiple multicast problems. In both cases the set of receivers for all multicast sessions is the same. What sets our problem apart from other problems studied in the literature, is that only one of these sessions is active

at each point in time. The problem that we address is that of code design. In particular we will show that it is possible to design a single code that can be used for all sessions.

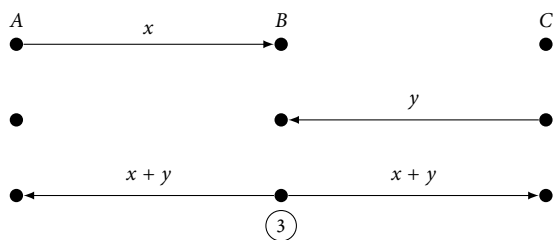
More precisely, the two scenarios that we consider are the following. The first one is that of information exchange on an undirected graph, studied in Chapter 2. There is a set of terminals positioned on an undirected graph. Each of the terminals is acting as a source and every terminal needs to receive all information transmitted by the other terminals. A potential application is video conferencing. A key ingredient of the problem is that over time the data rates at the sources can vary, *i.e.*, one participant is speaking and generating data at a relatively high rate, while the data rates of the other participants are fairly small. When a different participant begins to speak the data rates change. We model this scenario as a set of multicast sessions, one multicast session corresponding to a specific set of rates. An example of an information exchange configuration is given in Figure 1.5, where three terminals T_1 , T_2 and T_3 need to exchange information on the undirected butterfly network. This example will be discussed in more detail in Chapter 2.

The second scenario, to be covered in Chapter 3, is that of variable rate multicasting at minimum-cost. Consider a directed graph with a capacity and a cost associated with each edge. In this case we assume that there is a single source and a fixed set of receivers. In Chapter 3 we will give examples that demonstrate that there is a tradeoff between the throughput and the cost per delivered symbol. For each of the possible values of the throughput we consider the minimum-cost multicast solution, leading to a set of multicast sessions operating on different subgraphs.

The common element in both scenarios is that for each of the multicast sessions a network code is required. Of course, one can design a network code for each of the sessions individually. However, this will require a significant amount of resources, both at design time and in terms of storage and control at the intermediate nodes. In Chapters 2 and 3 we will see that we can design a single code for all multicast sessions.



(a) Solution without network coding: Transmissions 1 and 2 are only useful to nodes C and A, respectively.



(b) Network coding solution: Transmission 3 is useful to both nodes A and C.

Figure 1.6: Demonstrating the potential of network coding by exploiting broadcast: Exchanging bits x and y between nodes A and C.

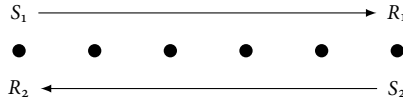


Figure 1.7: Information exchange on the line network.

1.6 Exploiting Broadcast

It was first observed in [81] that network coding provides a useful way of exploiting broadcast in wireless networks. To illustrate the basic principle, a simple example is discussed. In this example, depicted in Figure 1.6, nodes A and C need to exchange bits x and y . Figure 1.6a shows a flow using 4 transmissions, which is the minimum possible number if network coding is not allowed. One can observe that in this case transmissions 1 and 2 (originating at node B and received by nodes A and C) are useful only to nodes C and A , respectively. The network coding solution from Figure 1.6b uses only 3 transmissions to achieve the same end result. Network coding allows transmission 3 to be useful for both A and C , i.e. network coding increases the spatial efficiency. There are several ways in which the increased efficiency can be exploited. Obviously, since fewer transmissions are required, it allows to reduce the energy required to deliver bits x and y . But also, network coding requires less bandwidth to achieve the same throughput. Due to the lower spatial efficiency, solutions without network coding require more transmissions to be scheduled simultaneously in order to meet throughput constraints. This can only be achieved by utilizing more spectrum compared to network coding solutions. This thesis deals with the energy savings that can be obtained by exploiting broadcast and using network coding.

As another example consider information exchange on the line network, depicted in Figure 1.7. This is the configuration used in [81] and many of the resulting follow-up papers. The configuration consists of two source and destination pairs, S_1 to R_1 and S_2 to R_2 , located at the borders of the network. By extending the coding operation from the above example, as illustrated in Figure 1.6, it is possible to save one transmission at each interior node in the network. Hence, asymptotically, for a large number of nodes, the number of

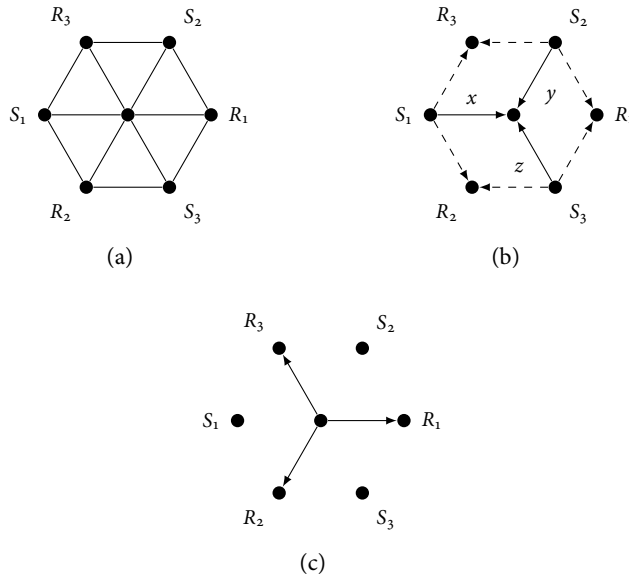


Figure 1.8: Network coding solution to three session multiple unicast configuration. Configuration and connectivity in (a). Transmissions from sources in (b). Note that each transmission is received by three nodes. The center nodes transmits $x + y + z$, see (c).

transmissions that is required can be reduced to 50%. Details of the coding scheme, which was first presented in [81], are provided in Chapter 5.

Yet another example is given in Figure 1.8. In this case there are three unicast sessions. The cheapest routing solution, *i.e.*, if network coding is not used, consists of having the center node retransmit three times. A network coding solution will have the center node retransmit the sum of three symbols, allowing all destinations to decode. Corresponding to the above case, extending this small example to a larger network, would demonstrate that network coding allows a reduction to 33% of the number of transmissions. This extension, and more generally finding lower bounds on the number of transmissions that can be saved, is the topic of Chapter 4 of this thesis.

1.7 Exploiting Superposition

In the previous section we saw that it might be beneficial to exploit broadcast in combination with network coding. The basic insight is that intermediate nodes in a network need not always forward all the information they receive. Rather, it can be sufficient for them to forward merely a function of that information. A natural follow-up observation is that if intermediate nodes are merely forwarding a function of their received information, then they actually do not have to receive all that information in the first place. Rather, as long as they manage to receive the particular function they need to forward, the overall networking solution will work properly. This is where *superposition* enters the picture. As was shown in [64, 65], whenever signals interfere, it can be more efficient for the decoder to obtain only a function of the transmitted messages, rather than all the messages individually. This is particularly interesting for the wireless medium where interference is linear and results in superposition.

If multiple nodes transmit simultaneously, then a receiving node that is within range of all of those transmitters receives a linear superposition of the transmitted signals. A classical way of treating this is to consider any superposition as an erasure/collision and to use clever scheduling to avoid this effect from occurring. However, more sophisticated approaches to physical-layer coding can deal with such linear superposition in other ways. For one, a receiver can first decode one signal, treating all others as noise. Then, assuming the decoding was correct, that signal can be subtracted from the received signal. This is referred to as successive cancellation decoding. In this thesis, we will not consider this option. Instead, we will consider a new way of exploiting the same superposition effect: Namely, to decode a *function* of the transmitted messages. In particular, the function that is decoded is a linear combination of the messages. It was shown in [64] that there exists channel codes that allow to decode sums of messages at high rate. In the remainder, we will refer to these types of codes as *computation codes*. An overview of some of the results on computation codes and related literature will be provided in Chapter 5.

As an example of the benefit of exploiting superposition through the use of computation coding, reconsider Figure 1.6. The important thing to observe is that if A and C are simultaneously transmitting, B is receiving a superposi-

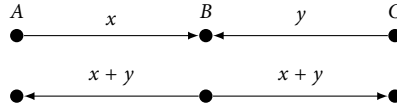


Figure 1.9: Exploiting superposition: Node B does not decode x and y individually, but decodes only $x + y$.

tion of the two signals (and noise). A computation code allows B to recover $x + y$. Hence, only two time slots are required, as illustrated in Figure 1.9.

In Chapter 5 we will investigate the impact of the use of computation codes on the *transport capacity* of wireless networks. This means that we study achievable rates for multiple unicast connections, *i.e.*, messages of every source node are of interest only to one destination node. For each source-destination pair, we evaluate the product of the rate achieved and the distance between source and destination. The transport capacity of the network, as introduced in [35], is then the sum of all of these products, maximized over all possible placements of unicast connections.

1.8 Summary of Results and Organization of the Thesis

Chapter 2 concentrates on the problem of information exchange on an undirected graph as introduced in Section 1.5. An important aspect of the problem is that rates vary over time. It is proven in Chapter 2 that the sum of the individual rates uniquely determines the feasibility of the problem. This result was previously presented in [53]. The proof given in Chapter 2 is new and based on subtree decomposition techniques [27]. For a large class of graphs we present upper and lower bounds on the achievable sum rate. These bounds are separated by a factor that is smaller than 2, which is an improvement of the general factor 2 that is known for arbitrary undirected graphs. The main contribution of the chapter is on the code design problem for different rates. It is shown that if a code for one rate tuple is given, codes for other rate tuples can be easily derived. In particular it will be shown

that this can be done in such a way that we can preserve 1) the coding points, and 2) the local coding coefficients used at these coding points. Preserving local coding vectors keeps complexity and storage overhead at the coding points low. Finally, it is shown that nodes in the network can determine the operating point based on the orientation of adjacent edges. This allows for decentralized operation of the network.

Chapter 3 deals with the case of variable rate multicast at minimum cost as introduced in Section 1.5. Due to the tradeoff between rate and cost per transmitted symbol, depending on quality of service requirements and available resources (e.g., battery levels) one will operate the network at varying rates. Designing new network codes for each of these rates will cause significant overhead. Therefore, a method is presented in Chapter 3 that allows for a single network code to be used at different rates. This code has a single set of local and global coding vectors for all rates.

Chapter 4 concerns the energy reduction that network coding can offer by exploiting broadcast in wireless networks. Lower bounds are provided on the maximum reduction by considering network coding solutions on networks for which the nodes are located at points of a lattice. The reduction is expressed in terms of the *energy benefit of network coding* which is the ratio of the minimum energy required by routing and network coding solutions, maximized over all configurations. Initially the energy benefit is analyzed by considering only the energy that is transmitted, ignoring overhead at transmitter and receiver. Moreover, the transmission range is assumed to be fixed. For this scenario it is shown that on a rectangular lattice the energy benefit is at least $2d/\lfloor\sqrt{d}\rfloor$, where d is the dimension of the network. Next, the case that the transmission range can be chosen freely is considered. It is shown, using a configuration on a hexagonal lattice, that the energy benefit is at least 3 in a two-dimensional lattice. Finally, the impact of ignoring energy consumption overhead at transmitter and receiver is considered. It is shown that taking this overhead into consideration can seriously influence the results obtained on the energy benefit of network coding. Also, it is demonstrated that if there is overhead it might be beneficial to

increase transmission power above the minimum required to achieve connectivity. This will reduce overall energy consumption by creating coding opportunities. This is an interesting observation, since much previous work has focussed on finding minimum transmit power configurations. Moreover, results on large random networks suggest that in terms of scaling, transmit power should be minimized.

Chapter 5 compares capacity bounds for four different deterministic models of wireless networks, representing four different ways of handling broadcast and superposition in the physical layer. In particular, the transport capacity under a multiple unicast traffic pattern is studied for a one-dimensional network of regularly spaced nodes on a line and for a two-dimensional network of nodes placed on a hexagonal lattice. The considered deterministic models are: (i) P/P, a model with exclusive transmission and reception, (ii) P/M, a model with simultaneous reception of the sum of the signals transmitted by all nearby nodes, (iii) B/P, a model with simultaneous transmission to all nearby nodes but exclusive reception, and (iv) B/M, a model with both simultaneous transmission and simultaneous reception. All four deterministic models are considered under half-duplex constraints. For the one-dimensional scenario, it is found that the transport capacity under B/M is twice that under P/P. For the two-dimensional scenario, it is found that the transport capacity under B/M is at least 2.5 times, and no more than six times, the transport capacity under P/P. The transport capacities under P/M and B/P fall between these bounds.

Finally, Chapter 6 provides a review of the results presented in this thesis and an outlook for further investigations.

The results that are presented in this thesis have been published in the following journal papers

- A—1 Jasper Goseling, Christina Fragouli and Suhas N. Diggavi, “Network Coding for Undirected Information Exchange”, *IEEE Communication Letters*, vol. 13, no. 1, pp. 25–27, 2009,
- A—2 Jasper Goseling, Ryutaroh Matsumoto, Tomohiko Uyematsu, and Jos H. Weber, “Lower Bounds on the Maximum Energy Benefit of Network

	Chapter 2	Chapter 3	Chapter 4	Chapter 5
A—1	•			
A—2			•	
A—3				•
B—1			•	
B—2		•		
B—3				•
B—4			•	
B—5			•	

Table 1.1: Relation between papers and chapters.

Coding for Wireless Multiple Unicast”, *EURASIP Journal on Wireless Communications and Networking*, vol. 2010, Article ID 605421, 13 pages, 2010, (Special Issue on Wireless Network Coding)

A—3 Jasper Goseling, Michael Gastpar and Jos H. Weber, “Line and Lattice Networks under Various Deterministic Interference Models”, *submitted to IEEE Transactions on Information Theory, Special Issue on Interference Networks*, April 2010,

and the following conference papers

B—1 Jasper Goseling and Jos H. Weber, “Energy Benefit of Network Coding for Multiple Unicast in Wireless Networks”, in *Proceedings of the 29th Symposium on Information Theory in the Benelux*, Leuven, Belgium, 2008, (Stichting Gauss, best young researcher paper award.)

B—2 Jasper Goseling and Jos H. Weber, “Multi-rate Network Coding for Minimum-Cost Multicasting”, in *Proceedings of the 2008 IEEE International Symposium on Information Theory*, pp. 36–40, Toronto, Canada, 2008,

B—3 Jasper Goseling, Michael Gastpar and Jos H. Weber, “Transport Capacity of Wireless Networks: Benefits from Multi-access Computation Coding”, in *Proceedings of the 30th Symposium on Information Theory in the Benelux*, Eindhoven, The Netherlands, 2009,

- B—4** Jasper Goseling, Ryutaroh Matsumoto, Tomohiko Uyematsu, and Jos H. Weber, “On the Energy Benefit of Network Coding for Wireless Multiple Unicast”, in *Proceedings of the 2009 IEEE International Symposium on Information Theory*, pp. 2567–2571, Seoul, Korea, 2009,
- B—5** Jasper Goseling and Jos H. Weber, “On the Energy Savings of Network Coding in Wireless Networks”, in *Proceedings of the 31st Symposium on Information Theory in the Benelux*, Rotterdam, The Netherlands, 2010.

The relation between the various chapters of this thesis and the above papers is depicted in Table 1.1.

Chapter 2

Network Coding for Undirected Information Exchange

Contents

2.1	Introduction	21
2.2	Model	22
2.3	Example	23
2.4	Rate Region	25
2.5	Preserving Coding Points	27
2.6	Preserving Local Coding Vectors	31
2.7	Discussion	32

2.1 Introduction

Consider a group of users in a network represented as an undirected graph that want to exchange information, *i.e.*, each user has information that needs to be received by all other users. This model arises in multimedia file exchange applications such as video-conferencing and internet games.

In this chapter we consider the use of network coding for such information exchange conferences. Network coding admits a larger rate region than

routing, at polynomial complexity [53]. We start by reviewing the characterization of the achievable rate region provided in [53]. We give an alternative proof for this result based on information flow decomposition techniques [27] and graph-theoretic properties. Our proof provides additional insight in the problem structure.

A major challenge that deployment of network coding for such applications faces, stems from the fact that during the conference duration, the rates at which users transmit will naturally vary. Employing a network coding solution that uses different sets of local coding vectors depending on the rates of the users, would result in unacceptable complexity. For example, it would require the intermediate nodes in the network to update their decoding operations accordingly.

Our main contribution is to prove that a common set of local coding vectors can be used to support all achievable rate tuples, thus allowing a smooth operation at different rates.

2.2 Model

We are given a network represented as an undirected graph $G = (V, E)$, and a set of terminals $\mathcal{T} \subseteq V$ of size $N \triangleq |\mathcal{T}|$. These terminals act as sources and receivers in an information exchange conference. Each terminal needs to receive all information transmitted by the other terminals. We will call $\{G, \mathcal{T}\}$ an information exchange configuration.

Assume time is slotted, and let rate R_i be the number of symbols that are generated per time-slot by the source located at terminal $T_i \in \mathcal{T}$, $i = 1, \dots, N$. We consider only integral rates.

Definition 2.1 (Achievable Rate Region). *The achievable rate region for an exchange configuration $\{G, \mathcal{T}\}$ consists of all tuples (R_1, R_2, \dots, R_N) for which there exists a valid linear network code that supports these rates.*

A code consists of an orientation of the graph and sets of global and local coding vectors. Furthermore, we assume that each edge in the graph has unit capacity, *i.e.*, it can carry one symbol per time-slot.

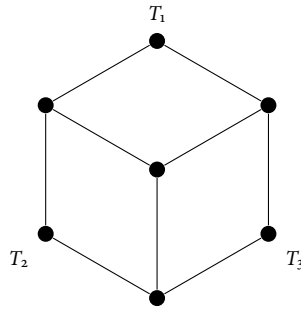


Figure 2.1: Three terminal information exchange configuration.

Definition 2.2 (Uniform Pairwise Min-cut). *A set of terminals $\mathcal{T} \subseteq V$ has uniform pairwise min-cut $h \in \mathbb{N}^+$ over a graph G if $\text{min-cut}(T_1, T_2) = h$, $\forall T_1, T_2 \in \mathcal{T}$.*

We are interested in minimal configurations, in the sense that removing any network edge would reduce the min-cut to smaller than h for at least one pair of terminals. Minimal configurations are desirable as they allow the conservation of network resources. Such configurations can be identified in polynomial time by first selecting edge disjoint paths between pairs of terminals, and then removing redundant edges [27].

2.3 Example

As an example consider a three terminal information exchange configuration on the undirected butterfly network, as depicted in Figure 2.1. First observe that this network has a uniform pairwise min-cut of 2. To demonstrate the benefit of network coding, consider the case that both T_1 and T_2 are transmitting at unit rate. It is clear that there is no routing solution that allows all nodes to receive all information. However, there do exist network coding solutions; one possibility is shown in Figure 2.2 on the next page, in which terminal T_1 transmits the symbol y and terminal T_2 transmits the symbol x . The case that terminal T_1 is transmitting at rate 2 and the other terminals are only receiving corresponds to the ‘traditional’ directed butterfly, which was discussed in

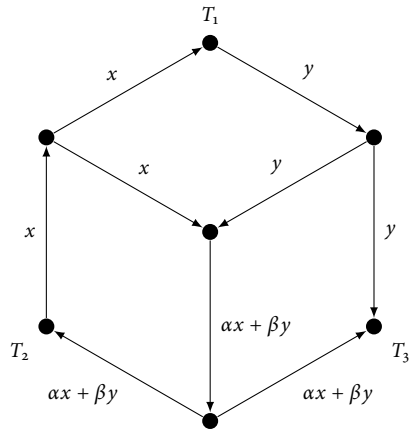


Figure 2.2: Terminals T_1 and T_2 transmitting at unit rate.

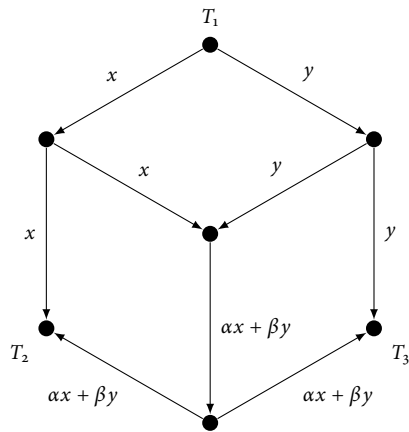


Figure 2.3: Terminal T_1 transmitting at rate two.

Section 1.4 and depicted for convenience in Figure 2.3. The coding operation performed by the center node is to retransmit the linear combination $\alpha x + \beta y$.

Besides the point that network coding can achieve rate tuples that can not be achieved with routing, we have two observations. The first is that the sum of the rates that are transmitted in the network are equal in the two examples demonstrated above. In the next section we present a result that demonstrates that the sum rate provides sufficient and necessary conditions for achievability of a rate tuple. The second observation is that the example solutions for rate tuples $(1, 1, 0)$ and $(2, 0, 0)$, as given in Figures 2.2 and 2.3 respectively, are very similar. More precisely, in both examples a single coding operation is performed at the same point in the network. We will see in Section 2.5 that it is always possible to choose the orientations corresponding to the different rate tuples in such a way that the coding points are the same for all rate tuples. Moreover, the local coding coefficients α and β are the same in both examples. In Section 2.6 it will be shown that a single set of local coding coefficients can be found that can be used for all rate tuples.

2.4 Rate Region

The next theorem shows that the achievable rate region can be completely characterized in terms of the maximum achievable sum-rate R^* .

Theorem 2.3. *A rate tuple (R_1, \dots, R_N) is achievable if and only if for all $i = 1, \dots, N$, a multicast session with only terminal T_i acting as a source of rate $R^* \triangleq \sum_{j=1}^N R_j$ is achievable.*

This result was first obtained in [53]. We provide an alternative proof in Section 2.5, but first we connect R^* to the pairwise min-cut between the terminals thereby giving a graph-theoretic interpretation. We start with a graph-theoretic result for networks that have a uniform pairwise min-cut. Let min-cut $(T, \mathcal{T} \setminus \{T\})$, $T \in \mathcal{T}$, be the value of a minimum cut that separates T from all terminals in $\mathcal{T} \setminus \{T\}$.

Lemma 2.4. *Consider an information exchange configuration $\{G, \mathcal{T}\}$, with uniform pairwise min-cut h . The minimum min-cut from a terminal to all other*

terminals is h :

$$\min_{T \in \mathcal{T}} \text{min-cut}(T, \mathcal{T} \setminus \{T\}) = h.$$

Proof. Let H be a Gomory-Hu tree (see e.g. [13]) constructed only on the set of terminal vertices. By the uniform pairwise min-cut assumption, every edge in H has weight h . Let T be any terminal node that is a leaf in H . The edge in H incident on T separates T from all other terminals. By the properties of a Gomory-Hu tree there is a capacity h cut in the original network, separating T from all other terminals, hence $\text{min-cut}(T, \mathcal{T} \setminus \{T\}) = h$. \square

Theorem 2.5. *Consider an exchange configuration $\{G, \mathcal{T}\}$ with uniform pairwise min-cut h . The maximum achievable sum rate satisfies $h \frac{N}{2(N-1)} \leq R^* \leq h$.*

Proof. We first show the upper bound. By Lemma 2.4 we know that there exists a terminal $T \in \mathcal{T}$ for which $\text{min-cut}(T, \mathcal{T} \setminus \{T\}) = h$. Consider any such minimum cut. The information from all sources needs to cross this cut.

For the lower bound we show that rate tuple $(\frac{h}{2(N-1)}, \dots, \frac{h}{2(N-1)})$ is achievable. Create a directed network by replacing each undirected edge with two oppositely directed edges of capacity $1/2$. Add a virtual source S' to the network and connect it to each terminal in \mathcal{T} using directed edges of capacity $h/(2(N-1))$. We will show that

$$\text{min-cut}(S', T) \geq Nh/(2(N-1)), \quad \forall T \in \mathcal{T}. \quad (2.1)$$

Consider any cut that separates the virtual source S' from a terminal T . The edge that connects S' to T has to cross this cut. In fact, if all terminals are on T 's side of the cut, all edges from the virtual source S' necessarily cross the cut which therefore has value at least $Nh/(2(N-1))$. If, on the other hand, a non-empty subset of terminals $\mathcal{T}_1 \subseteq \mathcal{T}$ is on the same side of the cut as the source, from construction $\text{min-cut}(\mathcal{T}_1, T) \geq h/2$. Adding the contribution of the direct edge from S' to T results in a cut value of at least $Nh/(2(N-1))$.

Since (2.1) is satisfied there exists a network code that allows to multicast rate $Nh/(2(N-1))$ from S' to all terminals. Any valid solution will require S' to send independent information to each terminal at rate $h/(2(N-1))$ and thus corresponds to a solution of the information exchange problem. \square

Note that the above result improves the general lower bound that was given in [53].

Procedure 1 Finding a new orientation

Input: Orientation of the graph that supports rate tuple (R_1, \dots, R_N) , $i, j \in \{1, \dots, N\}$, $i \neq j$, $R_i > 0$.

Output: Orientation with the same coding points that supports rate tuple $(\tilde{R}_1, \dots, \tilde{R}_N)$, $\tilde{R}_i = R_i - 1$, $\tilde{R}_j = R_j + 1$, $\tilde{R}_k = R_k$, $k \neq i, j$

- 1) Find R_i edge disjoint paths from T_i to T_j .
 - 2) Pick one of these paths.
 - 3) Reverse the orientation of the edges along this path.
-

2.5 Preserving Coding Points

Operating at different rate tuples requires different orientations of the edges in the network. We will see in this section that these orientations can be constructed in such a way that the coding points are the same for all orientations. We show this by means of subtree decomposition techniques.

The subtree decomposition captures the structure of the network and the coding solution by decomposing the network in trees that carry the same information [27]. The idea is to decompose the network into parts, each part being a tree, and thus called a subtree. We distinguish between source subtrees and coding subtrees. Each source subtree corresponds to one unit rate source, and thus a source emitting rate R_i results in R_i source subtrees. Each coding subtree starts with a coding point, an edge where linear combining occurs, and again represents a tree through which runs unit information rate. The linear combinations are represented by global coding vectors assigned to the subtrees. The local operations performed at the coding points are represented by local coding coefficients. Note that the number of source subtrees equals the dimension of the global coding vectors. Moreover, the number of coding subtrees equals the number of coding points.

As an illustrating example we have given in Figure 2.4b on the next page the subtree decomposition of the network from Figure 2.3, *i.e.*, for the undirected butterfly operated at rate tuple $(2, 0, 0)$. A notational difference from [27] is that we explicitly represent the coding point.

The idea presented in this section is that given an orientation of the graph that supports rate tuple (R_1, \dots, R_N) it is possible to construct an orientation

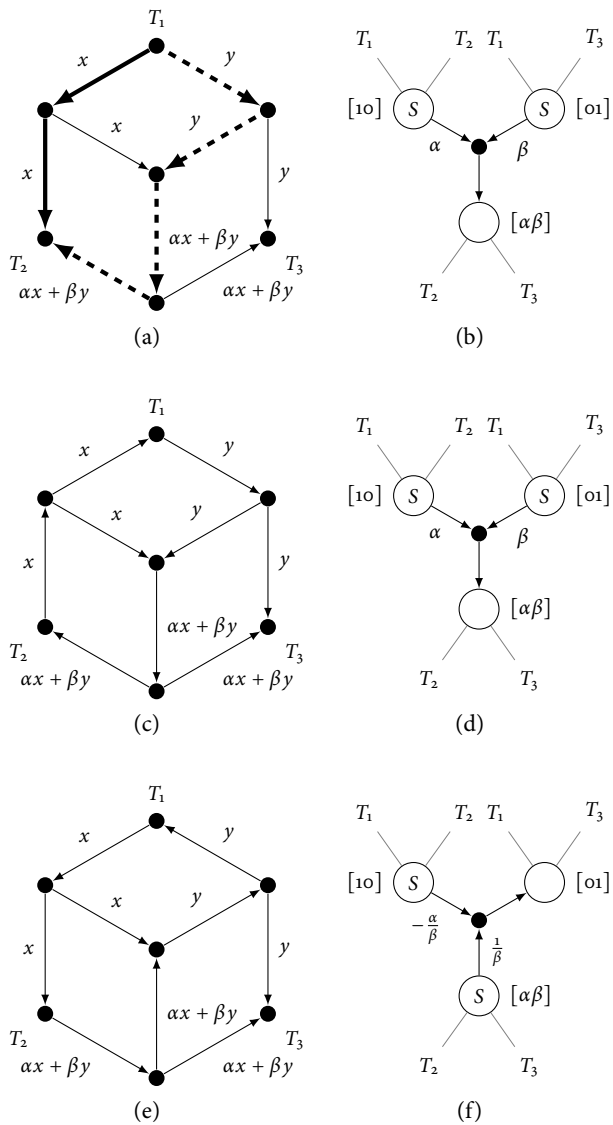


Figure 2.4: Illustrating Procedure 1.

of the graph that supports rate tuple $(\tilde{R}_1, \dots, \tilde{R}_N)$, $\tilde{R}_i = R_i - 1$, $\tilde{R}_j = R_j + 1$, $\tilde{R}_k = R_k$, $k \neq i, j$. By repeatedly applying this construction, orientations are obtained for all possible rate tuples. Procedure 1 provides a means of constructing a new orientation that supports rate tuple $(\tilde{R}_1, \dots, \tilde{R}_N)$. We illustrate the procedure by means of an example. On the butterfly, starting from an orientation for rate tuple $(2, 0, 0)$ we will obtain an orientation for the rate tuple $(1, 1, 0)$. In Figure 2.4a we have depicted the two (unique) disjoint paths from T_1 to T_2 . For convenience, the subtree corresponding to the orientation is given in Figure 2.4b. Now, the procedure allows to pick any one of the two paths. The orientation resulting from reversing the left path, depicted in solid lines, is given in Figure 2.4c. In this case the decomposition in subtrees is the same, as depicted in Figure 2.4d. The orientation resulting from reversing the right path, depicted in dashed lines, is given in Figure 2.4e. In this case the decomposition in subtrees is again the same, but some edges in the subtree graph are reoriented, as is illustrated in Figure 2.4f. Moreover, the roles of a source and a coding subtree are exchanged.

In general, application of Procedure 1 has the following effects:

1. The decomposition in subtrees is unaffected, *i.e.*, the same sets of edges are part of the same subtrees.
2. The role of a source and a coding subtree can interchange, causing the path between these subtrees to be reversed.

What is not clear from the above discussion is that the new orientation supports the intended rate tuple. To show that this is the case, we assume that for the original rate tuple and graph orientation a network code has been given. Now, we proceed in a formal way by assigning the same set of global coding vectors to the subtrees in the new orientation. Next, we find local coding coefficients that, starting from the global coding vectors of the source subtrees, result in the global coding vectors that have been assigned to the coding subtrees. This is a formal procedure, since the resulting code is not always a network code that can be implemented in practice. Figures 2.4e and 2.4f provide an example of this effect. Assume that terminal T_1 has symbol x to transmit and terminal T_2 the symbol y . Indeed, the terminal T_2 will not be able to transmit the coded symbol $\alpha x + \beta y$ over its outgoing edge, since it has

only symbol y available. The importance of this formal procedure lies in the fact that if there exists a network code with arbitrary global coding vectors assigned to the source subtrees and full rank systems observed by each of the terminals, then there must also be a network code in which the unit basis vectors are assigned to the source subtrees [49]. Hence, this shows that the graph orientation supports the desired rate tuple.

It needs to be shown that local coding coefficients leading to the right global coding vectors can always be found. First suppose that a single source and child coding subtree are exchanging roles.

Lemma 2.6. *Consider a valid code over a minimal subtree graph and assume we exchange the role of a source subtree and one of its children. There exist local coding vectors resulting in the same global coding vectors as the original code.*

Proof. W.l.o.g. assume that in the original graph subtrees C_1, \dots, C_k are parents of C_{k+1} , and that after the procedure we have C_2, \dots, C_{k+1} parents of C_1 . Let v_i denote the global coding vector associated with subtree C_i and $\langle v_1, \dots, v_k \rangle$ the space spanned by vectors v_1, \dots, v_k . Then $v_{k+1} \in \langle v_1, \dots, v_k \rangle$ and from properties of minimal configurations $v_{k+1} \notin \langle v_2, \dots, v_k \rangle$. This implies that $\langle v_1, \dots, v_k \rangle = \langle v_2, \dots, v_{k+1} \rangle$, i.e., v_2, \dots, v_{k+1} form a basis of the space $\langle v_1, \dots, v_k \rangle$. Thus $v_1 \in \langle v_2, \dots, v_{k+1} \rangle$, and we can always find the required local coding vector. \square

Theorem 2.7. *There exists a set of orientations on G , each supporting a different achievable rate tuple, such that the subtree decomposition and the coding points are the same for all these orientations.*

Proof. This follows from the above observations and the repeated application of Lemma 2.6. \square

Proof of Theorem 2.3. Procedure 1 allows, starting from any achievable rate tuple and a graph orientation that supports it, to obtain an orientation supporting a rate tuple in which a single terminal is acting as a source with a rate that is equal to the sum-rate of the original rate tuple, and vice versa. \square

Procedure 2 Preserving local coding vectors

Input: Network code at rate tuple $(R_l)_{l=1}^N$, $i, j \in \{1, \dots, N\}$, $i \neq j$, $R_i > 0$.

Output: Code using same local coding vectors, at rate tuple $(\tilde{R}_l)_{l=1}^N$, $\tilde{R}_i = R_i - 1$, $\tilde{R}_j = R_j + 1$, $\tilde{R}_k = R_k$, $k \neq i, j$.

- 1) Find R_i edge disjoint paths from T_i to T_j .
 - 2) Pick one of these paths.
 - 3) Reverse the orientation of the edges along this path.
 - 4) At each coding point keep the local coding vector coefficients of the edges that are not reoriented. At affected coding points, to the new incoming edge assign the coefficient of the edge that is now outgoing.
 - 5) Assign orthonormal basis vectors as global coding vectors to the source subtrees. The global coding vectors for the coding subtrees follow from the global coding vectors of the source subtrees and the local coding coefficients.
-

2.6 Preserving Local Coding Vectors

We will see in this section that it is not only possible to have the same coding points for all rate tuples, but that it is in fact possible to use, at each coding point, the same set of local coding coefficients for all rate tuples. This reduces the complexity at the coding points. It is shown that we can calculate *in advance* specifically chosen *universal* local coding vectors that can be reused for all rate tuples. Note that the global coding vectors may be different for each rate tuple.

Once universal local coding coefficients have been found, they can be used to construct network codes for different rate tuples using Procedure 2.

Theorem 2.8. *There exists a set of universal local coding vectors that can be repeatedly used in Procedure 2 and result in valid output codes.*

Proof. Start from any achievable rate tuple and an orientation of the graph supporting it. Assign orthonormal basis vectors as global coding vectors to the source subtrees. Following the algebraic framework [49], let the coefficients of the local coding vectors be variables. We show that there exists values for these variables that can be used as universal local coding vectors.

Consider the transfer matrices to each terminal for each of the codes that can be obtained by Procedure 2. By Theorem 2.7 we know that for the orientations obtained after Step 3) there exists a valid network code. Therefore, there also exists a code using any set of orthonormal basis vectors as global coding vectors at the source subtrees. Hence, the determinants of all these matrices are non-identically zero polynomials.

Consider the polynomial formed as the product of the above determinants. This is again a non-identically zero polynomial. Any set of coefficients for which the product polynomial evaluates to a non-zero value, results in suitable local coding vectors. \square

The theorem states that one can construct a suitable code that allows to preserve the same local coding vectors.

2.7 Discussion

In this chapter constructions have been provided that achieve arbitrary operating points in the achievable rate region for an undirected information exchange network, while using a single set of local coding vectors. Note that the approach lends itself to asynchronous network operation: the intermediate nodes in the network can deduce the coding operations they need to perform, based on the origin of the incoming packets, and without knowledge of the operating point. As a side result, we also get an alternative proof to the characterization of the exchange rate region. We also provide a proof for Theorem 2.5 based on graph-theoretic properties, that gives additional insight in our problem structure.

Chapter 3

Multi-Rate Network Coding

Contents

3.1	Introduction	33
3.2	Model	37
3.3	Network Coding at Minimum Cost	39
3.4	Multi-rate Network Coding	40
3.5	Discussion	45

3.1 Introduction

In this chapter we consider network coding on directed graphs that have capacities and costs assigned to the edges. The cost of an edge can represent, for instance, the energy required to transmit over this edge. There is a natural *tension between maximizing throughput and minimizing cost*. Consider e.g. the multicasting problem in the butterfly network depicted in Figure 3.1, with unit capacity edges and for each edge a cost one if it is used to transmit a symbol. Figure 3.2 shows the canonical network code that achieves the maximum possible throughput of 2, at a cost of $4\frac{1}{2}$ per symbol. Figure 3.3, on the other hand, shows a solution achieving a cost 4 per symbol at a reduced throughput of 1.

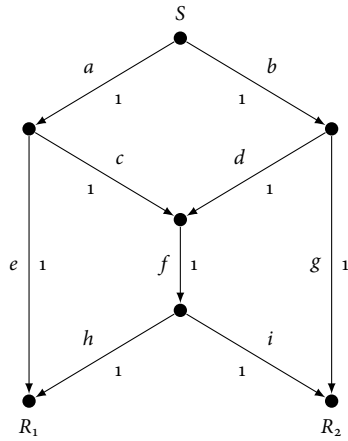


Figure 3.1: Butterfly network with source S , receivers R_1 and R_2 and unit capacity edges a, b, \dots, i of cost one.

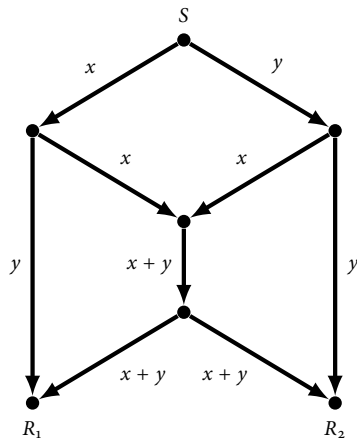


Figure 3.2: Multicast of two symbols x and y , i.e. at throughput 2, at a cost per symbol of $9/2 = 4\frac{1}{2}$.

It is well known that for multicasting on networks represented by directed graphs, network coding can be beneficial for the throughput [2]. Also, network coding with a cost criterion has been considered [60]. Existing work, however, has focussed either on maximizing throughput or minimizing cost.

In this chapter we show that a single network code can be used to *trade-off throughput against cost*. In other words that a single code can be used to operate at any achievable throughput–cost pair, subsequently referred to as an *operating point*. More precisely, we construct a code for which the source and intermediate nodes perform linear coding operations that do not have to be changed if a different operating point is used. The only difference between operating points is in which edges of the network are used. We refer to this type of code as a *multi-rate network code*. Our interest is in multi-rate codes that operate at the minimum possible cost for each of the values of the throughput that are achievable.

In [23] a network code is constructed, that, like our multi-rate code, allows to operate at different rates, while preserving local coding vectors. Cost is, however, not taken into consideration in [23]. The code that is constructed uses all edges of the network, making it unsuitable for minimum-cost operation. Also, we consider a fixed set of receivers, whereas in [23] the set of receivers at a specific rate are all nodes in the network with a sufficiently large min-cut.

The problem of constructing a network code for multiple operating points is closely related to the problem of constructing a network code that is robust against a set of edge failure patterns, a problem considered e.g. in [49] and [41]. The similarity to our work is that a single code needs to be constructed that is valid on different subgraphs. The difference is that in [41, 49] the supported rate on all subgraphs is the same, whereas we vary the rate.

In Section 3.2 we introduce our network model and some notation. Section 3.3 briefly discusses some issues related to network coding for minimum cost. In Section 3.4 we provide a construction for a minimum-cost multi-rate network code and show that it can be applied on all networks. In Section 3.5 we mention some interesting points for future research.

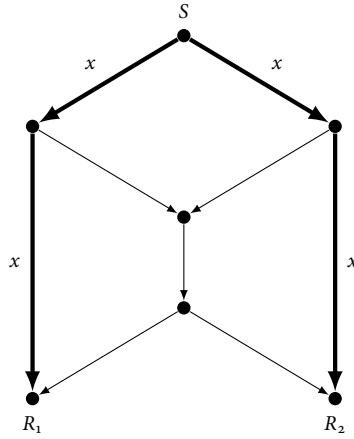


Figure 3.3: Multicast of one symbol x , i.e. at throughput 1, at a cost per symbol of $4/1 = 4$.

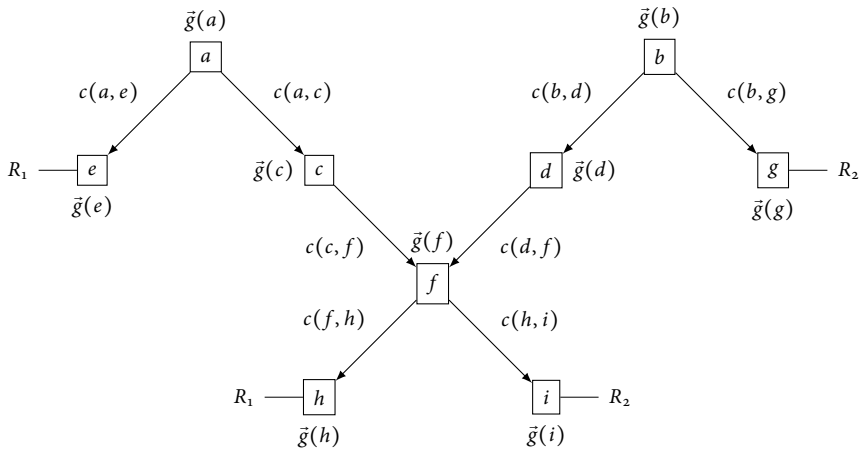


Figure 3.4: Line graph of the network from Figure 3.1, annotated with global coding vectors $\vec{g}(e)$, $e \in E$, and local coding coefficients $c(e, f)$, $(e, f) \in L$.

3.2 Model

Our interest is in networks represented by directed acyclic graphs (V, E) , i.e., graphs with vertex set V and edge set E , in which there is one source $S \in V$ that is supposed to multicast its information to a set of receivers $\mathcal{R} \subset V$. There is a non-negative cost associated with each edge. Throughout this chapter we will assume that all edges have unit capacity. However, our results are also valid for networks with edges of arbitrary capacity. We assume that there is no delay on the edges and that information flows through the acyclic network in zero time.

For vertex $v \in V$, let $\delta^+(v)$ and $\delta^-(v)$ be the sets of edges whose head respectively tail is v . Similarly for edge $e \in E$, let $\delta^+(e)$ be the set of edges whose head is equal to e 's tail, and $\delta^-(e)$ those whose tail is e 's head. Let (E, L) be the line graph of (V, E) , i.e.

$$L = \{(e, f) \mid e \in E, f \in \delta^-(e)\}. \quad (3.1)$$

Let \mathbb{F}_q be the field of operation and $x_n \in \mathbb{F}_q$, $n = 1, \dots, N$ the information symbols to be sent, collected in a row vector $x = [x_1, \dots, x_N]$. We call N the dimension of the code. Let $\vec{g}(e) \in \mathbb{F}_q^N$ be the global coding vector of edge $e \in E$, i.e. the inner product $\langle \vec{g}(e), x \rangle$ is transmitted over edge e . Associate with all $(e, f) \in L$ a local coding coefficient $c(e, f) \in \mathbb{F}_q$. The coding operation performed for an edge $f \in E$ is given by

$$\vec{g}(f) = \sum_{e \in \delta^+(f)} c(e, f) \vec{g}(e). \quad (3.2)$$

We will refer to $\vec{g}(f)$ as the global coding vector. The above definitions are illustrated in Figure 3.4. Note that a network code will, in general, not utilize all edges of the network. In that case, only a subset of the edges carries symbols and the above definitions apply to the corresponding subgraph.

Throughput is defined as the number of information symbols that are successfully decoded by all receivers. *Cost per symbol* is defined as the sum of the costs of all edges carrying a symbol, divided by the throughput.

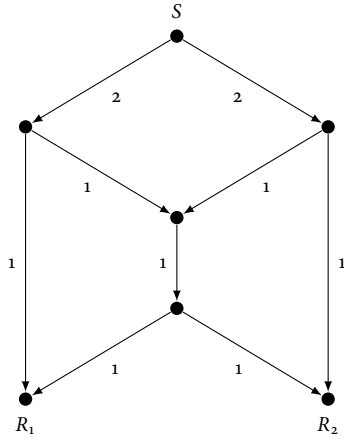


Figure 3.5: The network from Figure 3.1 with a different cost assignment on the edges such that the minimum-cost coding solution has throughput 2.

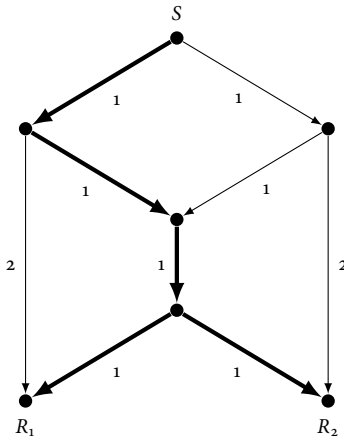


Figure 3.6: The network from Figure 3.1 with different costs on the edges. The thick edges depict a minimum cost solution at throughput 1.

3.3 Network Coding at Minimum Cost

For minimum-cost routing it is sufficient to use only a single path to each receiver, i.e. in a network with unit capacity edges there always exists a solution with throughput one achieving minimum cost over all possible rates. If network coding is allowed this is no longer true. Consider for example the network from Figure 3.1, but with costs on the edges as depicted in Figure 3.5.

It is easy to verify that each solution at throughput 1 has cost at least 6, whereas the canonical network code at throughput 2 has cost $5\frac{1}{2}$ per symbol. In fact, in this network there is no tradeoff between throughput and cost. This example also demonstrates that for networks represented by directed graphs network coding can achieve lower cost per symbol than routing only.

The above might suggest that the construction of a minimum-cost network code is more complex than finding a minimum-cost routing solution. However, it has been shown by Lun et al. that a minimum-cost network coding solution can be found in a distributed fashion in polynomial time [60]. The fact that the complexity of finding this solution is polynomial in time is surprising, since the corresponding routing problem is a Steiner tree problem that is known to be NP-complete [80].

The difference between the construction of an arbitrary network code and one that needs to operate at minimum cost is in the selection of the edges that are used by the code. For an arbitrary code one can select, independently for each receiver, any set of disjoint paths that meet the throughput requirements. If we consider the network in Figure 3.6 at throughput 1, we see that this is no longer the case for a minimum-cost network code. The edges that need to be used by the code can, however, be found in polynomial time by means of linear programming [60]. After the appropriate edges have been found, standard algorithms can be used to construct the minimum-cost network code, e.g. the algorithm presented in [41].

In the remainder of this chapter we assume that for each operating point a minimum-cost set of edges satisfying the throughput requirements is given. Note that these different sets of edges correspond to the different subgraphs that need to be considered when constructing a robust (in the sense that it is resilient against link failures) network code [41, 49]. The main difference is that in our case, the supported rate on each subgraph is different.

3.4 Multi-rate Network Coding

In this section we construct a network code for which the source is able to control the throughput. We refer to this type of code as a *multi-rate network code*.

Let h_1, h_2, \dots, h_K , positive integers, $h_1 > h_2 > \dots > h_K$, be the desired throughputs for operating points $1, \dots, K$ respectively. As stated in Section 3.3 we assume that for each operating point a set of minimum-cost edges is given. Let $E_k \subset E$ be the edges for operating point $k = 1, \dots, K$, with $L_k \subset L$ defined analogously to (3.1), *i.e.*,

$$L_k = \{(e, f) | e, f \in E_k, f \in \delta^-(e)\}. \quad (3.3)$$

Also, let $E_1^K = \bigcup_{k=1}^K E_k$ and $L_1^K = \bigcup_{k=1}^K L_k$.

3.4.1 Encoding and Decoding

The dimension of the code, *i.e.* the number of symbols in x , needs to be high enough to support throughput h_1 , the maximum throughput among the operating points. For the other operating points, not all information symbols in x will have to be used. In fact, since we operate at minimum cost, the number of coded symbols observed by a receiver will be too low to decode all information symbols.

We will construct a code in which, for each operating point, the source and receivers agree on which information symbols in x will be used to transmit actual information. We assume that at rate h_k the first h_k symbols are used. The remaining symbols are fixed at zero by the source.

The receivers will observe a number of coded symbols for which the coding vectors span a subspace of \mathbb{F}_q^N . If the dimension of this subspace is smaller than N , the observed symbols and their coding vectors by themselves are not sufficient to successfully decode, *i.e.* to solve the system of linear equation represented by the coding vectors. Knowledge about which information symbols are not used and fixed at zero makes decoding possible, however. The receiver can immediately eliminate the corresponding variables from the system and consider a reduced system of linear equations.

3.4.2 Code Construction

Our code is defined in terms of global coding vectors $\vec{g}^*(s)$, $s \in (\delta^-(S) \cap E_1^K)$ and local coding coefficients $c^*(e, f)$, $(e, f) \in L_1^K$. A node $v \in V$ in the network is provided with $c^*(e, f)$, for all $e, f \in E_1^K$ for which $e \in \delta^+(v)$ and $f \in \delta^-(v)$. Also, for all $e \in \delta^-(v)$ and all $k = 1, \dots, K$, v needs to know if $e \in E_k$.

We assume that all nodes in the network have knowledge of the operating point chosen by the source. Justification comes from practical considerations. Implementations of network coding that have been suggested, e.g. in [11], transmit in the header of a packet, a coding vector that is used by all symbols in the payload of the packet. We also include a description of the operating point in the header. The overhead in terms of throughput and cost of this is small.

At operating point k , an internal node $v \in V$ upon receiving coded symbols, for each outgoing edge $f \in \delta^-(v)$, transmits a symbol coded according to (3.2) if $f \in E_k$ and does not transmit anything on f otherwise. The receivers consider the (reduced) system of linear equations of dimension h_k as described in Section 3.4.1 and successfully decode.

3.4.3 Existence of a Valid Code

With each of the operating points obtained by the multi-rate code presented above we can associate a traditional network code, consisting of the coding vectors used at that operating point. For $k = 1, \dots, K$ this code, for $(e, f) \in L_1^K$, has local coding coefficients

$$c_k(e, f) = \begin{cases} c^*(e, f), & \text{if } (e, f) \in L_k \\ 0, & \text{otherwise.} \end{cases} \quad (3.4)$$

The global coding vectors transmitted by the source are

$$\vec{g}_k(s) = \begin{cases} \vec{g}^*(s), & \text{if } s \in (\delta^-(S) \cap E_k) \\ 0, & \text{otherwise,} \end{cases} \quad (3.5)$$

for $s \in (E_1^K \cap \delta^-(S))$. The remaining coding vectors are defined accordingly, following (3.2). Finally, the source utilizes the first h_k information symbols.

We need to find $\vec{g}^*(e)$ and $c^*(e, f)$ for which all K codes defined according to (3.4) and (3.5) are valid, i.e. the vectors $\vec{g}_k(e)$ allow all receivers to decode the first h_k information symbols assuming the remaining symbols are kept zero.

Theorem 3.1. *If q is sufficiently large, there exist valid global coding vectors $\vec{g}^*(s) \in \mathbb{F}_q^N$ and local coding coefficients $c^*(e, f) \in \mathbb{F}_q$, $s \in (\delta^-(S) \cap E_1^K)$, $(e, f) \in L_1^K$.*

Proof. Following the algebraic framework [49], introduce for all $(e, f) \in L_1^K$ an unknown over \mathbb{F}_q , i.e. let

$$c(e, f) = \alpha_{e,f}, \quad \forall (e, f) \in L_1^K. \quad (3.6)$$

Also introduce unknowns for the coding vectors transmitted by the source, i.e. let

$$\vec{g}(s) = [\dots \beta_{s,n} \dots]_{n=1}^N, \quad \forall s \in (\delta^-(S) \cap E_1^K). \quad (3.7)$$

All coding vectors in the network can be expressed in these unknowns. Since the network is acyclic, each entry of each coding vector is a bounded degree polynomial in these unknowns.

We construct matrices A_R^k , $R \in \mathcal{R}$, $k = 1, \dots, K$ that represent the system of linear equations that needs to be solved by receiver R at operating point k . First, let \tilde{A}_R^k be the concatenation of all $\vec{g}(e)$ for which $e \in E_1^K$ is observed by R and used at operating point k , i.e. if we label the respective edges as $\{e_1, e_2, \dots, e_{h_k}\} = \delta^+(R) \cap E_k$,

$$\tilde{A}_R^k = \begin{bmatrix} \vec{g}(e_1) \\ \vec{g}(e_2) \\ \vdots \\ \vec{g}(e_{h_k}) \end{bmatrix}. \quad (3.8)$$

Since at operating point k , the source only uses the first h_k information symbols, a receiver can eliminate the remaining symbols from the system by considering only the first h_k columns of \tilde{A}_R^k . Let these be given by the $h_k \times h_k$ matrix \hat{A}_R^k .

Also, since we need to consider the codes defined by (3.4) and (3.5), for all entries in \hat{A}_R^k put

$$\alpha_{e,f} = 0, \quad \forall (e, f) \notin L_k \quad (3.9)$$

and

$$\beta_{s,n} = 0, \quad \forall s \in (\delta^-(S) \cap (E_1^K \setminus E_k)), n = 1, \dots, N. \quad (3.10)$$

Denote the new matrix by A_R^k . Now, the codes defined by (3.4) and (3.5) are valid if all A_R^k , $R \in \mathcal{R}$, $k = 1, \dots, K$ are full rank matrices.

In (V, E_k) the source has, by assumption, min-cut h_k to each receiver. There exists therefore a routing solution, that routes information symbols $1, \dots, h_k$ over edges in E_k to receiver R . This routing solution corresponds to values of the unknowns $\alpha_{e,f}$, $(e, f) \in L_1^K$ and $\beta_{s,n}$, $s \in (\delta^-(S) \cap E_1^K)$, $n = 1, \dots, N$, that make the matrix A_R^k full rank. The determinant of A_R^k is, therefore, a non-zero polynomial in these unknowns. Moreover, since the degree of each entry is bounded, the degree of the determinant is bounded. Hence, it has only a finite number of zeros.

Now consider the polynomial that is the product of the determinants of all A_R^k . It has again a finite number of zeros. If the field \mathbb{F}_q is sufficiently large, there exist therefore values for $\alpha_{e,f}$, $(e, f) \in L_1^K$ and $\beta_{s,n}$, $s \in (\delta^-(S) \cap E_1^K)$, $n = 1, \dots, N$, for which this product polynomial evaluates to a non-zero value. Therefore, for these values of the unknowns all individual determinants also evaluate to non-zero and all A_R^k have full rank. \square

3.4.4 Example

We construct a minimum-cost multi-rate code for the butterfly network given in Figure 3.1 for the operating points depicted in Figures 3.2 and 3.3. We have $K = 2$, $h_1 = 2$, $h_2 = 1$, $E_1 = \{a, b, c, d, e, f, g, h, i\}$, $L_1 = \{(a, c), (a, e), (b, d), (b, g), (c, f), (d, f), (f, h), (f, i)\}$, $E_2 = \{a, b, e, g\}$, $L_2 = \{(a, e), (b, g)\}$.

One can verify that the canonical network code depicted in Figure 3.2 does not allow receiver R_2 to decode at operating point 2. There exists, however, the following solution over \mathbb{F}_2 . Take $c^*(e, f) = 1$, $\forall (e, f) \in L_1^2$, and

$$\vec{g}^*(a) = [1 \ 0], \quad \vec{g}^*(b) = [1 \ 1]. \quad (3.11)$$

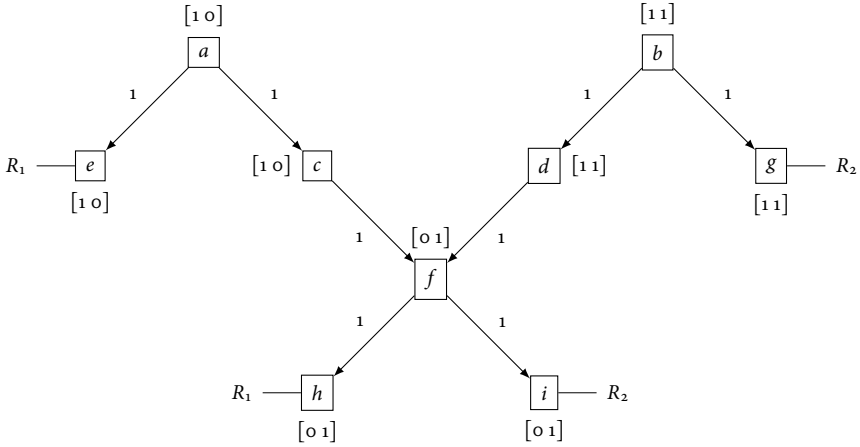


Figure 3.7: Line graph of the network of Figure 3.1 with global and local coding vectors for a multi-rate code for the operating points depicted in Figures 3.2 and 3.3.

For operating point 1, the global coding vectors for the other nodes in the network are depicted in Figure 3.7. At operating point 2 the coding vectors for edges not in E_2 are zero, the others are unaffected.

At operating point 1, receivers R_1 and R_2 obtain the system of linear equations represented by the matrices

$$\begin{bmatrix} \vec{g}(e) \\ \vec{g}(h) \end{bmatrix} = \begin{bmatrix} 1 & 0 \\ 0 & 1 \end{bmatrix} \quad \text{and} \quad \begin{bmatrix} \vec{g}(g) \\ \vec{g}(i) \end{bmatrix} = \begin{bmatrix} 1 & 1 \\ 0 & 1 \end{bmatrix} \quad (3.12)$$

respectively. Since these are full rank matrices both receivers can decode.

At operating point 2 receiver R_2 obtains only

$$\begin{bmatrix} \vec{g}(g) \end{bmatrix} = \begin{bmatrix} 1 & 1 \end{bmatrix}, \quad (3.13)$$

which corresponds to an underdetermined system, but since the source only uses the first information symbol the receiver can eliminate the second symbol and successfully decode. Receiver R_1 obtains

$$\begin{bmatrix} \vec{g}(e) \end{bmatrix} = \begin{bmatrix} 1 & 0 \end{bmatrix} \quad (3.14)$$

and can directly decode.

3.5 Discussion

In this chapter we have shown that network coding can be used to tradeoff throughput against cost. In the code that we construct, nodes need only one set of coding vectors. Based on the operating point, nodes either perform a linear coding operation that is the same for all operating points or do not transmit anything on specified edges.

The idea to use one network code to tradeoff throughput against cost, holds many interesting questions for future research. The example from Section 3.4.4 shows that the canonical network code on the butterfly network can not be used as the basis for a multi-rate code. There does, however, exist a multi-rate code over the field \mathbb{F}_2 , which is the smallest field required for any code of throughput 2. It will be interesting to see if there always exists a multi-rate code over a field not larger than would be required by any of the operating points individually.

From the proof of Theorem 3.1 it follows that a multi-rate code can be constructed by considering an appropriate algebraic structure. This, however, requires knowledge of the complete structure of the network. One could also try to find decentralized ways to construct a multi-rate code, using e.g. ideas presented in [39].

Chapter 4

The Energy Benefit of Network Coding

Contents

4.1	Introduction	47
4.2	Model and Problem Statement	50
4.3	Results	52
4.4	An Efficient Code on the Hexagonal Lattice	57
4.5	An Efficient Code on the Rectangular Lattice	65
4.6	Extended Energy Consumption Model	76
4.7	Discussion	87

4.1 Introduction

In recent years there has been significant interest in network coding with the aim of reducing energy consumption in wireless networks by exploiting broadcast. In this chapter we are interested in the energy benefit of network coding for wireless networks, which is the ratio of the minimum energy solution in a routing solution compared to the minimum energy network coding solution, maximized over all configurations.

It has been shown by Goel and Khanna [30] that the energy benefit of network coding for multicast problems in wireless networks is upper bounded by a constant. The problem of reducing energy consumption for many-to-many broadcast traffic in wireless networks has been studied by Fragouli et al. in [26] and Widmer and Le Boudec in [78], providing lower bounds on the energy benefit of network coding for specific topologies. More importantly, algorithms have been presented in [26,78] that allow to exploit these benefits in practical scenarios, *i.e.*, in a distributed fashion.

The above demonstrates that for multicast traffic and for many-to-many broadcast traffic, there is some understanding of the energy benefits of network coding and how to exploit them. In order to reduce energy consumption in practical networks, however, it is important to consider also multiple unicast traffic. Indeed, in practice a large part of the data will be generated by unicast sessions. For the case of multiple unicast traffic, contrary to multicast and broadcast, not much is known. This chapter deals with the energy benefits of network coding for wireless multiple unicast. Remember from the discussion in Chapter 1 that for multicast, the problem of minimum-cost routing is hard, whereas minimum-cost network coding is easy. In stark contrast, the problem of minimum-cost multiple unicast routing is easy. One constructs the minimum-cost solution, *i.e.*, the shortest path, for each session individually. The minimum-cost multiple unicast network coding problem, however, seems hard and in general very little is known.

Network coding for the multiple unicast problem in wireless networks was first studied by Wu et al. in [81], in which it was shown that in the information exchange problem on the line network the energy saving achieved by network coding is a factor two. The network codes that we construct in this work are in a sense a generalization of the results on one dimensional networks [81], to higher dimensional networks. The networks considered in this work are lattices. More specifically, the hexagonal lattice and the rectangular lattice. Effros et al. [19] and Kim et al. [48] have considered energy-efficient network codes on the hexagonal lattice. We improve the lower bounds on the energy savings of network on the hexagonal lattice given in [19]. More precisely, we improve the previously known bound of 2.4 and obtain a new bound of 3.

Kramer and Savari have developed techniques that can be used to up-

per bound the achievable throughputs in a multiple unicast problem [51]. No methods are known, however, to lower bound the cost of network coding solutions for a configuration. A lower bound to the ratio of the minimum energy consumption of routing and coding solutions for a given multiple unicast configuration was provided by Keshavarz-Haddad and Riedi in [47]. For the type of configurations used in this thesis, however, the results from [47] give the trivial lower bound of one. We will see, however, that network coding has large energy savings for these configurations.

The class of *decode-and-recombine* has been introduced in Chapter 1. We quickly restate the important properties of these codes: They satisfy the constraint that each symbol in each linear combination that is transmitted is explicitly known by the node transmitting that linear combination. This is a restriction from the general linear coding strategy, in which linear combinations of coded messages can be retransmitted. The use of a decode-and-recombine strategy results in reduced complexity. However, a question that has to be addressed is, whether the use of decode-and-recombine codes leads to a higher energy consumption than is strictly necessary. We answer this question affirmatively. An upper bound of three on the energy benefit of decode-and-recombine codes has been given by Liu et al. [57]. One of the contributions of this work is to show that larger energy benefits can be obtained by considering also other types of codes.

All the work that we referenced earlier in this section is based on the assumption that all the energy that is consumed by a device is emitted by the antenna. This is the model that we will use for most of this chapter. In the last part of this chapter, however, we consider a more detailed energy consumption model, taking also energy consumed by supporting circuitry into account.

This chapter is organized as follows. In Section 4.2 we specify our model and problem statement more precisely. Our main results are presented in Section 4.3. Constructions of configurations that allow a large energy benefit for network coding and proofs of our results are given in Sections 4.4 and 4.5. In Section 4.6 we provide an extension of the results from earlier sections to a more detailed energy consumption model. In Section 4.7, finally, we discuss our work.

4.2 Model and Problem Statement

Let $V \subset \mathbb{R}^d$ be the nodes of a d -dimensional wireless network. We consider a wireless network model with broadcast, where all nodes within range r of a transmitting node can receive, and nodes outside this range cannot. More precisely, given a transmission range r , a node v is broadcasting to all nodes in the set

$$\{u \in V \mid \|u - v\| \leq r\},$$

where $\|u - v\|$ denotes the Euclidean norm of $u - v$. Since we are interested in energy consumption only, we can schedule all transmissions sequentially. Hence, we can assume that there is no interference. We assume that signals are attenuated exponentially over distance with path loss exponent α . Moreover, we assume a fixed transmission rate. Hence, in order to have correct reception of a message, we require the signal to noise ratio to be above a certain threshold, *i.e.*, to have transmit power proportional to r^α . Summarizing: The energy required to transmit one unit of information to all other nodes within range r equals cr^α , where α is the path loss exponent and c some constant. In analyzing the energy consumption of nodes, we will consider only the energy consumed by transmitting. Receiver energy consumption as well as energy consumed by processing are assumed to be negligible compared to transmitter energy consumption. In particular, note that little additional processing is required for network coding, compared to the processing that is performed in a traditional wireless protocol stack. In Section 4.6 we will analyze the influence of the assumption that processing costs and receiver energy consumption are negligible.

The traffic pattern that we consider is multiple unicast. All symbols are from the field \mathbb{F}_2 , *i.e.*, they are bits and addition corresponds to the xor operation. The source of each unicast session has a sequence of source symbols that need to be delivered to the corresponding destination. Let M be the set of unicast sessions. We call $\{V, M, r\}$ a wireless multiple unicast configuration.

We will compare energy consumption of routing and network coding. Our goal is to establish lower bounds on the maximum of the ratio of the minimum energy required by routing and network coding solutions, where the maximum is over all configurations. We will refer to this ratio as the *energy benefit of network coding*. Let $\mathcal{E}_{\text{coding}}(V, M, r)$ and $\mathcal{E}_{\text{routing}}(V, M, r)$ be the

minimum energy required for network coding and routing solutions, respectively, for a configuration $\{V, M, r\}$. The energy consumption of a coding or routing scheme is defined as the time-average of the total energy spent by all nodes in the network to deliver one symbol for each unicast session. In analyzing coding schemes we will ignore the energy consumption in an initial startup phase and consider only steady-state behavior.

Note that the energy consumption per transmission equals cr^α . Therefore, the transmission range r is an important factor in the energy consumption. Therefore, it is of particular interest to optimize the transmission range such that energy consumption is minimized. In this work we consider two different quantities: 1) B_{fixed} , denoting the energy benefit that can be obtained if the transmission range is given and fixed and 2) B_{var} , denoting the energy benefit that can be obtained if one is allowed to optimize the transmission range. Note that the transmission range can be individually optimized for the routing and network coding scenarios. More precisely, the goal of this work is to establish lower bounds on

$$B_{\text{fixed}}(d) = \max_{V, M, r} \frac{\mathcal{E}_{\text{routing}}(V, M, r)}{\mathcal{E}_{\text{coding}}(V, M, r)},$$

where the maximization is over all node locations $V \subset \mathbb{R}^d$, multiple unicast sessions M and transmission ranges r , with the transmission range equal for the routing and network coding solutions, and

$$B_{\text{var}}(d) = \max_{V, M} \frac{\min_r \mathcal{E}_{\text{routing}}(V, M, r)}{\min_r \mathcal{E}_{\text{coding}}(V, M, r)},$$

where the maximization is over all node locations $V \subset \mathbb{R}^d$ and multiple unicast sessions M , with the transmission range optimized individually for the routing and network coding solutions. If no confusion can arise, we will omit dependency on d in the notation for B_{fixed} and B_{var} .

Since in B_{fixed} , r is equal for $\mathcal{E}_{\text{routing}}$ and $\mathcal{E}_{\text{coding}}$, the energy per transmission is equal in $\mathcal{E}_{\text{routing}}$ and $\mathcal{E}_{\text{coding}}$ and the benefit is equal to the ratio of the number of transmissions required in routing and network coding solutions.

Since we are interested in energy consumption only, we can assume that all transmissions are scheduled sequentially and/or that there is no interference. All coding and routing schemes that we consider proceed in time slots

or rounds. In each time slot all nodes are allowed to transmit one or more messages. We assume that the length of the time slot is large enough to accommodate sequential transmission of all messages in that round. Coding operations will be based on messages received in previous time slots only. Finally, we assume that all nodes have complete knowledge of the network topology and the network code that is being used.

To conclude this section, we introduce here some of the notation that will be used in the remainder of the chapter. The symbol transmitted by a node $v \in V$ in time slot t is denoted by $x_t(v)$. If v transmits more than one symbol in time slot t , these will be distinguished by a superscript, giving, for instance, $x_t^1(v)$ and $x_t^2(v)$. Nodes are represented by vectors. Given vectors $u = (u_1, \dots, u_d)$ and $v = (v_1, \dots, v_d)$, let $u_k^l \triangleq (u_k, \dots, u_l)$, $(u, v) \triangleq (u_1, \dots, u_d, v_1, \dots, v_d)$ and $u^{\setminus i} \triangleq (u_1, \dots, u_{i-1}, u_{i+1}, \dots, u_d) = (u_1^{i-1}, u_{i+1}^d)$.

Unicast sessions are denoted by $m^i(u)$, with i an integer and u a vector. We will see in Sections 4.4 and 4.5 that u defines the location of the source and i the relative location of the destination, *i.e.*, the direction of the session. In some cases $m^i(u)$ will be denoted as $m^i(u_1, u_2^d)$ or similar forms. The t -th source symbol of a session $m^i(u)$ is denoted by $m_t^i(u)$. The source and destination of session $m^i(u)$ are denoted by $s^i(u)$ and $r^i(u)$ respectively.

4.3 Results

We provide lower bounds on B_{var} and B_{fixed} .

Theorem 4.1. *The ratio of the minimum energy consumption of routing solutions and the minimum energy consumption of network coding solutions, maximized over all node locations, multiple unicast sessions and transmission ranges, with the transmission range equal for the routing and network coding solutions, is at least $2d/\lfloor\sqrt{d}\rfloor$, *i.e.*,*

$$B_{\text{fixed}}(d) \geq \frac{2d}{\lfloor\sqrt{d}\rfloor}.$$

The result states that B_{fixed} is at least 2, 4 and 6 for 1, 2 and 3-dimensional networks, respectively. The result that B_{fixed} is at least 2 in one dimensional networks also follows from the results in [81]. The lower bound 4 for 2-dimensional networks exceeds the previously known bound of 2.4 [19]. This

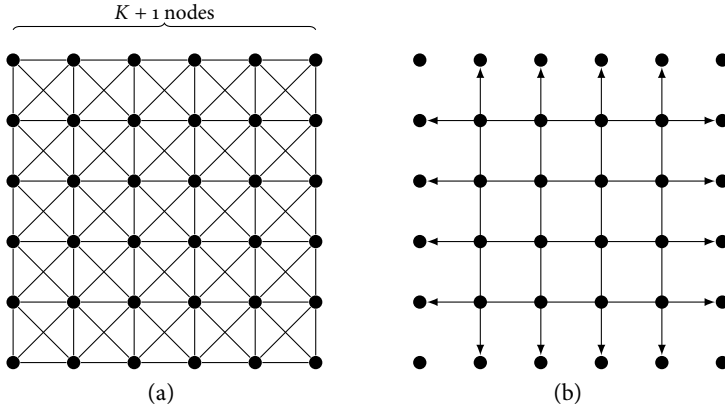


Figure 4.1: Configuration for which $\mathcal{E}_{\text{routing}}/\mathcal{E}_{\text{coding}} = 2d/\lfloor\sqrt{d}\rfloor$ is achievable, with $d = 2$ depicted here. Nodes are located at integer coordinates in a d -dimensional space, with connectivity given by $r = \sqrt{d}$, as depicted in (a). Unicast sessions are placed according to (b).

new lower bound is of particular interest, since it exceeds the upper bound of 3 for decode-and-recombine type network codes [57]. Indeed, the code that we construct does not follow a decode-and-recombine strategy. This shows that energy can be saved by considering strategies other than decode-and-recombine. No lower bounds for three dimensional networks have been previously established.

Before proving Theorem 4.1 in Section 4.5 we provide some intuition. The configuration used to prove Theorem 4.1 has nodes placed at a d -dimensional rectangular lattice, connectivity $r = \sqrt{d}$ and is parametrized by an integer K controlling the size of the network. The network is given in Figure 4.1 for $d = 2$ and $K = 5$. For $d = 2$ the result of Theorem 4.1 is obtained as follows. First consider the case of routing. Note, that the minimum-energy solution is to route all packets along the shortest path between source and destination. Therefore, all nodes in the interior of the network will need to transmit four times. Now, for the case of network coding, we will show in Section 4.5 that it is possible to construct a network code in which each node in the interior

of the network is transmitting only once in each time slot. Therefore, by considering large K and neglecting the energy consumption at the borders of the network the obtained energy benefit is 4.

In Section 4.5 we will consider the general case of arbitrary d . Again, the network coding solution will be such that each of the $K^d + O(K^{d-1})$ nodes in the interior of the network is transmitting only once in each time slot. In analyzing the routing solution some care needs to be taken. Since $r = \sqrt{d}$, the number of hops that need to be taken on the shortest path between source and destination equals $\lceil K/\lceil\sqrt{d}\rceil \rceil$. By noting that the number of sessions is roughly equal to the number of nodes at the border of the network, *i.e.*, $2dK^{d-1} + O(K^{d-2})$, and ignoring all transmission from nodes at the border of the network, we establish

$$B_{\text{fixed}}(d) \geq \lim_{K \rightarrow \infty} \frac{[2dK^{d-1} + O(K^{d-2})] \lceil K/\lceil\sqrt{d}\rceil \rceil}{K^d + O(K^{d-1})} \quad (4.1)$$

$$= \lim_{K \rightarrow \infty} \frac{2d/\lceil\sqrt{d}\rceil K^d + O(K^{d-1})}{K^d + O(K^{d-1})} \quad (4.2)$$

$$= \frac{2d}{\lceil\sqrt{d}\rceil}. \quad (4.3)$$

Details of the configuration and a proof of Theorem 4.1 are given in Section 4.5.

The configuration and network code construction used for Theorem 4.1 are not useful for obtaining bounds on B_{var} . Since, $r = \sqrt{d}$, the cost per transmission in the network coding scheme is $cd^{\alpha/2}$. One can verify, however, that the optimal transmission range under routing is $r = 1$. This requires K hops per session, with the cost per transmission equal c . Using the network code described above and the optimal routing solution at $r = 1$ gives

$$B_{\text{var}}(d) \geq \lim_{K \rightarrow \infty} \frac{cK [2dK^{d-1} + O(K^{d-2})]}{cd^{\alpha/2} [K^d + O(K^{d-1})]} \quad (4.4)$$

$$= 2d^{1-\alpha/2}, \quad (4.5)$$

which is at most 2, since $\alpha \geq 2$. Note that it was already shown in [81] that $B_{\text{var}}(1) \geq 2$ and in [19] that $B_{\text{var}}(2) \geq 2.4$.

By considering a different configuration we show that $B_{\text{var}}(2) \geq 3$.

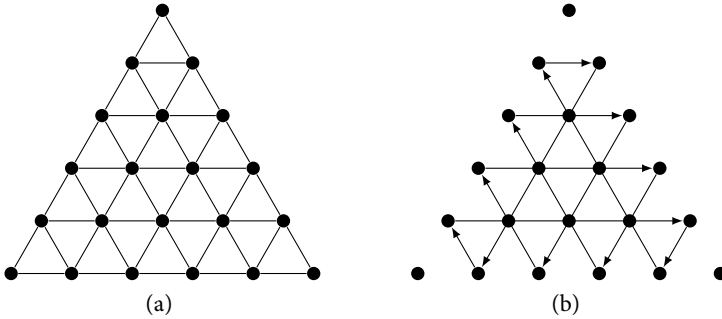


Figure 4.2: Configuration for which $\mathcal{E}_{\text{routing}}/\mathcal{E}_{\text{coding}} = 3$ is achievable. Nodes are a subset of the hexagonal lattice, with connectivity as depicted in (a). Unicast sessions are placed according to (b).

Theorem 4.2. *For 2-dimensional wireless networks, the ratio of the minimum energy consumption of routing solutions and the minimum energy consumption of network coding solutions, maximized over all node locations and multiple unicast sessions, with the transmission range optimized individually for the routing and network coding solutions, is at least 3, i.e., $B_{\text{var}}(2) \geq 3$.*

Here we provide an intuitive explanation of this result; details of the configuration and a proof of Theorem 4.2 are provided in Section 4.4. The result is established using a multiple unicast configuration on a subset of the 2-dimensional hexagonal lattice as depicted in Figure 4.2. The minimum cost routing solution on this network follows shortest paths for all sessions and will require all nodes in the interior of the network to transmit three times in order to deliver one symbol for each session. In Section 4.4 we construct a network code in which each node in the interior is only transmitting once per delivered symbol. By making the size of the network large, the influence of the borders becomes negligible. Hence, the energy benefit is 3.

Besides providing new lower bounds on the energy benefit of network, the network codes that are constructed in this chapter are of interest by themselves. They might lead to insight in how to operate in networks with another structure. Finally, even though the case $d > 3$ is not of any practical relevance, the bounds as well as the code constructions might lead to a better insight for

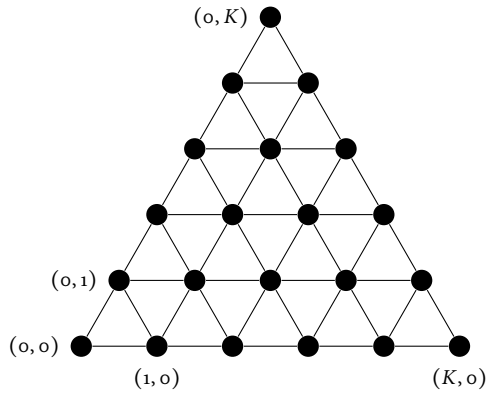


Figure 4.3: Nodes at a subset of the hexagonal lattice with the connectivity induced by a transmission range $r = 1$. The size of the network is controlled by K , with $K = 5$ in this figure.

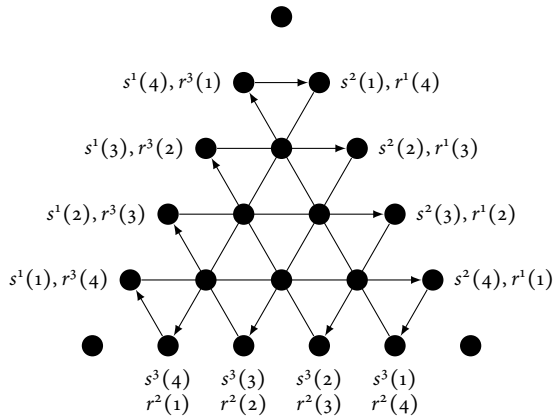


Figure 4.4: The unicast sessions on the network from Figure 4.3.

lower dimensional networks.

4.4 An Efficient Code on the Hexagonal Lattice

In this section we present a multiple unicast configuration in which the nodes form a subset of the hexagonal lattice. It will be shown that the energy benefit on this configuration is 3, proving Theorem 4.2. Since the code construction used here is less involved than the construction used to prove Theorem 4.1, we start with the proof of Theorem 4.2. This section is organized as follows. In Subsection 4.4.1 we present the configuration in more detail after which we give the construction of the network code in Subsection 4.4.2. Subsection 4.4.3 is used to prove that the code is valid. Finally, in Subsection 4.4.4 we analyze the energy consumption of the network code and prove Theorem 4.2.

4.4.1 Configuration

The size of the configuration is parametrized by a positive integer K . The nodes V form a subset of the hexagonal lattice. We index nodes with a tuple $(v_1, v_2) \in \mathbb{N}^2$. V is given by

$$V = \{(v_1, v_2) \mid v_1, v_2 \geq 0, v_1, v_2 \leq K, v_1 + v_2 \leq K\}. \quad (4.6)$$

The location of node $v \in V$ in \mathbb{R}^2 is given by vG , where

$$G = \begin{bmatrix} 1 & 0 \\ 1/2 & \sqrt{3}/2 \end{bmatrix}. \quad (4.7)$$

Let $\overset{\circ}{V}$ denote the interior of the network, *i.e.*,

$$\overset{\circ}{V} = \{v \in V \mid v_1, v_2 > 0, v_1, v_2 < K, v_1 + v_2 < K\}. \quad (4.8)$$

The transmission range that we are interested in is $r = 1$. This leads to connectivity between the six nearest neighbours. Hence, the neighbours of a node $(u_1, u_2) \in \overset{\circ}{V}$ are

$$(u_1-1, u_2+1), (u_1, u_2+1), (u_1-1, u_2), (u_1+1, u_2), (u_1, u_2-1), (u_1+1, u_2-1).$$

The nodes V and the connectivity are depicted in Figure 4.3.

There are $3(K-1)$ unicast sessions, denoted by $m^1(i)$, $m^2(i)$ and $m^3(i)$, $1 \leq i \leq K-1$. Sources and destinations of the sessions are positioned as follows

$$m^1(i) : \quad s^1(i) = (o, i), \quad r^1(i) = (K - i, i) \quad (4.9)$$

$$m^2(i) : \quad s^2(i) = (i, K - i), \quad r^2(i) = (i, o) \quad (4.10)$$

$$m^3(i) : \quad s^3(i) = (K - i, o), \quad r^3(i) = (o, K - i), \quad (4.11)$$

as depicted in Figure 4.4. Remember from Section 4.2, that session $m^j(i)$ has the sequence of source symbols $m_o^j(i), m_1^j(i), m_2^j(i), \dots$ to be transferred.

4.4.2 Network Code

The network code is such that in each time slot a new source symbol from each session is transmitted. Also, one symbol of each session is decoded by its destination in each time slot. After successfully decoding a symbol it is retransmitted by the destination in the next time slot. Nodes at the border will, therefore, transmit twice in each time slot. Nodes in the interior of the network transmit only once. The symbol that they transmit is a linear combination of one symbol from each of the sessions for which the shortest path between source and destination includes that node.

The operation of the network code is demonstrated in Figure 4.5 in which the transmissions of all nodes in the first four time slots are depicted. Different transmissions by the same node are separated by a comma. Note, moreover, that there is a startup phase, time slots 0 to 2, in which not all destinations are able to decode a symbol. From time slot 3 onwards all destinations decode one symbol in every time slot. In analyzing the energy consumption of the coding scheme, we will ignore the startup phase.

The symbol transmitted at $t = 3$ by the node with the dotted border can be obtained by summing all transmissions from nodes with a dashed border in earlier time slots. Indeed

$$\begin{aligned} m_1^1(3) + m_1^2(2) + m_o^1(1) + m_o^3(2) + m_2^2(1) + m_1^1(3) + m_2^1(2) \\ + m_o^3(2) + m_o^1(1) + m_1^2(2) + m_1^3(1) = m_2^1(2) + m_2^2(1) + m_1^3(1). \end{aligned} \quad (4.12)$$

This coding operation (*i.e.*, in time slot t a node transmits the sum of what was transmitted by its top-left neighbour in time slot $t - 2$, by its top right-neighbour in time slot $t - 1$, etc., as visualized in Figure 4.5) is performed by all nodes that are in the interior of the network. The idea behind the coding operation is to cancel, by means of the XOR operation, all symbols that should not be retransmitted. In (4.12), for instance, we have $m_1^1(3) + m_1^1(3) = 0$. The exact operation of the network code is made more precise in the remainder of this subsection. The coding operation for interior nodes is given in exact form in (4.17).

Nodes at the border of the network operate as follows. Let $0 < u_2 < K$. In time slot t node (o, u_2) transmits two symbols $x_t^1(o, u_2)$ and $x_t^3(o, u_2)$, where

$$\text{Left border: } \boxed{\begin{aligned} x_t^1(o, u_2) &= m_t^1(u_2), \\ x_t^3(o, u_2) &= m_{t-u_2}^3(K - u_2). \end{aligned}} \quad (4.13)$$

Since (o, u_2) is the source of session $m^1(u_2)$ it has source symbol $m_t^1(u_2)$ available. Also, (o, u_2) is the destination for session $m^3(K - u_2)$. It remains to be shown that symbol $m_{t-u_2}^3(K - u_2)$ can be decoded by (o, u_2) using the information obtained from its neighbours up to time slot t . For notational convenience let

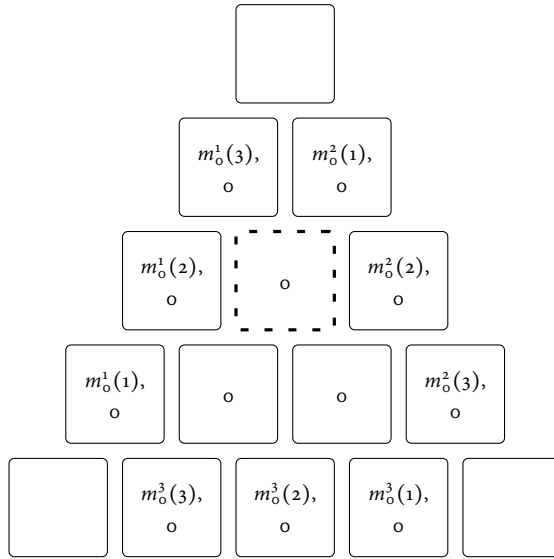
$$\text{Left border: } \boxed{x_t(o, u_2) \triangleq x_t^1(o, u_2) + x_t^3(o, u_2)}. \quad (4.14)$$

In similar fashion we have the following transmissions at the right and bottom borders of the network

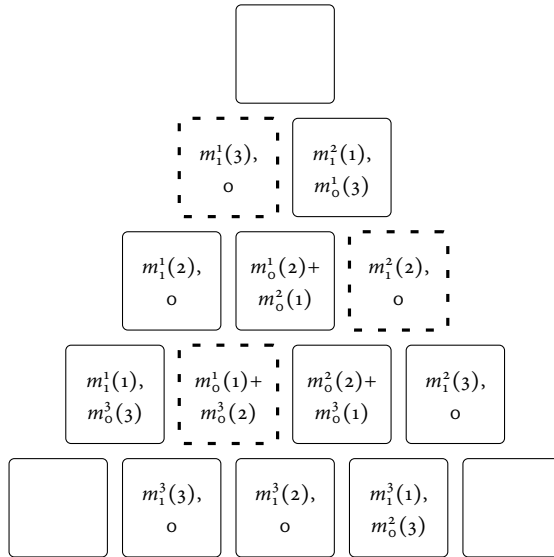
$$\text{Right border: } \boxed{\begin{aligned} x_t^1(v_1, v_2) &= m_{t-v_1}^1(v_2), \\ x_t^2(v_1, v_2) &= m_t^2(v_1), \\ x_t(v_1, v_2) &\triangleq x_t^1(v_1, v_2) + x_t^2(v_1, v_2), \end{aligned}} \quad (4.15)$$

$$\text{Bottom border: } \boxed{\begin{aligned} x_t^2(u_1, o) &= m_{t-K+u_1}^2(u_1), \\ x_t^3(u_1, o) &= m_t^3(K - u_1), \\ x_t(u_1, o) &\triangleq x_t^2(u_1, o) + x_t^3(u_1, o), \end{aligned}} \quad (4.16)$$

where $u_1, v_1, v_2 > 0$, $u_1, v_1, v_2 < K$ and $v_1 + v_2 = K$. Moreover, $x_t(v_1, v_2)$ and $x_t(u_1, o)$ are not symbols that are transmitted, but only notational shortcuts.

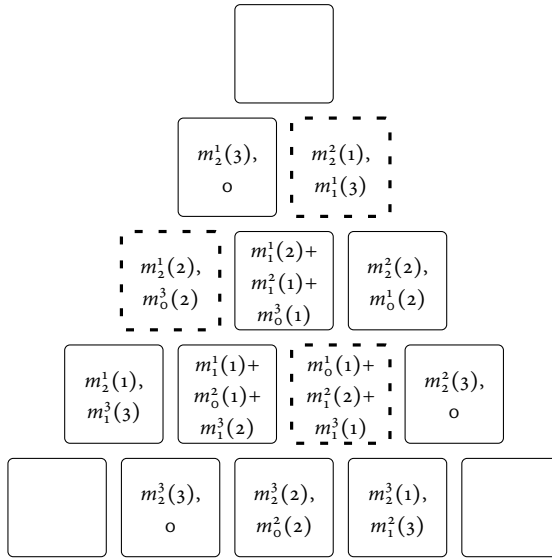


(a) $t = 0$

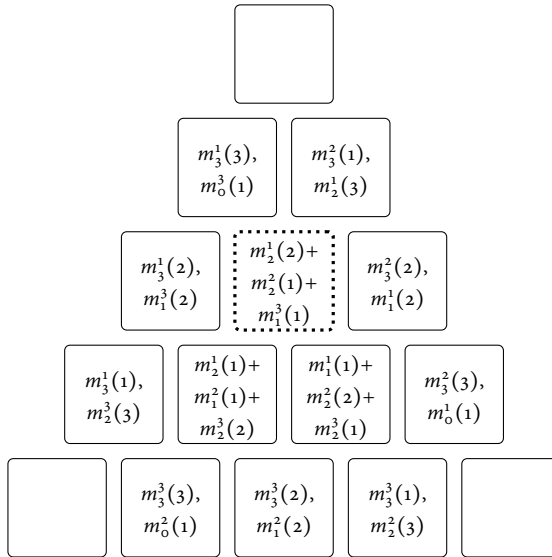


(b) $t = 1$

Figure 4.5: Example operation of the network code of Section 4.4, with $K = 4$. The transmissions of all nodes in the time slots $0, \dots, 3$ are depicted. Different transmissions by the same node are separated by a comma.



(c) $t = 2$



(d) $t = 3$

Figure 4.5: (Cont'd) The symbol transmitted at $t = 3$ by the node with dotted border can be obtained by summing all transmissions from nodes with a dashed border in earlier time slots.

Nodes in the interior of the network transmit once in each time slot. Let $(u_1, u_2) \in \overset{\circ}{V}$. The coding operation it performs is given by

$$\begin{aligned}
 x_t(u_1, u_2) &= x_{t-1}(u_1 - 1, u_2) \\
 &\quad + x_{t-2}(u_1 - 1, u_2 + 1) + x_{t-1}(u_1, u_2 + 1) \\
 &\quad + x_{t-3}(u_1, u_2) + x_{t-2}(u_1 + 1, u_2) \\
 &\quad + x_{t-2}(u_1, u_2 - 1) + x_{t-1}(u_1 + 1, u_2 - 1).
 \end{aligned} \tag{4.17}$$

4.4.3 Validity of the Network Code

We need to show that destinations can decode in time in order to retransmit the required symbols according to (4.13), (4.15) and (4.16). In order to do so we first analyze how data propagates through the network. If we look at the nodes in the network that transmit linear combinations that contain a certain source symbol, we see that symbols propagate exactly along the shortest paths between source and destination. This is made more precise in the following two lemmas.

Lemma 4.3. *Let $0 < u_2 < K$. Assume that the only non-zero source symbol transmitted in the network is $m_0^1(u_2)$ by node $(0, u_2)$ in time slot 0. Then, for all $t \geq 0$ and $(v_1, v_2) \in \overset{\circ}{V}$*

$$x_t(v_1, v_2) = \begin{cases} m_0^1(u_2), & \text{if } v_1 = t, v_2 = u_2, \\ 0, & \text{otherwise.} \end{cases} \tag{4.18}$$

Proof. We use induction over time. The base case is time slot $t = 0$, for which it is readily verified that the statement is true. Now, for the induction step suppose that the lemma holds for all t' smaller than t . This implies that for all $\tau > 0$ and $(v_1, v_2) \in \overset{\circ}{V}$,

$$x_{t-\tau}(v_1, v_2) = x_{t-\tau-1}(v_1 - 1, v_2). \tag{4.19}$$

Hence,

$$\begin{aligned}
x_t(v_1, v_2) &= x_{t-1}(v_1 - 1, v_2) + x_{t-2}(v_1 - 1, v_2 + 1) + x_{t-1}(v_1, v_2 + 1) \\
&\quad + x_{t-3}(v_1, v_2) + x_{t-2}(v_1 + 1, v_2) \\
&\quad + x_{t-2}(v_1, v_2 - 1) + x_{t-1}(v_1 + 1, v_2 - 1) \\
&= x_{t-1}(v_1 - 1, v_2) + x_{t-2}(v_1 - 1, v_2 + 1) + x_{t-2}(v_1 - 1, v_2 + 1) \\
&\quad + x_{t-3}(v_1, v_2) + x_{t-3}(v_1, v_2) \\
&\quad + x_{t-2}(v_1, v_2 - 1) + x_{t-2}(v_1, v_2 - 1) \\
&= x_{t-1}(v_1 - 1, v_2), \tag{4.20}
\end{aligned}$$

which by the induction hypothesis is equal to $m_0^1(u_2)$ if $v_1 = t$ and $v_2 = u_2$ and zero otherwise. \square

Lemma 4.4. *Let $(u_1, u_2) \in \overset{\circ}{V}$. We have*

$$x_t(u_1, u_2) = m_{t-u_1}^1(u_2) + m_{t-K+u_1+u_2}^2(u_1) + m_{t-u_2}^3(K - u_1 - u_2).$$

Proof. From Lemma 4.3, the time-invariance of the system, and the symmetry of the coding operation (4.17) of the internal nodes. \square

We are now ready to prove that the destinations can correctly decode source symbols. We present the decoding procedure for nodes on the right border of the network. The decoding procedures at the other borders can be obtained by exploiting the symmetry of the system.

Lemma 4.5. *Consider (u_1, u_2) , with $u_1 + u_2 = K$, $0 < u_2 < K$, i.e., the destination of session $m^1(u_2)$. It can decode symbol $m_{t-u_1}^1(u_2)$ at the end of time slot $t - 1$ as*

$$\begin{aligned}
&x_{t-2}^2(u_1 - 1, u_2 + 1) + x_{t-1}(u_1 - 1, u_2) + x_{t-3}^2(u_1, u_2) \\
&\quad + x_{t-2}(u_1, u_2 - 1) + x_{t-1}^1(u_1 + 1, u_2 - 1). \tag{4.21}
\end{aligned}$$

Proof. From Lemma 4.4 and (4.15) it follows that (4.21) equals

$$\begin{aligned}
&m_{t-u_1}^1(u_2) + m_{t-u_1-2}^1(u_2 - 1) + m_{t-u_1-2}^1(u_2 - 1) \\
&\quad + m_{t-2}^2(u_1 - 1) + m_{t-2}^2(u_1 - 1) + m_{t-3}^2(u_1) + m_{t-3}^2(u_1) \\
&\quad + m_{t-u_2-1}^3(1) + m_{t-u_2-1}^3(1) = m_{t-u_1}^1(u_2). \quad \square
\end{aligned}$$

4.4.4 Energy Consumption

The energy consumption of the network coding scheme presented above is given in the following lemma.

Lemma 4.6. $\min_r \mathcal{E}_{\text{coding}}(V, M, r) \leq \mathcal{E}_{\text{coding}}(V, M, 1) \leq \frac{c}{2}K^2 + O(K)$.

Proof. From (4.13)–(4.17) we have that each of the $3(K-1)$ nodes at the border that are source or destination are transmitting twice in each time slot. Each of the $(K-1)(K-2)/2$ internal nodes is transmitting once in each time slot. Since $r = 1$, the energy consumption per transmission is c . This gives

$$\mathcal{E}_{\text{coding}}(V, M, 1) \leq 6c(K-1) + c(K-1)(K-2)/2 = \frac{c}{2}K^2 + O(K). \quad \square$$

Next, we give the minimum energy required by a routing solution.

Lemma 4.7. $\min_r \mathcal{E}_{\text{routing}}(V, M, r) = \mathcal{E}_{\text{routing}}(V, M, 1) = \frac{3c}{2}K^2 + O(K)$.

Proof. Since we consider routing we need to take the shortest path for each session. Since the energy consumption per hop equals cr^α , the energy consumption under routing is minimized for $r = 1$. Now, we see that the number of transmissions required to deliver a symbol for the sessions $\{m^1(k)\}_{k=1}^{K-1}$ equals $K(K-1)/2$. Adding the transmissions for sessions of type 2 and 3 gives

$$\mathcal{E}_{\text{routing}}(V, M, 1) = \frac{3c}{2}K(K-1) = \frac{3c}{2}K^2 + O(K). \quad \square$$

Using the above two lemmas we are able to prove Theorem 4.2.

Proof of Theorem 4.2. Remember, that B_{var} is defined as the maximum of

$$\frac{\min_r \mathcal{E}_{\text{routing}}(V, M, r)}{\min_r \mathcal{E}_{\text{coding}}(V, M, r)}$$

over V and M . Hence, $\min_r \mathcal{E}_{\text{routing}}(V, M, r) / \min_r \mathcal{E}_{\text{coding}}(V, M, r)$ for any specific V and M will provide a lower bound to B_{var} .

In addition, any upper bound to $\min_r \mathcal{E}_{\text{coding}}(V, M, r)$ will result in a lower bound to B_{var} . Hence, from Lemmas 4.6 and 4.7 we have

$$\begin{aligned}
 B_{\text{var}}(2) &\geq \lim_{K \rightarrow \infty} \frac{\min_r \mathcal{E}_{\text{routing}}(V, M, r)}{\min_r \mathcal{E}_{\text{coding}}(V, M, r)} \\
 &\geq \lim_{K \rightarrow \infty} \frac{\mathcal{E}_{\text{routing}}(V, M, 1)}{\mathcal{E}_{\text{coding}}(V, M, 1)} \\
 &\geq \lim_{K \rightarrow \infty} \frac{\frac{3\epsilon}{2}K^2 + O(K)}{\frac{\epsilon}{2}K^2 + O(K)} \\
 &= 3. \quad \square
 \end{aligned}$$

4.5 An Efficient Code on the Rectangular Lattice

In this section we present a multiple unicast configuration in which the nodes are placed at integer coordinates in a d -dimensional space, *i.e.*, at the rectangular lattice.

4.5.1 Configuration

The size of the configuration is parametrized by a positive integer K . We have

$$V = \{(v_1, \dots, v_d) \mid 0 \leq v_i \leq K, i = 1, \dots, d\}. \quad (4.22)$$

The interior of the network is given by

$$\overset{\circ}{V} = \{v \in V \mid 0 < v_i < K, i = 1, \dots, d\}. \quad (4.23)$$

We will make us of

$$\tilde{V} = \{v \in V \mid \exists \text{ unique } i : v_i \in \{0, K\}\}, \quad (4.24)$$

which corresponds to those nodes that are part of exactly one face of the network.

The transmission range that will be used is $r = \sqrt{d}$. This transmission range induces a neighbourhood consisting of all neighbours within distance

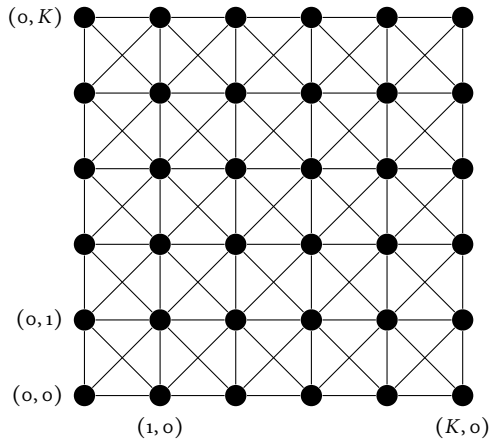


Figure 4.6: Nodes at a subset of the d -dimensional rectangular lattice, $d = 2$ depicted in the figure, with the connectivity induced by a transmission range $r = \sqrt{d}$. The size of the network is controlled by K , with $K = 5$ in this figure.

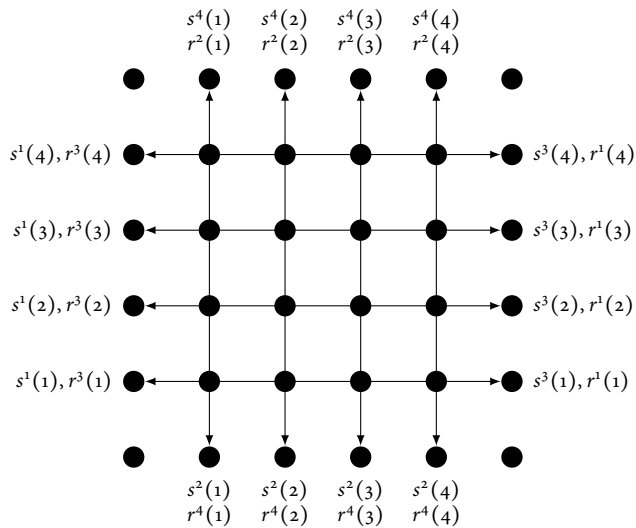


Figure 4.7: The unicast sessions on the network from Figure 4.6.

\sqrt{d} . The coding operation of our network code is based on only part of the neighbourhood, *i.e.*, it uses

$$N_v = \{u \in V \mid |u_i - v_i| \leq 1 \forall i, u \neq v\}. \quad (4.25)$$

Note, that for $d \leq 3$, N_v corresponds to the complete neighbourhood of v . We will be using $\text{dist}(u, v) \triangleq \|u - v\|_1 = \sum_{i=1}^d |u_i - v_i|$, *i.e.*, $\text{dist}(u, v)$ denotes the Manhattan distance from u to v . The network and its connectivity are depicted for $d = 2$ in Figure 4.6.

A source is located at each $v \in \bar{V}$. Therefore, there are $|\bar{V}| = 2d(K - 1)^{d-1}$ sessions. If $v_i = 0$, we denote the session corresponding to this source by $m^i(v^{\setminus i})$. Recall from Section 4.2 that $v^{\setminus i}$ denotes the $d - 1$ dimensional vector obtained by removing the i -th element from v . If $v_i = K$, we denote the session by $m^{d+i}(v^{\setminus i})$. The destination of each session is located at the other side of the network, *i.e.*, we have $r^i(v^{\setminus i}) = s^{d+i}(v^{\setminus i})$ and $r^{d+i}(v^{\setminus i}) = s^i(v^{\setminus i})$. The positions of sources and destinations are depicted for $d = 2$ in Figure 4.7. It can be seen that $m^i(v^{\setminus i})$ and $m^{d+i}(v^{\setminus i})$ form oppositely directed sessions.

4.5.2 Network code

We introduce sets $\Theta_\delta \subset \{1, \dots, 2d\}$, $0 \leq \delta \leq d$, which are defined recursively as follows

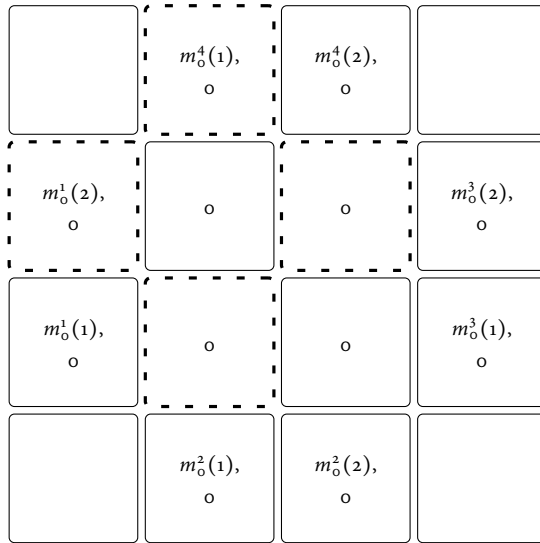
$$\Theta_d = \{d\}, \quad (4.26)$$

$$\Theta_\delta = (\Theta_{\delta+1} - 1) \Delta (\Theta_{\delta+1} + 1), \quad 0 < \delta < d, \quad (4.27)$$

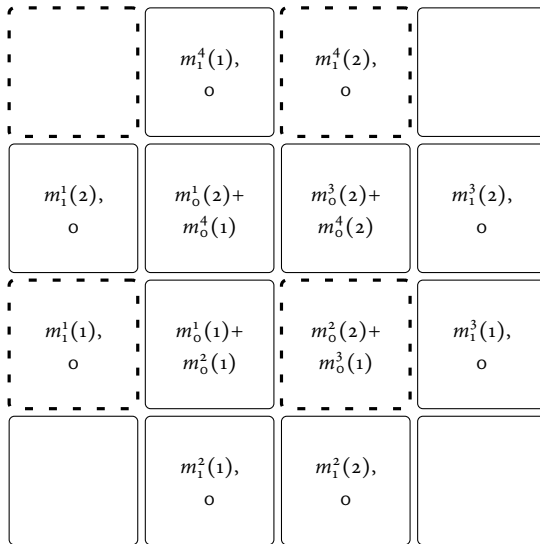
$$\Theta_0 = ((\Theta_1 - 1) \Delta (\Theta_1 + 1)) \setminus \{0\}, \quad (4.28)$$

where Δ denotes symmetric difference and $\Theta_\delta \pm 1 = \{\tau \pm 1 \mid \tau \in \Theta_\delta\}$. Note, that irrespective of d we have $1 \in \Theta_1$. As an example for $d = 2$ we have $\Theta_2 = \{2\}$, $\Theta_1 = \{1, 3\}$ and $\Theta_0 = \{4\}$.

The scheme is very similar in flavour to the scheme presented in Section 4.4, its operation is demonstrated in Figure 4.8 in which, for $d = 2$ and $K = 3$, the transmissions of all nodes in the first four time slots are depicted. The operation of the scheme is such that in time slot t sources transmit the t -th source symbol and destinations decode the $(t - K)$ -th source symbol. Besides transmitting a new source symbol in each time slot, sources/destinations

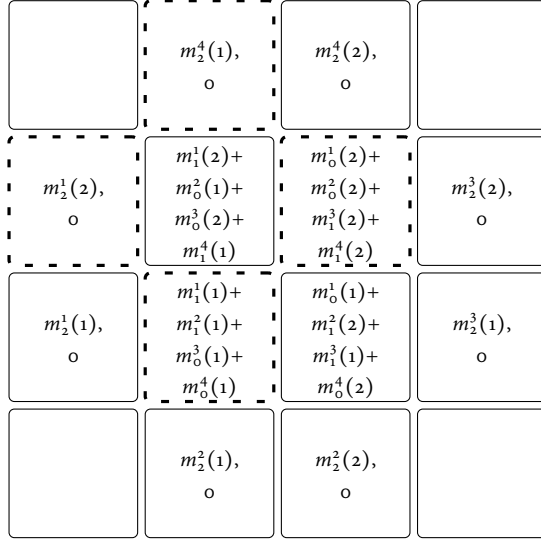


(a) $t = 0$

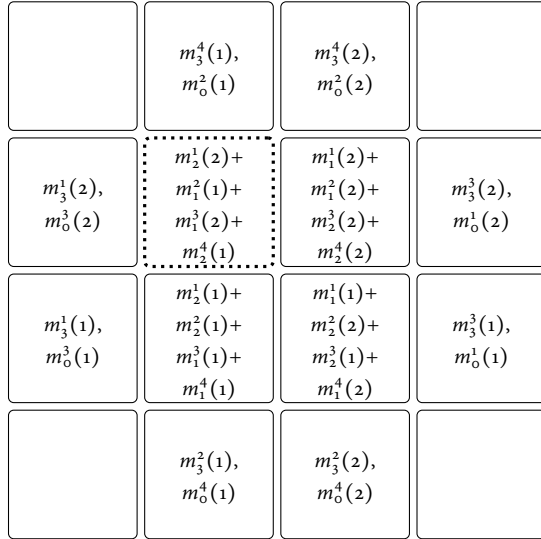


(b) $t = 1$

Figure 4.8: Example operation of the network code of Section 4.5, with $K = 3$. The transmissions of all nodes in the time slots $0, \dots, 3$ are depicted. Different transmissions by the same node are separated by a comma.



(c) $t = 2$



(d) $t = 3$

Figure 4.8: (Cont'd) The symbol transmitted at $t = 3$ by the node with dotted border can be obtained by summing all transmissions from nodes with a dashed border in earlier time slots.

will also retransmit the symbol that has been decoded in that time slot, *i.e.*, they transmit two different symbols in each time slot. In the figure, different transmissions by the same node are separated by a comma. Nodes in the interior of the network transmit only once. The symbol that they transmit is a linear combination of one symbol from each of the sessions for which the shortest path between source and destination includes that node. The symbol transmitted at $t = 3$ by the node with the dotted border can be obtained by summing all transmissions from nodes with a dashed border in earlier time slots. This coding operation is performed by all nodes that are in the interior of the network. The exact operation of the network code is made more precise in the remainder of this subsection. The coding operation for interior nodes is given in exact form in (4.32).

Let node $v \in \bar{V}$. Remember, that $v \in \bar{V}$ implies that there exists a unique i such that $v_i \in \{0, K\}$. Node v transmits

$$x_t^i(v) = m_{t-v_i}^i(v^i) \quad (4.29)$$

and

$$x_t^{d+i}(v) = m_{t-K+v_i}^{d+i}(v^i). \quad (4.30)$$

For notational convenience, let

$$x_t(v) \triangleq x_t^i(v) + x_t^{d+i}(v). \quad (4.31)$$

The coding operation performed by an internal node is as follows

$$x_t(v) = \sum_{u \in N_v \cup \{v\}} \sum_{\tau \in \Theta_{\text{dist}(u,v)}} x_{t-\tau}(u). \quad (4.32)$$

4.5.3 Validity of the Network Code

The following result follows directly from the definition of the sets Θ_δ , but is stated here as a lemma because of its importance in the remainder of the chapter.

Lemma 4.8. Let $\{x_t\}$ be a sequence of symbols from \mathbb{F}_2 and let $0 < \delta < d$. We have

$$\sum_{\tau \in \Theta_\delta} x_{t-\tau} = \sum_{\tau \in \Theta_{\delta+1}} [x_{t-\tau+1} + x_{t-\tau-1}], \quad (4.33)$$

$$\sum_{\tau \in \Theta_0} x_{t-\tau} = \sum_{\tau \in \Theta_1 \setminus \{1\}} x_{t-\tau+1} + \sum_{\tau \in \Theta_1} x_{t-\tau-1}. \quad (4.34)$$

Lemma 4.9. Consider node $(o, u_2^d) \in \bar{V}$. Assume that the only non-zero source symbol transmitted in the network is $m_o^1(u_2^d)$ by node (o, u_2^d) in time slot o . Then

$$x_t(v) = \begin{cases} m_o^1(u_2^d), & \text{if } v_1 = t, v_2^d = u_2^d, \\ 0, & \text{otherwise,} \end{cases} \quad (4.35)$$

for all $v \in V$ and $t \geq o$.

Proof. We use induction over t . At time $t = o$ the lemma holds, giving us our base case. Now suppose that the lemma holds for all time slots smaller than t . If $v \in \bar{V}$ the lemma follows directly from (4.29)–(4.31). In the remainder we consider $u \in \overset{\circ}{V}$. From the induction hypothesis it follows that for any $t' < t$

$$x_{t'}(u) = x_{t'-1}(u_1 - 1, u_2^d). \quad (4.36)$$

If $u_1 = K - 1$, it follows from (4.29) and the induction hypothesis that

$$x_{t'-1}(u) = x_{t'}(u_1 + 1, u_2^d). \quad (4.37)$$

Now, at t the coding operation performed by u can be decomposed as

$$x_t(u) = \sum_{w \in N_u \cup \{v\}} \sum_{\tau \in \Theta_{\text{dist}(w,u)}} x_{t-\tau}(w) = \sum_{\substack{w \in N_u: \\ w_1 = u_1}} g(w),$$

where

$$\begin{aligned} g(w) = & \sum_{\tau \in \Theta_{\text{dist}(w,u)+1}} x_{t-\tau}(w_1 - 1, w_2^d) \\ & + \sum_{\tau \in \Theta_{\text{dist}(w,u)}} x_{t-\tau}(w) + \sum_{\tau \in \Theta_{\text{dist}(w,u)+1}} x_{t-\tau}(w_1 + 1, w_2^d). \end{aligned} \quad (4.38)$$

In the remainder we show that

$$g(w) = \begin{cases} x_{t-1}(w_1 - 1, w_2^d), & \text{if } w = u \\ 0, & \text{otherwise,} \end{cases} \quad (4.39)$$

which proves the lemma, since by the induction hypothesis $x_{t-1}(u_1 - 1, u_2^d) = m_0^1(u_2^d)$ if $u_1 = t$ and zero otherwise.

For $w \neq u$ we have

$$\begin{aligned} g(w) &= \sum_{\tau \in \Theta_{\text{dist}(w,u)+1}} x_{t-\tau}(w_1 - 1, w_2^d) + \sum_{\tau \in \Theta_{\text{dist}(w,u)}} x_{t-\tau}(w) \\ &\quad + \sum_{\tau \in \Theta_{\text{dist}(w,u)+1}} x_{t-\tau}(w_1 + 1, w_2^d) \\ &= \sum_{\tau \in \Theta_{\text{dist}(w,u)+1}} x_{t-\tau}(w_1 - 1, w_2^d) + \sum_{\tau \in \Theta_{\text{dist}(w,u)+1}} x_{t-\tau+1}(w) \\ &\quad + \sum_{\tau \in \Theta_{\text{dist}(w,u)+1}} x_{t-\tau-1}(w) + \sum_{\tau \in \Theta_{\text{dist}(w,u)+1}} x_{t-\tau}(w_1 + 1, w_2^d) \\ &= \sum_{\tau \in \Theta_{\text{dist}(w,u)+1}} x_{t-\tau}(w_1 - 1, w_2^d) + \sum_{\tau \in \Theta_{\text{dist}(w,u)+1}} x_{t-\tau}(w_1 - 1, w_2^d) \\ &\quad + \sum_{\tau \in \Theta_{\text{dist}(w,u)+1}} x_{t-\tau}(w_1 + 1, w_2^d) + \sum_{\tau \in \Theta_{\text{dist}(w,u)+1}} x_{t-\tau}(w_1 + 1, w_2^d) \\ &= 0, \end{aligned}$$

where the second equality follows from Lemma 4.8, the third equality follows from (4.36)–(4.37) and the last equality holds because we work over \mathbb{F}_2 .

For $w = u$ we have

$$\begin{aligned} g(u) &= \sum_{\tau \in \Theta_1} x_{t-\tau}(u_1 - 1, u_2^d) + \sum_{\tau \in \Theta_0} x_{t-\tau}(u) \\ &\quad + \sum_{\tau \in \Theta_1} x_{t-\tau}(u_1 + 1, u_2^d) \\ &= \sum_{\tau \in \Theta_1} x_{t-\tau}(u_1 - 1, u_2^d) + \sum_{\tau \in \Theta_1 \setminus \{1\}} x_{t-\tau+1}(u) \\ &\quad + \sum_{\tau \in \Theta_1} x_{t-\tau-1}(u) + \sum_{\tau \in \Theta_1} x_{t-\tau}(u_1 + 1, u_2^d) \end{aligned}$$

$$\begin{aligned}
&= \sum_{\tau \in \Theta_1} x_{t-\tau}(u_1 - 1, u_2^d) + \sum_{\tau \in \Theta_1 \setminus \{1\}} x_{t-\tau}(u_1 - 1, u_2^d) \\
&\quad + \sum_{\tau \in \Theta_1} x_{t-\tau}(u_1 + 1, u_2^d) + \sum_{\tau \in \Theta_1} x_{t-\tau}(u_1 + 1, u_2^d) \\
&= x_{t-1}(u_1 - 1, u_2^d). \quad \square
\end{aligned}$$

Lemma 4.10. Let $u \in \overset{\circ}{V}$

$$x_t(u) = \sum_{i=1}^d \left[m_{t-u_i}^i(u^i) + m_{t-K+u_i}^{d+i}(u^i) \right]. \quad (4.40)$$

Proof. By linearity, time-invariance and symmetry of (4.32) together with Lemma 4.9. \square

We are now ready to prove that the destinations can correctly decode source symbols. We present the decoding procedure for nodes on the right border of the network, *i.e.*, for nodes of type $(K, u_2^d) \in \bar{V}$. The decoding procedures at the other borders can be obtained by exploiting the symmetry of the system.

Lemma 4.11. Consider node $u = (K, u_2^d) \in \bar{V}$. At the end of time slot $t - 1$ it can decode symbol $m_{t-K}^1(u_2^d)$ as

$$\begin{aligned}
&\sum_{\substack{v \in N_u: \\ v_1 < K}} \sum_{\tau \in \Theta_{\text{dist}(u,v)}} x_{t-\tau}(v) + \sum_{\substack{v \in N_u: \\ v_1 = K}} \sum_{\tau \in \Theta_{\text{dist}(u,v)+1}} [x_{t-\tau+1}^1(v) + x_{t-\tau-1}^{d+1}(v)] \\
&\quad + \sum_{\tau \in \Theta_1 \setminus \{1\}} x_{t-\tau+1}^1(u) + \sum_{\tau \in \Theta_1} x_{t-\tau-1}^{d+1}(u). \quad (4.41)
\end{aligned}$$

Proof. First note that all terms in (4.41) correspond to symbols that have been received by (K, u_2^d) before or in time slot $t - 1$.

Now, from Lemma 4.10 we have

$$\begin{aligned}
& \sum_{\substack{v \in N_u: \\ v_1 < K}} \sum_{\tau \in \Theta_{\text{dist}(u,v)}} x_{t-\tau}(v) \\
&= \sum_{\substack{v \in N_u: \\ v_1 < K}} \sum_{\tau \in \Theta_{\text{dist}(u,v)}} \sum_{i=1}^d [m_{t-v_i-\tau}^i(v^i) + m_{t-K+v_i-\tau}^{d+i}(v^i)] \\
&= \sum_{\substack{v \in N_u: \\ v_1 < K}} \sum_{\tau \in \Theta_{\text{dist}(u,v)}} [m_{t-v_1-\tau}^1(v^1) + m_{t-K+v_1-\tau}^{d+1}(v^1)] \\
&\quad + \sum_{i=2}^d \left[\sum_{\substack{v \in N_u: \\ v_1 < K, v_i = u_i}} \left[\sum_{\tau \in \Theta_{\text{dist}(u,v)+1}} m_{t-v_i+1-\tau}^i(v^i) \right. \right. \\
&\quad + \sum_{\tau \in \Theta_{\text{dist}(u,v)}} m_{t-v_i-\tau}^i(v^i) + \sum_{\tau \in \Theta_{\text{dist}(u,v)+1}} m_{t-v_i-1-\tau}^i(v^i) \\
&\quad + \sum_{\tau \in \Theta_{\text{dist}(u,v)+1}} m_{t-v_i+1-\tau}^{d+i}(v^i) + \sum_{\tau \in \Theta_{\text{dist}(u,v)}} m_{t-v_i-\tau}^{d+i}(v^i) \\
&\quad \left. \left. + \sum_{\tau \in \Theta_{\text{dist}(u,v)+1}} m_{t-v_i-1-\tau}^{d+i}(v^i) \right] \right] \\
&\stackrel{(a)}{=} \sum_{\substack{v \in N_u: \\ v_1 < K}} \sum_{\tau \in \Theta_{\text{dist}(u,v)}} [m_{t-v_1-\tau}^1(v^1) + m_{t-K+v_1-\tau}^{d+1}(v^1)] \\
&= \sum_{\tau \in \Theta_1} [m_{t-K+1-\tau}^1(u^1) + m_{t-1-\tau}^{d+1}(u^1)] \\
&\quad + \sum_{\substack{v \in N_u: \\ v_1 = K}} \sum_{\tau \in \Theta_{\text{dist}(u,v)+1}} [m_{t-K+1-\tau}^1(v^1) + m_{t-1-\tau}^{d+1}(v^1)] \quad (4.42)
\end{aligned}$$

where (a) holds, because for $\text{dist}(u, v) > 0$ Lemma 4.8 gives

$$\begin{aligned}
& \sum_{\tau \in \Theta_{\text{dist}(u,v)+1}} m_{t-v_i+1-\tau}^i(v^i) + \sum_{\tau \in \Theta_{\text{dist}(u,v)}} m_{t-v_i-\tau}^i(v^i) \\
&\quad + \sum_{\tau \in \Theta_{\text{dist}(u,v)+1}} m_{t-v_i-1-\tau}^i(v^i) = 0
\end{aligned}$$

and

$$\sum_{\tau \in \Theta_{\text{dist}(u,v)+1}} m_{t-v_i+1-\tau}^{d+i}(v^{\setminus i}) + \sum_{\tau \in \Theta_{\text{dist}(u,v)}} m_{t-v_i-\tau}^{d+i}(v^{\setminus i}) + \sum_{\tau \in \Theta_{\text{dist}(u,v)+1}} m_{t-v_i-1-\tau}^{d+i}(v^{\setminus i}) = 0.$$

From (4.29) and (4.30) it follows that

$$\begin{aligned} \sum_{\substack{v \in N_u: \\ v_1=K}} \sum_{\tau \in \Theta_{\text{dist}(u,v)+1}} [x_{t-\tau+1}^1(v) + x_{t-\tau-1}^{d+1}(v)] \\ = \sum_{\substack{v \in N_u: \\ v_1=K}} \sum_{\tau \in \Theta_{\text{dist}(u,v)+1}} [m_{t-K+1-\tau}^1(v^{\setminus 1}) + m_{t-1-\tau}^{d+1}(v^{\setminus 1})] \quad (4.43) \end{aligned}$$

and

$$\begin{aligned} \sum_{\tau \in \Theta_1 \setminus \{1\}} x_{t-\tau+1}^1(u) + \sum_{\tau \in \Theta_1} x_{t-\tau-1}^{d+1}(u) \\ = \sum_{\tau \in \Theta_1 \setminus \{1\}} m_{t-K+1-\tau}^1(u^{\setminus 1}) + \sum_{\tau \in \Theta_1} m_{t-1-\tau}^{d+1}(u^{\setminus 1}). \quad (4.44) \end{aligned}$$

The proof of the lemma follows by adding the final expressions from (4.42), (4.43) and (4.44) and observing that the outcome is $m_{t-K}^1(u_2^d)$. \square

4.5.4 Energy Consumption

The energy consumption of the network coding scheme presented above provides an upper bound to $\min_r \mathcal{E}_{\text{coding}}(V, M, r)$.

Lemma 4.12. $\mathcal{E}_{\text{coding}}(V, M, \sqrt{d}) \leq 4cd^{1+\alpha/2}(K-1)^{d-1} + cd^{\alpha/2}(K-1)^d$.

Proof. All transmissions are over distance \sqrt{d} and cost $cd^{\alpha/2}$. The nodes in \bar{V} are transmitting twice. On each of the $2d$ sides of the network there are $(K-1)^{d-1}$ nodes from \bar{V} , hence $|\bar{V}| = 2d(K-1)^{d-1}$. This gives $2|\bar{V}| = 4d(K-1)^{d-1}$ transmissions. In addition, there are $(K-1)^d$ nodes in the interior, that are all transmitting once. \square

Next, we give the minimum energy required by a routing solution.

Lemma 4.13. $\mathcal{E}_{\text{routing}}(V, M, \sqrt{d}) = 2cd^{1+\alpha/2} \lceil K/\lfloor \sqrt{d} \rfloor \rceil (K-1)^{d-1}$.

Proof. Since, the transmission range is equal to \sqrt{d} , a routing solution requires $\lceil K/\lfloor \sqrt{d} \rfloor \rceil$ transmissions per session. Moreover, there are $|\tilde{V}| = 2d(K-1)^{d-1}$ sessions. \square

Using the above two lemmas we are able to prove Theorem 4.1.

Proof of Theorem 4.1. Lemmas 4.12 and 4.13 give

$$\begin{aligned} B_{\text{fixed}}(d) &\geq \lim_{K \rightarrow \infty} \frac{\mathcal{E}_{\text{routing}}(V, M, \sqrt{d})}{\mathcal{E}_{\text{coding}}(V, M, \sqrt{d})} \\ &\geq \lim_{K \rightarrow \infty} \frac{2cd^{1+\alpha/2} \lceil K/\lfloor \sqrt{d} \rfloor \rceil (K-1)^{d-1}}{cd^{\alpha/2} [4d(K-1)^{d-1} + (K-1)^d]} \\ &= \frac{2d}{\lfloor \sqrt{d} \rfloor}. \end{aligned} \quad \square$$

4.6 Extended Energy Consumption Model

The analysis in the first part of this chapter has been based on the model that all the energy that is consumed in a wireless device is emitted by the antenna. In the remainder of this chapter we will consider the impact of more detailed energy consumption models on the results obtained earlier in this chapter. The energy consumption of a wireless device is modeled by including not only the energy emitted while transmitting, but also energy consumed by supporting circuitry. In particular also receiver energy consumption is taken into account. It is shown that under this model, compared to traditional routing, the energy reduction offered by network coding is significantly different from results reported in the literature based on an energy consumption model that includes the energy emitted while transmitting only. Moreover, it is illustrated that energy can be saved by increasing the transmission power. Whereas this causes individual transmissions to consume more energy, overall energy consumption can be reduced since more coding opportunities arise.

An important contribution to the energy consumption is formed by the energy that is emitted while transmitting. Therefore, optimizing the transmit power in multi-hop networks has been the topic of many studies, for instance [28, 34, 79]. By considering only the transmitted energy, it is concluded that it is optimal to keep the transmit power as low as possible, while ensuring connectivity. Hence, one should take many short hops instead of less hops over a larger distance.

There are applications in which the transmit power is so large that the energy consumption is dominated by the transmit energy. However, there are also many applications in which the transmit power is relatively low and other contributions to the energy consumption can not be neglected, for instance, in wireless sensor networks. The other contributions consist of, for instance, energy consumed by supporting circuitry while transmitting, as well as energy consumed while receiving. Examples of exact values of the energy consumed while transmitting and receiving at various transmit power levels can be found in the literature [22] as well as in manufacturer specifications of devices, *e.g.*, [77]. These values demonstrate that: 1) energy consumed while receiving is not always negligible, and 2) transmitter energy consumption is not always dominated by the transmitted energy. In [10] this observation has been used to demonstrate that it is not always optimal to take the shortest possible hops. Indeed, if, independent of the hop distance, a large amount of energy is consumed in each hop, it might be optimal to take few long hops. In this section we will consider the consequence of the above observations on the energy consumption in the configurations discussed earlier in this chapter. For these configurations we will analyze the use of network coding under a more detailed energy consumption model. In addition we will consider an increased transmission range for reducing energy consumption.

4.6.1 Extended Model

Most of the model is equivalent to the model used in the previous parts of this chapter, *i.e.*, as defined in Section 4.2. The difference is that energy consumption of a device is separated in two quantities: $E_{\text{tx}}(r)$ and E_{rx} denoting the energy required to transmit a symbol at transmission range r and the energy required to receive a symbol respectively. Again, since we are interested

in energy consumption only, we can schedule all transmissions sequentially. Hence, we can assume that there is no interference. We assume that signals are attenuated exponentially over distance with path loss exponent α . Moreover, we assume a fixed transmission rate. Hence, in order to have correct reception of a message, we require the signal to noise ratio to be above a certain threshold, *i.e.*, to have transmit power proportional to r^α , where r is the distance over which transmission takes place. We assume that each node within transmission range r is capable of receiving the transmitted symbol without error. Besides the energy that is emitted while transmitting, there is an additional part independent of the transmission range. This leads to the following relation between the transmission range and the energy consumption per transmitted symbol at the transmitter

$$E_{\text{tx}}(r) = \kappa_2(\kappa_1 + r^\alpha), \quad (4.45)$$

where κ_1 and κ_2 are constants. The values of the constants depend on the hardware and the communication protocols that are being used. In this thesis we will not deal with an interpretation of or exact values for these parameters. Since we will compare the energy consumption of various routing and coding schemes their values will only enter the analysis by means of the relation between the different parameters. We comment here on the values that can be expected in practical devices. Depending on the operating regime, the value of κ_1 can range from being negligible compared to r^α , to being of the same order of magnitude or even larger than r^α . The specifications of a device in which κ_1 is larger than r^α are given in [77]. In addition similar measurements are presented in [22] for other devices. Also the value of E_{tx} can range from being negligible compared to r^α , to being larger than r^α , again see, *e.g.*, [22, 77].

4.6.2 To code or not to code

Reconsider the example presented in Chapter 1 of three sessions with nodes located according to a (single) hexagon. For convenience, Figure 4.9 illustrates the example. Remember, from Chapter 1 that a solution without network coding would require six transmissions in order to transfer one symbol for each session. The network coding solution uses only four transmissions.

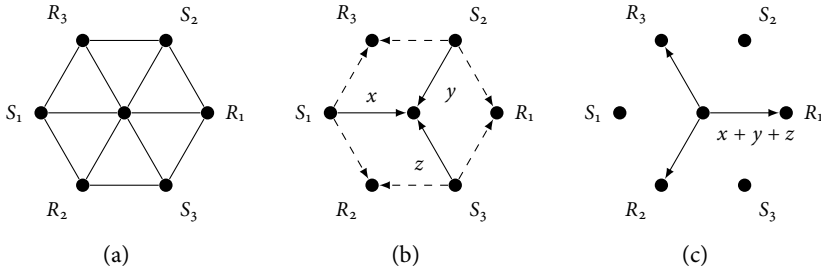


Figure 4.9: Network coding solution to three session multiple unicast configuration. Configuration and connectivity in (a). Transmissions from sources and center node in (b) and (c) respectively.

The last transmission $x + y + z$ by the center node, depicted in Figure 4.9c, is useful for all sinks. The first contribution of this section deals with the observation that the network coding solution requires each sink to receive three symbols, whereas without network coding only one symbol needs to be received. Hence, there is a tension between the energy saved by reducing the numbers of transmissions and the additional energy spend by the sinks in receiving more symbols. We will explore this tradeoff in more detail for two configurations: 1) information exchange on the line network and 2) the hexagonal lattice as introduced in Section 4.4. Both configurations will be analyzed for the limit of a large network. The energy benefit of network coding under the extended energy consumption model will be denoted as $\tilde{B}_{\text{line}}^{\text{code}}$ and $\tilde{B}_{\text{hex}}^{\text{code}}$ for the line network and the hexagonal lattice respectively.

We start this section with a discussion on information exchange in the network of K uniformly spaced nodes on a line with interdistance one. There are two oppositely directed unicast sessions with sources and destinations at the boundaries of the network. We assume that in both the network coding and routing case $r = 1$. For notational convenience, the dependence of E_{tx} on r will be left implicit. Note that a routing solution requires all nodes except for the two boundary nodes to transmit and receive twice. In addition, it is known that a network coding solution exists that uses one transmission at each of those nodes using a piggy-backing strategy [81] (see also Chapter 5),

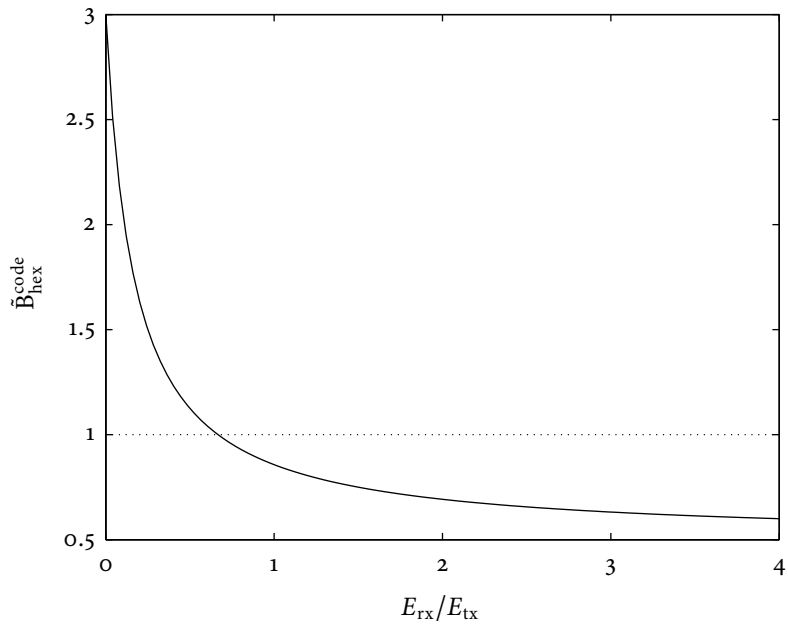


Figure 4.10: The energy benefit of network coding for the configuration from Section 4.4 under the extended energy consumption model as a function of $E_{\text{rx}}/E_{\text{tx}}$.

again each node needs to receive twice. Since we consider $K \rightarrow \infty$ we can ignore the nodes at the boundary. It follows that the energy benefit, $\tilde{B}_{\text{line}}^{\text{code}}$ is

$$\tilde{B}_{\text{line}}^{\text{code}} = \frac{2E_{\text{tx}} + 2E_{\text{rx}}}{E_{\text{tx}} + 2E_{\text{rx}}} = \frac{2 + 2\frac{E_{\text{rx}}}{E_{\text{tx}}}}{1 + 2\frac{E_{\text{rx}}}{E_{\text{tx}}}}. \quad (4.46)$$

If $E_{\text{rx}} = 0$ we see that $\tilde{B}_{\text{line}}^{\text{code}} = 2$. However, if $E_{\text{rx}} = E_{\text{tx}}$, for instance, this reduces to $\tilde{B}_{\text{line}}^{\text{code}} = \frac{4}{3}$, which differs significantly from the benefit of 2 which is usually presented in the literature. Finally, note that the ratio is always larger than one, *i.e.*, the network coding solution will always perform better than the routing solution. We will see that there are also configurations in which, for certain ranges of parameter values, known coding solutions perform worse than routing solutions.

The second configuration that we consider is that of Section 4.4, the natural extension of Figure 4.9 to a larger network. First note that the optimal routing solution is transmitting data along the shortest paths between sources and destinations. Hence, a routing solution requires each interior node to transmit and receive three times. From Section 4.4 we know that a network coding solution exists in which each interior node is transmitting once in order to deliver a symbol for each session. Moreover each node at the border is transmitting twice, hence this contribution to the energy consumption can be neglected for large networks. In Section 4.4 we did not consider receiver energy consumption. Inspection of the proposed code shows that each interior node needs to receive six times. Note, finally that the energy consumption of this particular network code forms an upper bound to the minimum energy required by any network code. Hence the benefit can be lower bounded as

$$\tilde{B}_{\text{hex}}^{\text{code}} \geq \frac{3E_{\text{tx}} + 3E_{\text{rx}}}{E_{\text{tx}} + 6E_{\text{rx}}} = 3 \frac{1 + \frac{E_{\text{rx}}}{E_{\text{tx}}}}{1 + 6\frac{E_{\text{rx}}}{E_{\text{tx}}}}. \quad (4.47)$$

This recovers the result from Section 4.4 that if $E_{\text{rx}} = 0$ then $\tilde{B}_{\text{hex}}^{\text{code}} \geq 3$. Moreover we can conclude that we have a benefit larger than one if $E_{\text{tx}} > 3E_{\text{rx}}/2$. However, for $E_{\text{tx}} \leq 3E_{\text{rx}}/2$ no code is known that achieves better than routing. We have plotted this bound on $\tilde{B}_{\text{hex}}^{\text{code}}$ as a function of $E_{\text{rx}}/E_{\text{tx}}$ in Figure 4.10.

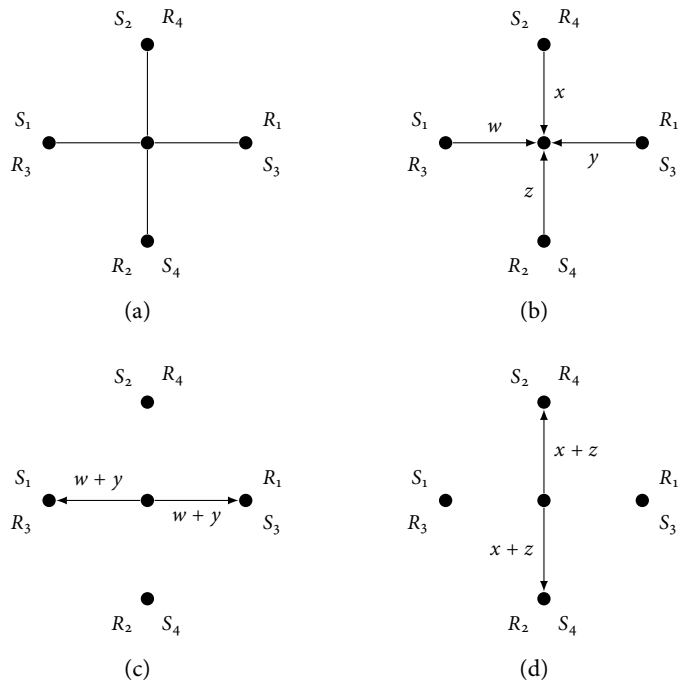


Figure 4.11: Network coding solution to the four session multiple unicast configuration depicted in (a). The solution depicted in (b)–(d) performs coding for the horizontal and vertical sessions independently and uses a total of 8 transmissions.

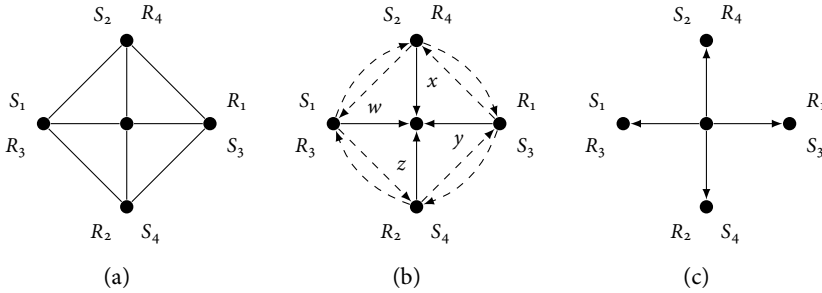


Figure 4.12: The four session configuration from Figure 4.11 with increased transmission range leading to connectivity as in (a). The network coding solution depicted in (b) and (c) uses 5 transmissions.

The main message is that taking receiving energy consumption into account can significantly influence results on the energy benefit of network coding.

4.6.3 Transmission range

The second observation made regarding the extended energy consumption model is that by increasing the transmission power, the transmission range is increased and more nodes are able to receive each message, hence potentially creating coding opportunities and enabling more efficient operation. Again, we illustrate by means of an example. In Figure 4.11 we have depicted a configuration with four multicast sessions and a coding solution in which the center nodes transmits twice. Note that this coding solution is using the well-known piggy-backing strategy [81] for the horizontal and vertical sessions independently. In Figure 4.12 we have depicted the topology resulting from an increased transmission range and a corresponding network coding solution in which the center node is transmitting only once. Hence the number of transmissions is reduced by increasing the transmission range. Obviously, there is a tension between the increased efficiency and the additional energy spend by increasing the transmit power. Moreover, receiver energy consumption is increased since more transmissions need to be overheard.

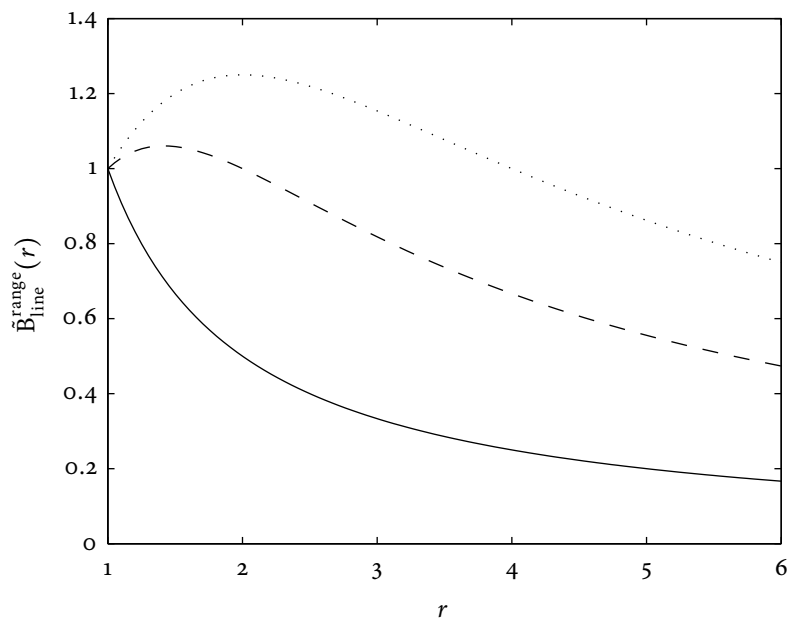


Figure 4.13: The benefit of increasing the transmission range in the line network under the extended energy consumption model for $\alpha = 2$ and $\beta = 0, 2, 4$ in solid, dashed and dotted lines respectively.

We consider the influence of the transmission power on the overall energy consumption for two families of configurations, the line network that was also used in the previous section and the configuration from Section 4.5. Let $\tilde{B}_{\text{line}}^{\text{range}}(r)$ and $\tilde{B}_{\text{rect}}^{\text{range}}(r)$ denote the benefit of increasing from transmission range 1 to r for the line and rectangular lattice network under the extended energy consumption model respectively. More precisely, the benefit is defined as the ratio of the minimum energy consumption at ranges 1 and r in the limit $K \rightarrow \infty$. We start with the line network for which we have seen in the previous section that independent of the value of $E_{\text{rx}}/E_{\text{tx}}$ it is beneficial to use network coding. Therefore, we will compare the energy consumption of the network coding solution given in the previous section at various transmission powers, *i.e.*, at ranges 1 and r . Observe that at transmission range r only every $\lfloor r \rfloor$ th node needs to participate in a coding scheme. The other nodes can remain inactive. Hence, it is straightforward to derive

$$\tilde{B}_{\text{line}}^{\text{range}}(r) = \frac{\lfloor r \rfloor (E_{\text{tx}}(1) + 2E_{\text{rx}})}{E_{\text{tx}}(r) + 2E_{\text{rx}}} = \frac{\lfloor r \rfloor (1 + \beta)}{r^\alpha + \beta}, \quad (4.48)$$

where, for notational convenience, we have introduced $\beta = \kappa_1 + 2E_{\text{rx}}/\kappa_2$. In order to characterize the behavior of $\tilde{B}_{\text{line}}^{\text{range}}(r)$ we analyze

$$\tilde{\tilde{B}}_{\text{line}}^{\text{range}}(r) = \frac{r(1 + \beta)}{r^\alpha + \beta}, \quad (4.49)$$

which is an upper bound to $\tilde{B}_{\text{line}}^{\text{range}}(r)$. The maximum of $\tilde{\tilde{B}}_{\text{line}}^{\text{range}}(r)$ is attained at

$$r = \sqrt[\alpha]{\frac{\beta}{\alpha - 1}}. \quad (4.50)$$

Finally, we determine the values of β for which $\tilde{\tilde{B}}_{\text{line}}^{\text{range}}(r) \leq 1$ for all $r \geq 1$, *i.e.*, for which it is not beneficial to increase the transmission range. From $\tilde{\tilde{B}}_{\text{line}}^{\text{range}}(1) = 1$, the value of the derivative and continuity, it follows that

$$\beta < \alpha - 1 \Rightarrow \tilde{\tilde{B}}_{\text{line}}^{\text{range}}(r) \leq 1, \quad r \geq 1. \quad (4.51)$$

We have plotted the values of $\tilde{\tilde{B}}_{\text{line}}^{\text{range}}(r)$ as function of r for $\alpha = 2$ and various values β in Figure 4.13. In Figure 4.13 we have used $\alpha = 2$ in which case

the above expression for the maximizing transmission range, Equation (4.50), reduces to $r = \sqrt{\beta}$.

Next, we consider the energy consumption in configuration from Section 4.5 in two dimensions. First, note that for each pair of oppositely directed sessions it is possible to use the line network information exchange network coding scheme that was discussed in the previous section. From this discussion it follows that network coding always reduce energy consumption. Therefore, we will compare network coding solutions at various transmission ranges. In contrast to the first part of this section we will compare $r = 1$ and $r = \sqrt{2}$ only. At $r = 1$ we use the information exchange scheme from [81] for pairs of oppositely directed sessions. Hence each interior node needs to transmit twice and receive four times.

For $r = \sqrt{2}$ we use the code that was constructed in Section 4.5. Note that at $r = \sqrt{2}$ each node in the interior of the network has 8 neighbours. In order to deliver one symbol for each of the sessions, the code requires each interior node to receive from all 8 neighbours. In addition one transmission is required. The nodes at the border transmit twice and receive at most eight times. Hence, the contributions from the border nodes can be neglected. It follows that

$$\tilde{B}_{\text{rect}}^{\text{range}}(\sqrt{2}) \geq \frac{2E_{\text{tx}}(1) + 4E_{\text{rx}}}{E_{\text{tx}}(\sqrt{2}) + 8E_{\text{rx}}} = \frac{2\kappa_1 + 2 + 4E_{\text{rx}}/\kappa_2}{\kappa_1 + 2^{\alpha/2} + 8E_{\text{rx}}/\kappa_2}. \quad (4.52)$$

It follows that the benefit is larger than one if

$$E_{\text{rx}} < \frac{\kappa_2 (\kappa_1 + 2 - 2^{\alpha/2})}{4}. \quad (4.53)$$

This means that in the configuration depicted in Figure 4.1 it is beneficial to increase the transmission range from $r = 1$ to $r = \sqrt{2}$ if the above condition is satisfied. Note, that increasing from $r = 1$ to $r = \sqrt{2}$ does not affect the number of hops on the shortest path between any source and destination. Hence, the reduced energy consumption comes from more efficient coding that is possible at $r = \sqrt{2}$. In contrast, in the line network, as discussed in the first part of this section, lower energy consumption arose from a reduction in the number of hops.

4.7 Discussion

We have given several constructions of energy-efficient network codes. These constructions serve to show that compared to plain routing, network coding has the potential of reducing energy consumption in wireless networks. Since we have provided only codes that are based on a centralized design, it remains to be shown in future work if and how this potential can be exploited using practical codes. Moreover, it would also be of interest to consider the energy-benefit in topologies in which the nodes are not positioned at a lattice, for instance, random networks. We have provided lower bounds on the energy benefit of network coding for wireless multiple unicast. Another open problem is to find upper bounds on the benefit.

In addition it has been demonstrated that considering an energy consumption model that include overhead at the transmitter as well as receiver energy consumption might have significant impact on the results. Moreover, it has been shown that by increasing the transmission power it is possible to reduce the overall energy consumption in the network since more coding opportunities are created.

Chapter 5

The Transport Capacity of Line and Lattice Networks

Contents

5.1	Introduction	89
5.2	Computation Coding	92
5.3	Model and Notation	93
5.4	Main Results	97
5.5	Upper Bounds	103
5.6	Achievable Schemes	123
5.7	Extension to Gaussian Models	136
5.8	Discussion	138
5.A	Proof of Lemma 5.28	139

5.1 Introduction

As discussed in Section 1.7 of the introductory chapter of this thesis, a natural follow-up observation, starting from the insight that intermediate nodes in a network need not always forward all the information they receive, is that then they actually do not have to receive all that information in the first place.

Rather, as long as they manage to receive the particular function they need to forward, the overall networking solution will work properly. This is where *superposition* enters the picture. As was shown in [64, 65], whenever signals interfere, it can be more efficient for the decoder to obtain only a function of the transmitted messages, rather than all the messages individually. This is particularly interesting for the wireless medium where interference is linear and results in superposition. Based on recent results from [64, 65] we will consider models in which nodes are able to decode the sum of the messages transmitted by their neighbours. The idea of exploiting superposition in this way has been the topic of [64, 65] as well as many other recent studies, some of which will be reviewed in Section 5.2.

The classical means of operating a wireless network, turning the physical layer into a network of reliable point-to-point bit pipes, removes both broadcast and superposition. This results in an abstraction of the wireless medium in which reliable communication is most naturally captured by a deterministic model. In this chapter we introduce other deterministic models, capturing the effects of exploiting broadcast and/or superposition by decoding linear functions. We study four models that are denoted as P/P, B/P, P/M and B/M. The first position denotes whether symbols are transmitted to a single neighbour (P(oint-to-point)) or to all neighbours (B(roadcast)). The second position denotes whether multiple transmissions to a node cause interference (P(oint-to-point)) or that nodes receive the sum of all symbols that are transmitted by neighbours (M(ulti-access)). More precisely we introduce the following models:

1. P/P: Neither broadcast nor superposition are exploited, *i.e.*, a single transmission can be received by at most one device and multiple transmissions to the same device result in a collision.
2. B/P: Transmissions are received by all neighbours. However, multiple transmissions to the same device lead to a collision.
3. P/M: Nodes can decode the sum of all transmissions by neighbouring nodes. However, a single transmission can be received by at most one device.

4. B/M: Finally, the most interesting deterministic network model considered in this chapter is the combination of the above two effects into a model that involves both the broadcast and the superposition effects.

Our goal in this chapter is to compare the performance attainable under these four deterministic models. For the performance measure in this chapter, we study achievable rates for *multiple unicast connections*, i.e., messages of every source node are of interest only to one destination node. This is by contrast to several other problems of interest, such as for example the multicasting problem where one source node may be of interest to many destinations. Finally, the particular figure of merit that we consider in this chapter will be the so-called *transport capacity*: For each source-destination pair, we evaluate the product of the rate achieved and the distance between source and destination. The transport capacity of the network, as introduced in [35], is then the sum of all of these products, maximized over all possible placements of unicast connections. Obviously, there are other interesting performance measures to study, for instance, the maximum achievable common rate in a random multiple unicast configuration, as studied in many recent papers like, for instance [67, 82]. Since no single number can fully characterize ‘the’ capacity of a network we believe that several performance measures should be explored.

We establish upper and lower bounds on the transport capacity under the four different deterministic network models for two specific arrangements of the nodes in the network. Our results are the following:

1. We consider a network where all the nodes are arranged in a line and obtain tight capacity bounds for all models. We find that the capacity under B/P and P/M is 33% larger than the capacity under P/P. Moreover, the capacity under B/M is twice the capacity under P/P.
2. We consider a network in which the nodes are arranged on a two-dimensional hexagonal lattice. Here we find that the capacity under B/M is at least 2.5 times, and no more than six times, the transport capacity under P/P. The transport capacities under P/M and B/P fall between these bounds.

For the line network our upper and lower bounds are tight in the sense that

the difference is a constant independent of the network size. For the two-dimensional case our bounds are not tight. Finding the optimal network coding solution for multiple unicast appears to be a hard (and open) problem. This claim is supported by the fact that linear network codes are not sufficient to achieve capacity [16].

By contrast to a growing body of literature on deterministic models, see *e.g.*, [4, 5, 18, 31, 83], our main emphasis is not on (approximate) capacity results. Instead, we consider maximum attainable performance under specific operating constraints. For the P/P model these operating constraints correspond to first reducing the wireless medium to a network of reliable point-to-point links. For the other models considered in this chapter there is also a reduction to reliable links, but these are no longer point-to-point. All models correspond, in a sense, to different means of handling the wireless medium in a (OSI) layered overall system architecture. Indeed, we will see in this chapter how our results can be applied to obtain achievable rates for Gaussian network models by specifically considering a simple version with local interference only.

The remainder of this chapter is organized as follows. In Section 5.2 we review some of the recent work on exploiting superposition. In Section 5.3, we introduce the problem and the four different deterministic interference models that are considered. In Section 5.4 we provide upper and lower bounds. In Sections 5.5 and 5.6 we present proofs of our bounds. In Section 5.7 we outline the application of our results to Gaussian network models. In Section 5.8 we conclude this chapter with a discussion of the results.

5.2 Computation Coding

Exploiting superposition in combination with network coding by recovering a sum of different messages has been considered in many recent papers. The concept is known under various names, such as analog network coding [3, 45], physical layer network coding [36, 56, 58, 87, 88], joint physical layer coding and network coding [62, 70], layer-2 combining [76] and computation coding [61, 63–65].

Many of the recent studies [36, 45, 56, 76, 87, 88] have focussed on uncoded transmissions and the corresponding detection problems. In these works the

performance of these strategies in communicating a single sum of messages to a specific receiver is analyzed. In [45] the influence of imperfect synchronization between nodes is considered and measurement results from a testbed are presented. The diversity-multiplexing tradeoff of a physical-layer network coding system is studied in [56]. Of course, if these uncoded strategies are used in larger networks a method will need to be devised to prevent the amplification of noise and/or the propagation of errors. This problem has not been addressed in previous work based on uncoded transmissions. In [87] the benefit of physical layer network coding in a line network is studied under the assumption that there is no propagation of errors.

By contrast to performing uncoded transmissions, our focus is reliable communication over each link. In [64] it has been demonstrated that if N nodes communicate to a single receiver in a Gaussian multiple-access channel, the maximum achievable rate R for reliable communication satisfies

$$\frac{1}{2} \log \left(\frac{1}{N} + P \right) \leq R \leq \frac{1}{2} \log(1 + P), \quad (5.1)$$

where P is an individual power constraint for each of the transmitters. Starting from the results in [64] we assume that nodes are able to reliably decode the sum of the messages. Similar arguments have been used for specific small network examples, e.g., [61–63, 70]. The difference with our work is that we consider networks of arbitrary size.

In [58] the scaling behaviour of the capacity of random networks is studied under physical-layer network coding. It is shown that exploiting superposition by decoding sums of messages does not affect the scaling behaviour. Our focus is on networks with specific node placement and analysis of the constants involved.

5.3 Model and Notation

5.3.1 Network

We model a wireless network as a directed graph (V, E) , where V is the set of nodes and $E \subseteq V \times V$ are the edges. If $(u, v) \in E$, information can be reliably transmitted from u to v . The interaction between nodes is specified in more

detail below for each of the four models. We assume that $(u, v) \in E$ implies $(v, u) \in E$, *i.e.*, that the interaction between nodes is symmetric.

5.3.2 Communication Models

Time is slotted. Symbols are from the finite field \mathbb{F}_q . In the remainder the base of the logarithm in entropy and mutual information measures is q , *i.e.*, the unit of information is the q -ary symbol. In all four models each link can carry one q -ary symbol per time slot. Hence the links have unit capacity. Let $X_v[t]$ and $Y_v[t]$ be the symbols transmitted and received respectively, by node v in time slot t . For $S \subseteq V$, let $X^S[t] = \{X_v[t] | v \in S\}$ and $Y^S[t] = \{Y_v[t] | v \in S\}$. Let

$$N_v = \{w \in V | (v, w) \in E\} \cup \{v\}, \quad (5.2)$$

i.e., N_v is the neighbourhood of v including v itself. The channel output Y_v depends only on X^{N_v} , the channel inputs of neighbouring nodes in the same time slot. The relation between Y_v and X^{N_v} is independent of time and therefore dependence on the time slot is often omitted in the notation.

All our models will respect half-duplex constraints, meaning that no node can simultaneously transmit and receive. Formally, we model this by extending the channel input alphabet with a “silent” symbol σ denoting that a node is not transmitting. Moreover, formally, for any node v that is transmitting in time slot t , its corresponding received signal $Y_v[t]$ is set to an independent random variable, uniformly distributed over the entire alphabet. This means that v does not get any information.¹ We restrict our attention to transmission strategies in which the transmission schedule is fixed ahead of time, *i.e.*, strategies for which

$$P(X_v[t] = \sigma) \in \{0, 1\}. \quad (5.3)$$

Note that even though half-duplex constraints are modelled by means of a uniformly distributed channel output, the model is otherwise deterministic in nature.

The exact functional relation is now specified for each of the models that were introduced in Section 5.1. The four models are denoted by P/P, B/P,

¹Another way to model collisions due to interference, would be to extend the output alphabet with an erasure symbol. This, however, creates a covert channel.

P/M and B/M. The first position denotes whether symbols are transmitted to a single neighbour (P) or broadcast to all neighbours (B). The second position denotes whether multiple transmissions to a node cause interference (P) or that nodes receive the sum of all symbols that are transmitted by neighbours (M). To simplify notation we introduce random variables Z_v , $v \in V$, uniformly distributed over \mathbb{F}_q . Each Z_v is independent of all other random variables. In addition, for the P/P and P/M models we introduce, for each node $v \in V$, a variable A_v that denotes the neighbour that v is transmitting to. Since the transmission schedule is fixed ahead of time

$$P(A_v[t] = w) \in \{0, 1\}, \quad (5.4)$$

for all $v, w \in V$.

The models are defined as follows.

P/P: Neither broadcast nor superposition are exploited, *i.e.*, a single transmission can be received by at most one device and multiple transmissions to the same device result in a collision. This means that $Y_v = X_u$ if u is the only neighbour of v that is transmitting and also v itself is not transmitting. Otherwise $Y_v = Z_v$, *i.e.*, a uniformly distributed random variable. This gives

$$\text{P/P: } Y_v = \begin{cases} X_u, & \text{if } u \in N_v, X_u \neq \sigma, A_u = v, \forall w \in N_v \setminus \{u\}: X_w = \sigma, \\ Z_v, & \text{otherwise.} \end{cases} \quad (5.5)$$

P/M: Superposition is exploited, but broadcast is not. A transmission from u to v prevents other transmissions from u , but other transmissions to v are allowed. If v is not transmitting itself, it receives the sum of all symbols that are transmitted to v by its neighbours, *i.e.*,

$$\text{P/M: } Y_v = \begin{cases} \sum_{u \in N_v: X_u \neq \sigma} X_u, & \text{if } X_v = \sigma \text{ and } \exists u \in N_v: X_u \neq \sigma \text{ and} \\ & \forall w \in N_v: (X_w \neq \sigma \rightarrow A_w = v), \\ Z_v, & \text{otherwise.} \end{cases} \quad (5.6)$$

B/P: Broadcast is exploited, but superposition is not. A transmission from u to v prevents other transmissions to v , but other transmissions from u are allowed. Since u is broadcasting to all its neighbours we don't need the variables A_v in the B/P model. This gives

$$\text{B/P: } Y_v = \begin{cases} X_u, & \text{if } u \in N_v, X_u \neq \sigma, \forall w \in N_v \setminus \{u\}: X_w = \sigma, \\ Z_v, & \text{otherwise.} \end{cases} \quad (5.7)$$

B/M: Both broadcast and superposition are exploited. Each node that is not transmitting receives the sum of the symbols transmitted by all its neighbours, *i.e.*,

$$\text{B/M: } Y_v = \begin{cases} \sum_{u \in N_v: X_u \neq \sigma} X_u, & \text{if } X_v = \sigma \text{ and } \exists u \in N_v: X_u \neq \sigma, \\ Z_v, & \text{otherwise.} \end{cases} \quad (5.8)$$

5.3.3 Transport Capacity

The traffic pattern that we consider is multiple unicast. For a set of K unicast sessions, let S_k and D_k denote the source and destination respectively, of the k th session, and R_k its throughput. Each subset $\Gamma \subseteq V$ of nodes induces a partition of V and hence a directed cut. We will, therefore, often refer to a set of nodes as a cut. For $\Gamma \subseteq V$, let $\bar{\Gamma} = V \setminus \Gamma$ and

$$K_\Gamma = \{k | S_k \in \Gamma, D_k \notin \Gamma\}. \quad (5.9)$$

Our measure of interest is the *transport capacity* of a network which is defined as the maximum, over all configurations of unicast sessions on a given network and all possible transmission strategies, of $\sum_{k=1}^K \text{dist}(S_k, D_k) R_k$, where $\text{dist}(S_k, D_k)$ is the number of hops on the shortest path from S_k to D_k , *i.e.*, the transport capacity is the maximum number of q -ary symbols \times hops per time slot that can be transported in the network. We will derive upper and lower bounds on the transport capacity of some networks under the different models.

5.3.4 Notation

Finally, we define some notation. If $f(L) = o(g(L))$ for a function $f : \mathbb{N} \rightarrow \mathbb{R}$ then

$$\lim_{L \rightarrow \infty} \frac{f(L)}{g(L)} = o.$$

Similarly, $f(L, M) = o(g(L, M))$ for a function $g : \mathbb{N}^2 \rightarrow \mathbb{R}$ means that

$$\lim_{L \rightarrow \infty} \frac{f(L, L)}{g(L, L)} = o.$$

The floor and ceiling operations are denoted by $\lfloor x \rfloor$ and $\lceil x \rceil$ respectively, *i.e.*, $\lfloor x \rfloor = \max\{y \in \mathbb{Z} \mid y \leq x\}$ and $\lceil x \rceil = \min\{y \in \mathbb{Z} \mid y \geq x\}$. For integers a, b and $p > 0$, $a \equiv b \pmod{p}$ means that a and b are congruent modulo p , *i.e.*, that $a - b$ is divisible by p . Finally, $a = b \pmod{p}$ means that the remainder of a divided by p is b .

5.4 Main Results

5.4.1 Line Network

We consider the line network represented by (V, E) , where

$$V = \{0, 1, \dots, L\}, \quad E = \{(u, v) \subseteq V \times V \mid |u - v| = 1\}. \quad (5.10)$$

The throughput of multiple unicast on the line network in a model that allows for broadcast and coding was first studied in [81]. The extension to models that allow for superposition has been treated in [45, 87]. We give bounds on the transport capacity of the line network under the different models. The coding scheme used to achieve the lower bounds was also used in previous work [45, 81, 87]. Results similar to Theorems 5.2 and 5.4 have appeared in [81] and [87] respectively. The proof techniques that are developed are new and will be used to analyze the hexagonal lattice. For the P/P and B/M models we have exact results for the transport capacity of the line network. For the B/P and P/M models we provide upper and lower bounds that are separated by at most $\frac{2}{3}$.

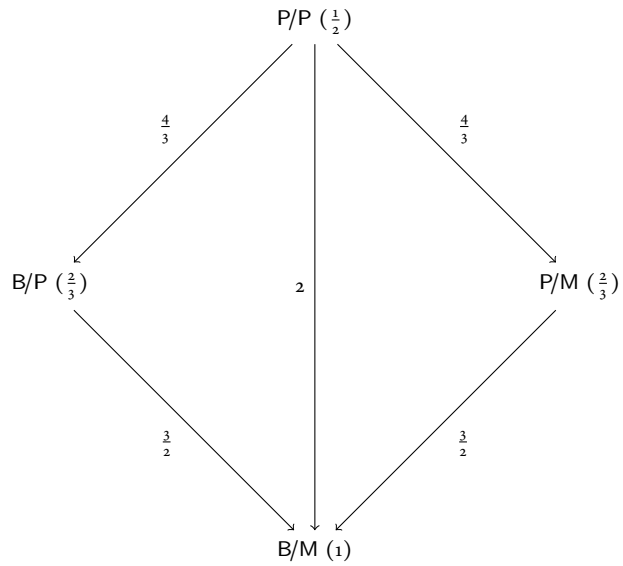


Figure 5.1: Transport capacity of the line network under different models. For each model in parentheses is $\lim_{L \rightarrow \infty} \frac{C^{\text{line}}(L)}{L}$. Labels next to arrows denote the multiplicative improvement obtained by moving from one model to the next.

Theorem 5.1. *The transport capacity $C_{P/P}^{\text{line}}(L)$ of the $L + 1$ node line network under the P/P model is*

$$C_{P/P}^{\text{line}}(L) = \left\lfloor \frac{1}{2}L \right\rfloor.$$

Theorem 5.2. *The transport capacity $C_{B/P}^{\text{line}}(L)$ of the $L + 1$ node line network under the B/P model satisfies*

$$\frac{2}{3}L \leq C_{B/P}^{\text{line}}(L) \leq \left\lfloor \frac{2}{3}L \right\rfloor.$$

Theorem 5.3. *The transport capacity $C_{P/M}^{\text{line}}(L)$ of the $L + 1$ node line network under the P/M model satisfies*

$$\frac{2}{3}L \leq C_{P/M}^{\text{line}}(L) \leq \left\lfloor \frac{2}{3}L \right\rfloor.$$

Theorem 5.4. *The transport capacity $C_{B/M}^{\text{line}}(L)$ of the $L + 1$ node line network under the B/M model is*

$$C_{B/M}^{\text{line}}(L) = L.$$

Figure 5.1 gives an overview of the results from Theorems 5.1–5.4. The figure presents the value of $\lim_{L \rightarrow \infty} \frac{C^{\text{line}}(L)}{L}$ for each model. Moreover, the labels next to arrows denote the multiplicative improvement obtained by moving from one model to the next. One can observe that moving from P/P to B/P or P/M gives an improvement of approximately 33%. However, the combined effect of B/P and P/M, *i.e.*, moving from P/P to B/M gives an improvement of 100%. Note that the combined effects of multiaccess and broadcast are larger than the sum of their individual contributions. We will provide some intuition for this in Section 5.5.1.

5.4.2 Hexagonal Network

In this section we consider a network of size $(L + 1) \times (M + 1)$ with nodes located on the hexagonal lattice and edges between nearest neighbours. We

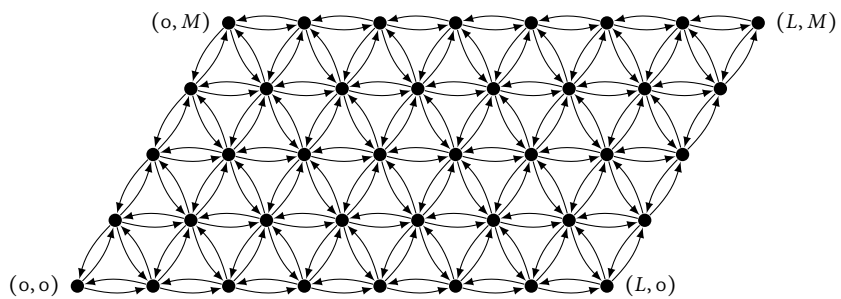


Figure 5.2: Nodes located at the hexagonal lattice with connectivity between nearest neighbours, $L = 7$, $M = 4$.

index nodes with a tuple $(u_1, u_2) \in \mathbb{N}^2$. The location in \mathbb{R}^2 of (u_1, u_2) is $(u_1, u_2)G_\Lambda$, with $G_\Lambda = \begin{bmatrix} 1 & 0 \\ 1/2 & \sqrt{3}/2 \end{bmatrix}$. Now, we consider (V, E) with

$$V = \{(u_1, u_2) \mid 0 \leq u_1 \leq L, 0 \leq u_2 \leq M\},$$

$$E = \{((u_1, u_2), (v_1, v_2)) \in V \times V \mid \|(u_1 - v_1, u_2 - v_2)G_\Lambda\|_2 = 1\}.$$

The hexagonal network is illustrated in Figure 5.2. Note, that the number of edges in (V, E) is $6LM + 2(L + M)$.

Theorem 5.5. *The transport capacity $C_{P/P}^{\text{hex}}(L, M)$ of the $(L + 1) \times (M + 1)$ node hexagonal network under the P/P model satisfies*

$$\frac{1}{3}LM + o(LM) \leq C_{P/P}^{\text{hex}}(L, M) \leq \frac{2}{5}LM + o(LM).$$

Theorem 5.6. *The transport capacity $C_{P/M}^{\text{hex}}(L, M)$ of the $(L + 1) \times (M + 1)$ node hexagonal network under the P/M model satisfies*

$$\frac{2}{5}LM + o(LM) \leq C_{P/M}^{\text{hex}}(L, M) \leq \frac{6}{7}LM + o(LM).$$

Theorem 5.7. *The transport capacity $C_{B/P}^{\text{hex}}(L, M)$ of the $(L + 1) \times (M + 1)$ node hexagonal network under the B/P model satisfies*

$$\frac{2}{5}LM + o(LM) \leq C_{B/P}^{\text{hex}}(L, M) \leq \frac{6}{7}LM + o(LM).$$

Theorem 5.8. *The transport capacity $C_{B/M}^{\text{hex}}(L, M)$ of the $(L + 1) \times (M + 1)$ node hexagonal network under the B/M model satisfies*

$$C_{B/M}^{\text{hex}}(L, M) \leq 2LM + o(LM).$$

Moreover, if $q = 2$, then it satisfies

$$C_{B/M}^{\text{hex}}(L, M) \geq LM + o(LM).$$

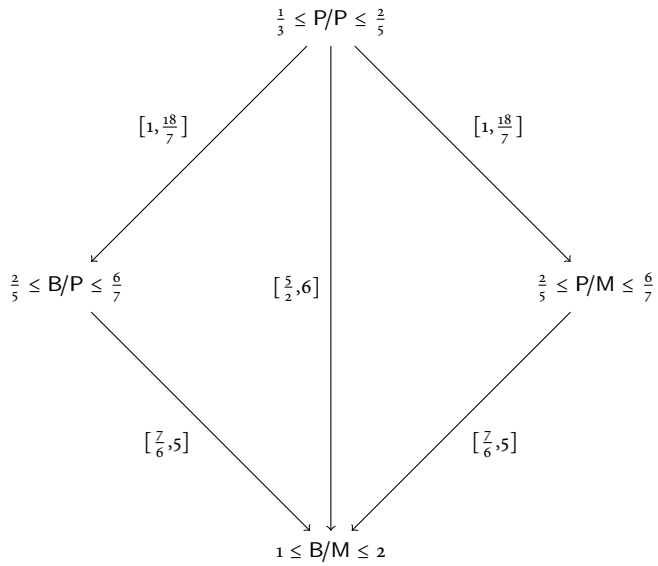


Figure 5.3: Transport capacity of the hexagonal lattice under different models, assuming $q = 2$. For each model lower and upper bounds on $\lim_{L \rightarrow \infty, M \rightarrow \infty} \frac{C^{\text{hex}}(L, M)}{LM}$ are presented. Labels next to arrows denote the range (lower and upper bounds) of the multiplicative improvement obtained by moving from one model to the next.

Note that the lower bound of the above theorem holds only for $q = 2$. We do not believe that $q = 2$ is a necessary condition, but have not been able to prove the result for arbitrary q . Based on the proof techniques used for Theorems 5.6 and 5.7 it is possible to obtain other (weaker) lower bounds for arbitrary q , but for the purpose of clarity of exposition those have been omitted from this thesis.

Figure 5.3 gives an overview of the results from Theorems 5.5–5.8. The figure presents lower and upper bounds to the value of $\lim_{L \rightarrow \infty, M \rightarrow \infty} \frac{C^{\text{hex}}(L, M)}{LM}$ for each model. Moreover, the labels next to arrows denote the range (upper and lower bounds) of the multiplicative improvement obtained by moving from one model to the next.

5.5 Upper Bounds

In this section we give proofs for the upper bounds of Theorems 5.1–5.8. In Subsection 5.5.1 constraint graphs are introduced that capture the structure of the topology and some of the constraints imposed by the communication models. Subsection 5.5.2 deals with upper bounds for the line network. The upper bounds for the hexagonal lattice are derived in Subsection 5.5.3.

5.5.1 Constraint graphs

We capture some of the structure of the topology and the communication models in (undirected) graphs $(E, \mathcal{J}_{B/M})$, $(E, \mathcal{J}_{B/P})$, $(E, \mathcal{J}_{P/M})$ and $(E, \mathcal{J}_{P/P})$. These graphs capture the idea that if $\langle (u, v), (u', v') \rangle$ is an edge, then it is not possible that $I(X_u; Y_v)$ and $I(X_{u'}; Y_{v'})$ are both positive. Before specifying the constraint graphs precisely, we provide some intuition. We consider Figure 5.4, depicting subsets of edges of the line network, and first focus on the P/P model, Figure 5.4a. Assume that $I(X_2; Y_3) > 0$, *i.e.*, that information is transmitted across the thick edge $(2, 3)$ in the network. Then, for all other edges (u', v') in the figure it is true that under the P/P model $I(X_{u'}; Y_{v'}) = 0$. We discuss why this is true for each of these edges. First, remember that one of the assumptions made in Section 2.2 is that the transmission schedule is fixed ahead of time, *i.e.*, that for all $v \in V$, $P(X_v = \sigma) \in \{0, 1\}$ and

$P(A_v = u) \in \{0, 1\}$. Together with (5.5) this implies that $I(X_2; Y_3) > 0$ gives

$$P(X_2 = \sigma) = 0, \quad P(X_3 = \sigma) = 1, \quad P(A_2 = 3) = 1. \quad (5.11)$$

Now, again from (5.5), achieving $I(X_1; Y_2) > 0$ or $I(X_3; Y_2) > 0$ on edges $(1, 2)$ or $(3, 2)$ respectively, would require $X_2 = \sigma$, contradicting (5.11). In other words transmissions to node 2 are not possible due to half-duplex constraints. In similar fashion $I(X_3; Y_4) > 0$ would violate half-duplex constraints, since it requires $X_3 \neq \sigma$. Achieving $I(X_2; Y_1) > 0$ would require $A_2 = 1$, which again contradicts (5.11). Note that under the B/P and B/M models, *i.e.*, when broadcast can be exploited, $I(X_2; Y_1)$ and $(X_2; Y_3)$ can be simultaneously positive. Achieving $I(X_4; Y_3) > 0$ would require $X_4 \neq \sigma$. However, by (5.5), it is not possible to have node $4 \in N_3 \setminus \{2\}$ to transmit. In other words: a transmission from node 4 causes a collision at 3. Under the P/M and B/M models, *i.e.*, when superposition is exploited, $I(X_4; Y_3)$ and $(X_2; Y_3)$ can be simultaneously positive. Finally, similar arguments hold for edges $(0, 1)$ and $(4, 5)$. It can be seen that $I(X_0; Y_1)$ and $I(X_4; Y_5)$ can only be positive under the B/M model, *i.e.*, if both broadcast and interference are exploited. In the next four lemmas we define the constraints graphs for arbitrary networks and for all four models. An extension to the above ideas is that we allow for arbitrary conditioning in the mutual information terms. Note that we do not allow for loops in the constraint graphs, *i.e.*, $\langle (u, v), (u, v) \rangle$ is never an edge.

Lemma 5.9. *Consider the P/P model and let $\mathcal{J}_{P/P}$, a set of unordered pairs of E , be defined as*

$$\langle (u, v), (u', v') \rangle \in \mathcal{J}_{P/P} \text{ iff } u' \in N_v \text{ or } u \in N_{v'}. \quad (5.12)$$

Consider arbitrary subsets $U, W, U', W' \subseteq V$ and assume $\langle (u, v), (u', v') \rangle \in \mathcal{J}_{P/P}$. There does not exist a joint distribution on X^V and A^V satisfying $P(X_w = \sigma) \in \{0, 1\}$ and $P(A_w = w') \in \{0, 1\}$ for all $w, w' \in V$ such that both

$$I(X_u, A_u; Y_v | X^U, A^U, Y^W) > 0$$

and

$$I(X_{u'}, A_{u'}; Y_{v'} | X^{U'}, A^{U'}, Y^{W'}) > 0$$

Proof. Assume

$$I(X_u, A_u; Y_v | X^U, A^U, Y^W) > 0$$

and

$$I(X_{u'}, A_{u'}; Y_{v'} | X^{U'}, A^{U'}, Y^{W'}) > 0.$$

By (5.3), (5.4) and (5.5) we have

$$P(X_u = \sigma) = 0, \tag{5.13}$$

$$P(A_u = \nu) = 1, \tag{5.14}$$

$$P(X_w = \sigma) = 1, \text{ for all } w \in N_v \setminus \{u\}, \tag{5.15}$$

$$P(X_{u'} = \sigma) = 0, \tag{5.16}$$

$$P(A_{u'} = \nu') = 1, \text{ and} \tag{5.17}$$

$$P(X_{w'} = \sigma) = 1, \text{ for all } w' \in N_{v'} \setminus \{u'\}. \tag{5.18}$$

Since $\langle (u, \nu), (u', \nu') \rangle \in \mathcal{J}_{P/M}$, we have $u' \in N_v$ or $u \in N_{v'}$. Now, if $u \neq u'$, then $u' \in N_v \setminus \{u\}$ or $u \in N_{v'} \setminus \{u'\}$ and we have a contradiction between (5.15) and (5.16) or (5.13) and (5.18) respectively. If $u = u'$ then $\nu' \neq \nu$, since $(u, \nu) \neq (u', \nu')$ and we obtain a contradiction between (5.14) and (5.17). \square

Lemma 5.10. Consider the P/M model and let $\mathcal{J}_{P/M}$, a set of unordered pairs of E , be defined as

$$\langle (u, \nu), (u', \nu') \rangle \in \mathcal{J}_{P/M} \text{ iff } \nu' \neq \nu \text{ and } (u' \in N_\nu \text{ or } u \in N_{\nu'}). \tag{5.19}$$

Consider arbitrary subsets $U, W, U', W' \subseteq V$ and assume $\langle (u, \nu), (u', \nu') \rangle \in \mathcal{J}_{P/M}$. There does not exist a joint distribution on X^V and A^V satisfying $P(X_w = \sigma) \in \{0, 1\}$ and $P(A_w = w') \in \{0, 1\}$ for all $w, w' \in V$ such that both

$$I(X_u, A_u; Y_v | X^U, A^U, Y^W) > 0$$

and

$$I(X_{u'}, A_{u'}; Y_{v'} | X^{U'}, A^{U'}, Y^{W'}) > 0.$$

Proof. Assume

$$I(X_u, A_u; Y_v | X^U, A^U, Y^W) > 0$$

and

$$I(X_{u'}, A_{u'}; Y_{v'} | X^{U'}, A^{U'}, Y^{W'}) > 0.$$

By (5.3), (5.4) and (5.6) we have

$$P(X_u = \sigma) = 0, \quad (5.20)$$

$$P(A_u = \nu) = 1, \quad (5.21)$$

$$P(X_w = \sigma) = 0 \longrightarrow P(A_w = \nu) = 1, \text{ for all } w \in N_\nu, \quad (5.22)$$

$$P(X_{u'} = \sigma) = 0, \quad (5.23)$$

$$P(A_{u'} = \nu') = 1, \text{ and} \quad (5.24)$$

$$P(X_{w'} = \sigma) = 0 \longrightarrow P(A_{w'} = \nu') = 1, \text{ for all } w' \in N_{\nu'}. \quad (5.25)$$

Suppose that $u' \in N_\nu$. By (5.22) and (5.23) we need $P(A_{u'} = \nu) = 1$, but this contradicts (5.24), since $\nu' \neq \nu$. In similar fashion (5.20), (5.21) and (5.25) contradict in the case that $u \in N_{\nu'}$. \square

Lemma 5.11. *Consider the B/P model and let $\mathcal{J}_{B/P}$, a set of unordered pairs of E , be defined as*

$$\langle (u, \nu), (u', \nu') \rangle \in \mathcal{J}_{B/P} \quad \text{iff} \quad u' \in N_\nu \setminus \{u\} \text{ or } u \in N_{\nu'} \setminus \{u'\}. \quad (5.26)$$

Consider arbitrary subsets $U, W, U', W' \subseteq V$ and assume $\langle (u, \nu), (u', \nu') \rangle \in \mathcal{J}_{B/P}$. There does not exist a joint distribution on X^V satisfying $P(X_w = \sigma) \in \{0, 1\}$ for all $w \in V$ such that both

$$I(X_u; Y_\nu | X^U, Y^W) > 0$$

and

$$I(X_{u'}; Y_{\nu'} | X^{U'}, Y^{W'}) > 0.$$

Proof. Assume $I(X_u; Y_\nu | X^U, Y^W) > 0$ and $I(X_{u'}; Y_{\nu'} | X^{U'}, Y^{W'}) > 0$. By (5.3) and (5.7) we have $P(X_u = \sigma) = 0$, $P(X_w = \sigma) = 1$ for all $w \in N_\nu \setminus \{u\}$, $P(X_{u'} = \sigma) = 0$ and $P(X_{w'} = \sigma) = 1$ for all $w' \in N_{\nu'} \setminus \{u'\}$. Since $\langle (u, \nu), (u', \nu') \rangle \in \mathcal{J}_{B/P}$ we have $u' \in N_\nu \setminus \{u\}$ or $u \in N_{\nu'} \setminus \{u'\}$, leading to a contradiction. \square

Lemma 5.12. Consider the B/M model and let $\mathcal{J}_{\text{B/M}}$, a set of unordered pairs of E , be defined as

$$\langle (u, v), (u', v') \rangle \in \mathcal{J}_{\text{B/M}} \quad \text{iff} \quad u' = v \text{ or } u = v'. \quad (5.27)$$

Consider arbitrary subsets $U, W, U', W' \subseteq V$ and assume $\langle (u, v), (u', v') \rangle \in \mathcal{J}_{\text{B/M}}$. There does not exist a joint distribution on X^V satisfying $P(X_w = \sigma) \in \{0, 1\}$ for all $w \in V$ such that both

$$I(X_u; Y_v | X^U, Y^W) > 0$$

and

$$I(X_{u'}; Y_{v'} | X^{U'}, Y^{W'}) > 0.$$

Proof. Assume $I(X_u; Y_v | X^U, Y^W) > 0$ and $I(X_{u'}; Y_{v'} | X^{U'}, Y^{W'}) > 0$. By (5.3) and (5.8) we have $P(X_u = \sigma) = 0$, $P(X_v = \sigma) = 1$, $P(X_{u'} = \sigma) = 0$ and $P(X_{v'} = \sigma) = 1$. Since $\langle (u, v), (u', v') \rangle \in \mathcal{J}_{\text{B/M}}$ we have $u' = v$ or $u = v'$, leading to a contradiction. \square

The constraint graphs, as defined by (5.12), (5.19), (5.26) and (5.27), are illustrated in Figures 5.4 and 5.5 on the next page for the line and hexagonal network respectively. Since the constraint graphs for the hexagonal network have many edges, we will not draw these graphs. Instead we will illustrate the constraint graphs as done in Figure 5.5, or, for instance, by presenting sets of edges that form a clique in a constraint graph. It will be shown in the next two subsections that the transport capacity can be upper bounded in terms of the number of edges (u, v) in the graph (V, E) for which $I(X_u; Y_v)$ can be simultaneously positive. By Lemmas 5.9–5.12 it follows that this number is the size of the maximum independent set in the constraint graphs. Remember that an independent set of a graph is a set of vertices, no two of which are adjacent [6]. Since finding the size of the maximum independent set is a NP-complete problem [44], we will derive upper bounds on this size. Note, finally, that our constraint graphs are very similar to the conflict graph, introduced in [42], where upper bounds are derived for multi-commodity flow problems in which network coding is not allowed.

A careful look at the constraint graphs of the line and hexagonal networks provides some intuition on the fact that the combined effects of multiaccess



(a) P/P



(b) B/P



(c) P/M



(d) B/M

Figure 5.4: Illustration of the constraint graphs of the line network under the various models. In thin lines the edges that interfere with the thick edge, *i.e.*, in thin lines the set of edges (u', v') for which $\langle (u, v), (u', v') \rangle$ is in the constraint graph, where (u, v) is the thick edge.

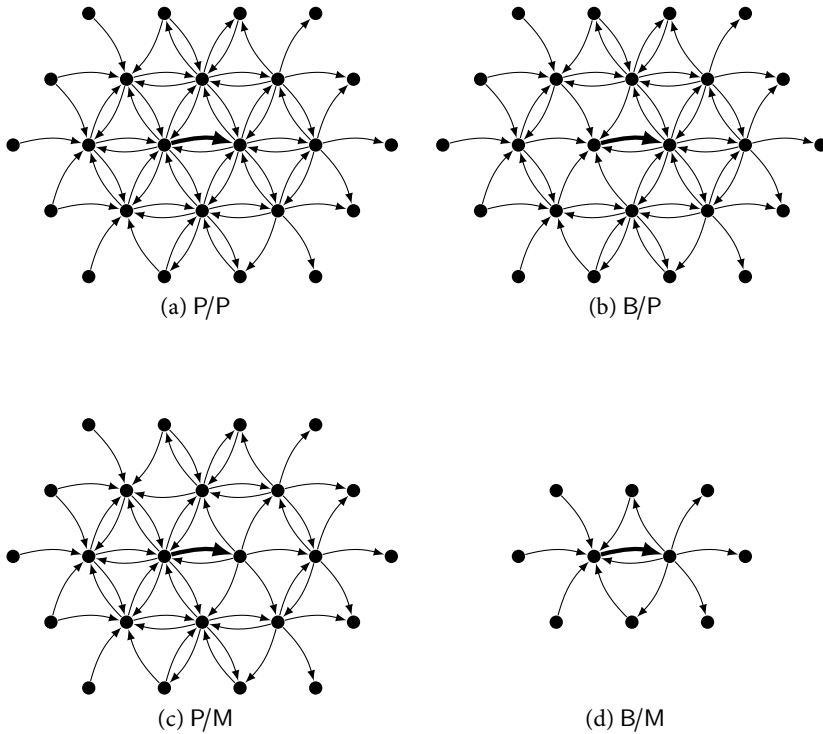


Figure 5.5: Illustration of the constraint graphs of the hexagonal network under the various models. In thin lines the edges that interfere with the thick edge, *i.e.*, in thin lines the set of edges (u', v') for which $\langle (u, v), (u', v') \rangle$ is in the constraint graph, where (u, v) is the thick edge.

and broadcast are larger than the sum of their individual contributions, as observed in Section ???. We observe that $(E, \mathcal{J}_{B/P})$ and $(E, \mathcal{J}_{P/M})$ are subgraphs of $(E, \mathcal{J}_{P/P})$. However, taking the intersection of $(E, \mathcal{J}_{B/P})$ and $(E, \mathcal{J}_{P/M})$ does not give $(E, \mathcal{J}_{B/M})$. Therefore, the effect of exploiting both superposition and broadcast is larger than their individual contributions. The constraint graphs also provide some intuition on why the benefit in the hexagonal network is larger than in the line network. If we compare the ratio of the number of edges in $(E, \mathcal{J}_{P/P})$ and $(E, \mathcal{J}_{B/M})$, we see that this difference is much larger for the hexagonal network. Hence, larger benefits can be expected in the hexagonal network.

5.5.2 Line Network

The following lemma establishes the upper bound of Theorem 5.4.

Lemma 5.13. *The transport capacity $C_{B/M}^{\text{line}}(L)$ of the $L + 1$ node line network under the B/M model is upper bounded by*

$$C_{B/M}^{\text{line}}(L) \leq L.$$

Proof. Let a set of unicast sessions and a network coding strategy over T time slots achieving rate R_k for session $k = 1, \dots, K$, be given. For $i = 0, \dots, L - 1$, let $\Gamma_i = \{0, \dots, i\}$, $\bar{\Gamma}_i = \{i + 1, \dots, L\}$, and $\mathcal{S} = \{\Gamma_i, \bar{\Gamma}_i | i = 0, \dots, L - 1\}$. Since a unicast session over d hops crosses d cuts from \mathcal{S} ,

$$\sum_{S \in \mathcal{S}} \sum_{k \in K_S} R_k = \sum_{k=1}^K \text{dist}(S_k, D_k) R_k. \quad (5.28)$$

We start developing a cut-set bound following the line of proof found in [14, Theorem 14.10.1], for instance. This gives

$$\sum_{k \in K_{\Gamma_i}} R_k \leq \frac{1}{T} \sum_{t=1}^T I(X^{\Gamma_i}[t]; Y^{\bar{\Gamma}_i}[t] | X^{\bar{\Gamma}_i}[t]). \quad (5.29)$$

Summing the LHS and RHS in (5.29) over all $2L$ cuts in \mathcal{S} and using (5.28)

give

$$\sum_{k=1}^K \text{dist}(S_k, D_k) R_k \leq \frac{1}{T} \sum_{t=1}^T \sum_{i=0}^{L-1} [I(X^{\Gamma_i}[t]; Y^{\bar{\Gamma}_i}[t] | X^{\bar{\Gamma}_i}[t]) + I(X^{\bar{\Gamma}_i}[t]; Y^{\Gamma_i}[t] | X^{\Gamma_i}[t])], \quad (5.30)$$

where the second term on the RHS corresponds to reverse cuts $\bar{\Gamma}_i$. Now, due to the fact that the transmission schedule is fixed ahead of time, $P(X_\nu[t] = \sigma) \in \{0, 1\}$ for each t and each $\nu \in V$. We proceed by upper bounding the RHS as

$$\sum_{k=1}^K \text{dist}(S_k, D_k) R_k \leq \max_t \sum_{i=0}^{L-1} [I(X^{\Gamma_i}[t]; Y^{\bar{\Gamma}_i}[t] | X^{\bar{\Gamma}_i}[t]) + I(X^{\bar{\Gamma}_i}[t]; Y^{\Gamma_i}[t] | X^{\Gamma_i}[t])]. \quad (5.31)$$

This means, that for any achievable transport capacity, there must exist a joint distribution on X_ν , with $P(X_\nu = \sigma) \in \{0, 1\}$ for each $\nu \in V$, satisfying

$$\sum_{k=1}^K \text{dist}(S_k, D_k) R_k \leq \sum_{i=0}^{L-1} [I(X^{\Gamma_i}; Y^{\bar{\Gamma}_i} | X^{\bar{\Gamma}_i}) + I(X^{\bar{\Gamma}_i}; Y^{\Gamma_i} | X^{\Gamma_i})] \quad (5.32)$$

$$\leq \sum_{i=0}^{L-1} [I(X_i; Y_{i+1} | X^{\bar{\Gamma}_i}) + I(X_{i+1}; Y_i | X^{\Gamma_i})], \quad (5.33)$$

where the second inequality follows after decomposing the mutual information terms and using (5.8).²

We now argue that for all probability distributions of this kind, the right hand side of (5.33) is upper bounded by L . From (5.8) it follows that each term individually can be at most one. Therefore, it is sufficient to show that at most L terms in (5.33) can be made positive. By Lemma 5.12, this number is exactly the size of the maximum independent set in the constraint graph $(E, \mathcal{J}_{B/M})$,

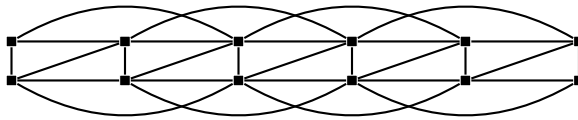
²A more common form of the cut-set bound is to introduce a time-sharing variable and perform an averaging argument instead of taking the maximum over t on the RHS. In general, however, the averaged distribution does not satisfy the condition that $P(X_\nu = \sigma) \in \{0, 1\}$ for all $\nu \in V$.



(a) Constraint graph $(E, \mathcal{J}_{B/M})$ for the line network, where E is represented by square shaped nodes and $\mathcal{J}_{B/M}$ by solid lines. Moreover, the line network (V, E) is depicted by circle shaped nodes and dotted lines.



(b) (E, \mathcal{J}') , where $\mathcal{J}' \subset \mathcal{J}_{B/M}$.



(c) Constraint graph $(E, \mathcal{J}_{B/P})$ for the line network. (V, E) is now omitted for clarity.



(d) (E, \mathcal{J}') , where $\mathcal{J}' \subset \mathcal{J}_{B/P}$.

Figure 5.6: Line network. Interference relations under the B/M and B/P models.

which is depicted in Figure 5.6a. Since the size of the maximum independent set can not decrease in size by removing some of the edges of $(E, \mathcal{J}_{B/M})$, we consider the graph given in 5.6b. Since this graph consists of disjoint components which are cliques, the maximum independent set is upper bound by the number of components, which is L . \square

The following lemma establishes the upper bound of Theorem 5.2.

Lemma 5.14. *The transport capacity $C_{B/P}^{\text{line}}(L)$ of the $L + 1$ node line network under the B/P model is upper bounded by*

$$C_{B/P}^{\text{line}}(L) \leq \left\lceil \frac{2}{3}L \right\rceil.$$

Proof. We apply Lemma 5.11 by starting from (5.33) and considering the constraint graph $(E, \mathcal{J}_{B/P})$ as given in Figure 5.6c. Again, by removing edges we get the graph depicted in Figure 5.6d, which consists of disjoint components which are cliques. In counting the number of cliques we need to take into account edge effects. It can easily be verified that we have $2 \left\lfloor \frac{L}{3} \right\rfloor + (L \bmod 3) = \left\lceil \frac{2L}{3} \right\rceil$ cliques. \square

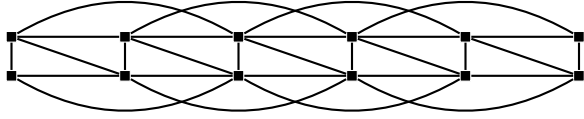
The following lemma establishes the upper bound of Theorem 5.3.

Lemma 5.15. *The transport capacity $C_{P/M}^{\text{line}}(L)$ of the $L + 1$ node line network under the P/M model is upper bounded by*

$$C_{P/M}^{\text{line}}(L) \leq \left\lceil \frac{2}{3}L \right\rceil.$$

Proof. We apply Lemma 5.10 by starting from (5.33) and considering the constraint graph $(E, \mathcal{J}_{P/M})$ as given in Figure 5.7a. Again, by removing edges we get the graph depicted in Figure 5.7b, which consists of disjoint components which are cliques. Now, by similarity to Figure 5.6d, the size of the maximum independent set equals that of the B/P case. \square

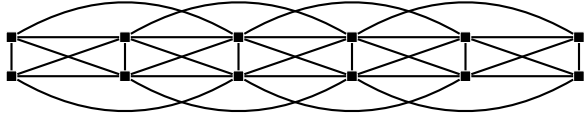
The following lemma establishes the upper bound of Theorem 5.1.



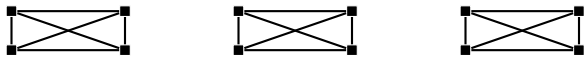
(a) Constraint graph $(E, \mathcal{J}_{P/M})$ for the line network.



(b) (E, \mathcal{J}') , where $\mathcal{J}' \subset \mathcal{J}_{P/M}$.



(c) Constraint graph $(E, \mathcal{J}_{P/P})$ for the line network.



(d) (E, \mathcal{J}') , where $\mathcal{J}' \subset \mathcal{J}_{P/P}$.

Figure 5.7: Line network. Interference relations under the P/M and P/P models.

Lemma 5.16. *The transport capacity $C_{P/P}^{\text{line}}(L)$ of the $L + 1$ node line network under the P/P model is upper bounded by*

$$C_{P/P}^{\text{line}}(L) \leq \left\lceil \frac{1}{2}L \right\rceil.$$

Proof. We apply Lemma 5.9 by starting from (5.33) and considering the constraint graph $(E, \mathcal{J}_{P/P})$ as given in Figure 5.7c. Again, by removing links we get the graph depicted in Figure 5.7d, which consists of disjoint components which are cliques. It can easily be verified that we have $\lfloor \frac{L}{2} \rfloor + (L \bmod 2) = \lceil \frac{L}{2} \rceil$ cliques. \square

5.5.3 Hexagonal Lattice

In this section we establish the upper bounds of Theorems 5.5–5.8. The following lemma establishes the upper bound of Theorem 5.8.

Lemma 5.17. *The transport capacity $C_{B/M}^{\text{hex}}(L, M)$ of the $(L + 1) \times (M + 1)$ node hexagonal network under the B/M model is upper bounded by*

$$C_{B/M}^{\text{hex}}(L, M) \leq 2LM + 2(L + M).$$

Proof. Consider the cuts

$$\Gamma_i^1 = \{(u_1, u_2) \in V \mid u_1 \leq i\}, \quad i = 0, \dots, L - 1, \quad (5.34)$$

$$\Gamma_i^2 = \{(u_1, u_2) \in V \mid u_2 \leq i\}, \quad i = 0, \dots, M - 1, \quad (5.35)$$

$$\Gamma_i^3 = \{(u_1, u_2) \in V \mid u_1 + u_2 \leq i\}, \quad i = 0, \dots, L + M - 1. \quad (5.36)$$

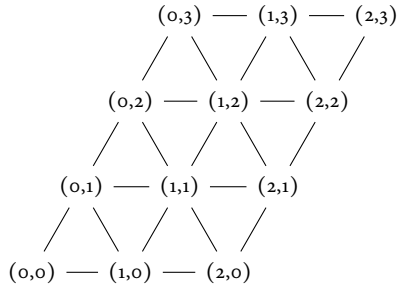
Let

$$\mathcal{S} = \{\Gamma_i^1, \bar{\Gamma}_i^1\}_{i=0}^{L-1} \cup \{\Gamma_i^2, \bar{\Gamma}_i^2\}_{i=0}^{M-1} \cup \{\Gamma_i^3, \bar{\Gamma}_i^3\}_{i=0}^{L+M-1}, \quad (5.37)$$

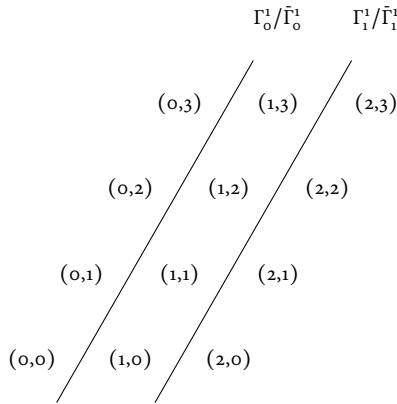
where we have used the notation $\bar{\Gamma}_i^j = V \setminus \Gamma_i^j$. Figure 5.8 on the next page depicts (V, E) and the lines inducing the cuts in \mathcal{S} .

Since on the shortest path between two nodes, the number of cuts crossed on each hop is 2 and no cut is crossed more than once,

$$\sum_{S \in \mathcal{S}} \sum_{k \in K_S} R_k = 2 \sum_{k=1}^K \text{dist}(S_k, D_k) R_k. \quad (5.38)$$

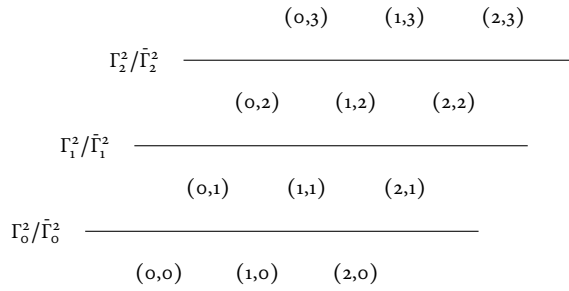


(a) Hexagonal network (V, E) for $L = 2, M = 3$.

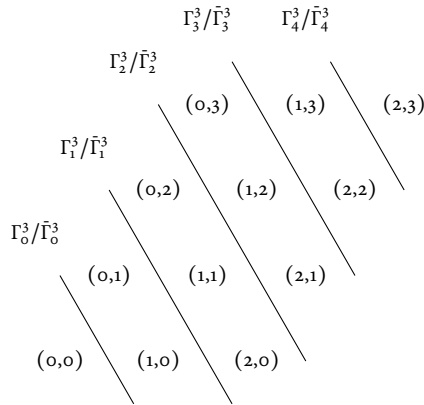


(b) Lines inducing the partitions Γ_i^1 and $\bar{\Gamma}_i^1, i = 0, \dots, L - 1$.

Figure 5.8: Hexagonal network with vertices located at the hexagonal lattices and edges between nearest neighbours. Moreover, lines inducing the cuts used to upper bound its transport capacity.



(c) Lines inducing the partitions Γ_i^2 and $\bar{\Gamma}_i^2$, $i = 0, \dots, M - 1$.



(d) Lines inducing the partitions Γ_i^3 and $\bar{\Gamma}_i^3$, $i = 0, \dots, L + M - 1$.

Figure 5.8: (Cont'd) Hexagonal network with vertices located at the hexagonal lattices and edges between nearest neighbours. Moreover, lines inducing the cuts used to upper bound its transport capacity.

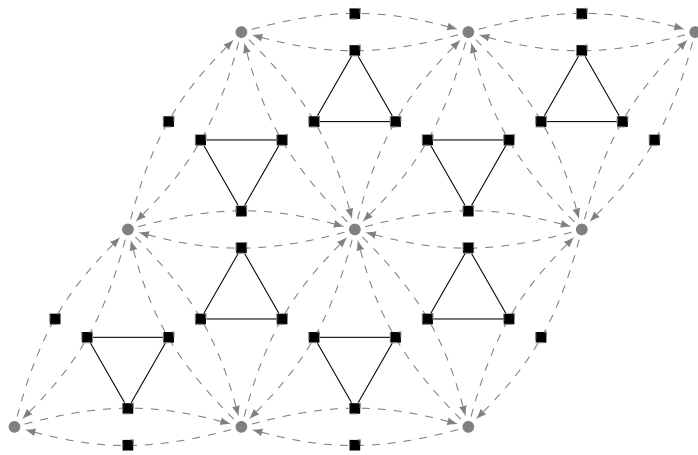


Figure 5.9: Subgraph of the constraint graph $(E, \mathcal{J}_{B/M})$. Depicted are (E, \mathcal{J}') , $\mathcal{J}' \subset \mathcal{J}_{B/M}$, with E as square vertices and \mathcal{J}' as solid lines and the hexagonal network (V, E) in round vertices and dashed lines.

Developing a cut-set bound in similar fashion to the proof of Lemma 5.13 and summing over all cuts leads to

$$2 \sum_{k=1}^K \text{dist}(S_k, D_k) R_k \leq \sum_{i=0}^{L-1} [I(X_i^{\Gamma^1}; Y_i^{\bar{\Gamma}^1} | X_i^{\bar{\Gamma}^1}) + I(X_i^{\bar{\Gamma}^1}; Y_i^{\Gamma^1} | X_i^{\Gamma^1})] \quad (5.39)$$

$$+ \sum_{i=0}^{M-1} [I(X_i^{\Gamma^2}; Y_i^{\bar{\Gamma}^2} | X_i^{\bar{\Gamma}^2}) + I(X_i^{\bar{\Gamma}^2}; Y_i^{\Gamma^2} | X_i^{\Gamma^2})] \quad (5.40)$$

$$+ \sum_{i=0}^{L+M-1} [I(X_i^{\Gamma^3}; Y_i^{\bar{\Gamma}^3} | X_i^{\bar{\Gamma}^3}) + I(X_i^{\bar{\Gamma}^3}; Y_i^{\Gamma^3} | X_i^{\Gamma^3})], \quad (5.41)$$

which is the equivalent of (5.32). By decomposing the mutual information terms on the RHS we obtain

$$\sum_{k=1}^K \text{dist}(S_k, D_k) R_k \leq \frac{1}{2} \sum_{(u,v) \in E} \left[I(X_u; Y_v | X^{A(u,v)}, Y^{B(u,v)}) \right. \\ \left. + I(X_v; Y_u | X^{C(u,v)}, Y^{D(u,v)}) \right]. \quad (5.42)$$

The sets $A(u, v)$, $B(u, v)$, $C(u, v)$ and $D(u, v)$ capture the conditioning terms. We will apply Lemma 5.12 which does not depend on the conditioning. Therefore, these sets do not affect the remainder and we will leave them unspecified. From (5.42) and Lemma 5.12 it follows that the transport capacity is upper bounded by the size of the maximum independent set in the constraint graph $(E, \mathcal{J}_{B/M})$. Note that any 3-cycle in the hexagonal network (V, E) forms a clique in the constraint graph $(E, \mathcal{J}_{B/M})$. Therefore, we construct a set $\mathcal{J}' \subset \mathcal{J}_{B/M}$ consisting of 3-cycles and some unconnected nodes. Figure 5.9 depicts \mathcal{J}' . It can be readily verified that there are $2LM$ cycles and $2(L+M)$ unconnected nodes. Therefore, the size of the maximum independent set is upper bounded by $2LM + 2(L+M)$. \square

The following lemma establishes the upper bound of Theorem 5.7.

Lemma 5.18. *The transport capacity $C_{B/P}^{\text{hex}}(L, M)$ of the $(L+1) \times (M+1)$ node hexagonal network under the B/P model is upper bounded by*

$$C_{B/P}^{\text{hex}}(L, M) \leq \frac{6}{7}LM + o(LM).$$

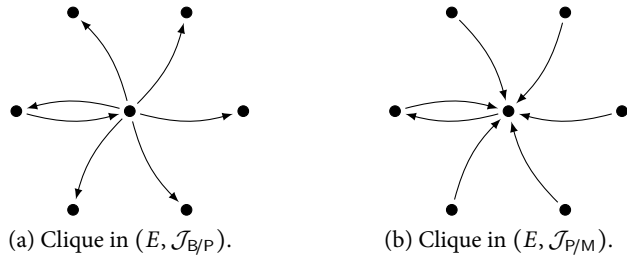


Figure 5.10: Subgraphs of the hexagonal network such that the edges form a clique in the constraint graph $(E, \mathcal{J}_{B/P})$ and $(E, \mathcal{J}_{P/M})$ respectively.

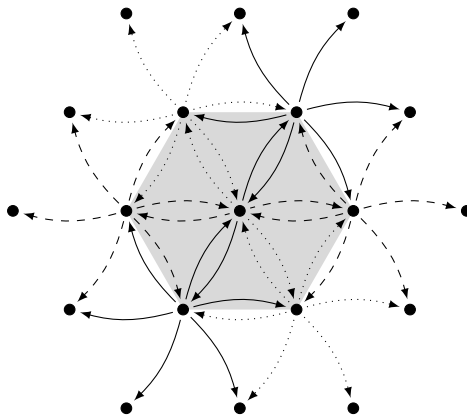


Figure 5.11: Six cliques as given in 5.10a.

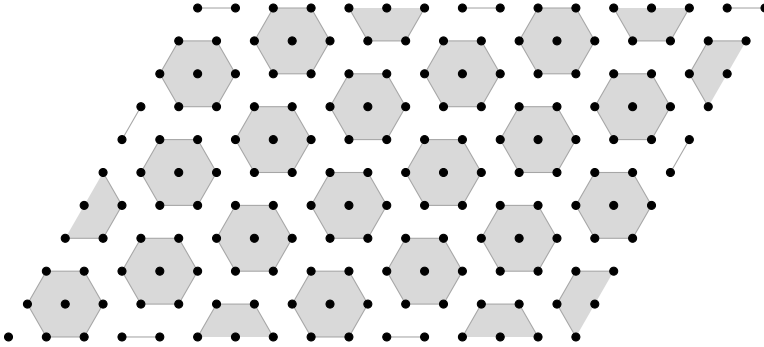


Figure 5.12: Tiling the structure from 5.11.

Proof. We use the same line of proof as used for Lemma 5.17. The set of edges depicted in Figure 5.10a form a clique in the constraint graph $(E, \mathcal{J}_{B/P})$. Figures 5.11 and 5.12 illustrate that based on this clique the size of the maximum independent set of $(E, \mathcal{J}_{B/P})$ can be upper bounded by $\frac{6}{7}LM + o(LM)$. In Figure 5.11 six cliques from Figure 5.10a are depicted. In Figure 5.12 the resulting graph is tiled around the hexagonal network, ensuring that all edges are covered exactly once. \square

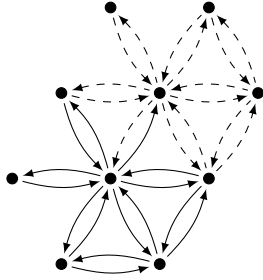
The following lemma establishes the upper bound of Theorem 5.6.

Lemma 5.19. *The transport capacity $C_{P/M}^{\text{hex}}(L, M)$ of the $(L+1) \times (M+1)$ node hexagonal network under the P/M model is upper bounded by*

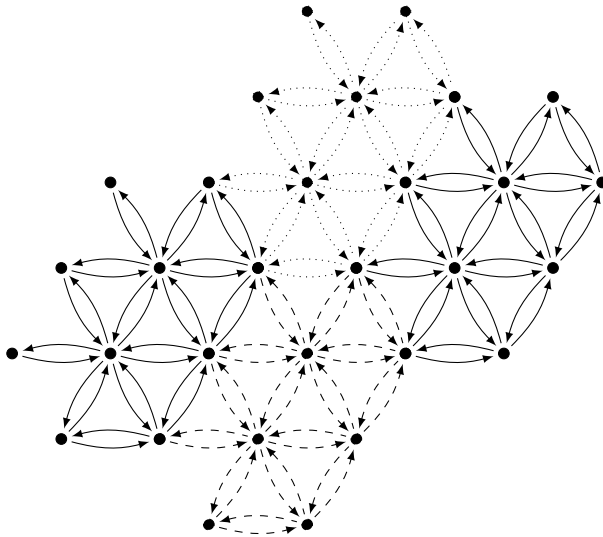
$$C_{P/M}^{\text{hex}}(L, M) \leq \frac{6}{7}LM + o(LM).$$

Proof. This result follows using the proof of Lemma 5.18 with the edges from Figure 5.10b as a clique and a tiling of cliques as depicted in Figures 5.11 and 5.12. \square

The following lemma establishes the upper bound of Theorem 5.5.



(a) Two cliques of $(E, \mathcal{J}_{P/P})$.



(b) Tiling the structure of (a).

Figure 5.13: Subgraphs of the hexagonal network for which the edges form a clique in the constraint graph $(E, \mathcal{J}_{P/P})$.

Lemma 5.20. *The transport capacity $C_{P/P}^{\text{hex}}(L, M)$ of the $(L + 1) \times (M + 1)$ node hexagonal network under the P/P model is upper bounded by*

$$C_{P/P}^{\text{hex}}(L, M) \leq \frac{2}{5}LM + o(LM).$$

Proof. Again, we use the same line of proof as used for Lemma 5.17. Consider the set of edges depicted in Figure 5.13a. The set is partitioned in two, such that the edges in each partition form a clique in the constraint graph $(E, \mathcal{J}_{P/P})$. This means that the size of the maximum independent set of this subset of $(E, \mathcal{J}_{P/P})$ is 2. Also, the set of edges from Figure 5.13a can be tiled around in such a way that all edges in (V, E) are covered exactly once. This is depicted in Figure 5.13b. From Figure 5.13b it is clear that the number of times that the set from Figure 5.13a is used in the tiling is $LM/5 + o(LM)$. Hence the size of the maximum independent set is at most $\frac{2}{5}LM + o(LM)$. \square

5.6 Achievable Schemes

5.6.1 Line Network

In this section we establish the lower bounds of Theorems 5.1–5.4. The following lemma establishes the lower bound of Theorem 5.4.

Lemma 5.21. *The transport capacity $C_{B/M}^{\text{line}}(L)$ of the $L + 1$ node line network under the B/M model satisfies*

$$C_{B/M}^{\text{line}}(L) \geq L.$$

Proof. We consider the multiple unicast configuration in which two sessions have sources and receivers at the endpoints of the network, *i.e.*,

$$\begin{aligned} S_1 &= 0, & D_1 &= L, \\ S_2 &= L, & D_2 &= 0. \end{aligned} \tag{5.43}$$

Let $\{m[t]\}$ and $\{\bar{m}[t]\}$ be the sequence of source symbols transmitted by S_1 and S_2 respectively. We will show that the nodes in the network are able to operate in such a fashion that the symbols transmitted are as depicted in Figure 5.14.

Communication proceeds in rounds. Each round consists of two time slots. In the first time slot the even nodes transmit; in the second time slot the odd nodes transmit. Round o starts at time slot o . Let $\tilde{x}_i[r]$ be the symbol transmitted by node i in round r . This gives

$$x_i[t] = \begin{cases} \tilde{x}_i[\lfloor t/2 \rfloor], & \text{if } t \equiv i \pmod{2}, \\ \sigma, & \text{otherwise.} \end{cases} \quad (5.44)$$

Note, that each node receives one useful symbol in each round. Each node is transmitting in one of the time slots in each round and is not able to receive due to half-duplex constraints. Let $\tilde{y}_i[r]$ denote the symbol received by node i in round r . It is readily verified that $\tilde{y}_i[r] = \tilde{x}_{i-1}[r]\mathbf{1}_{\{i>0\}} + \tilde{x}_{i+1}[r]\mathbf{1}_{\{i<L\}}$.

Now we specify what symbols $\tilde{x}_i[r]$ are transmitted. In round o the only non-zero symbols that are transmitted are $\tilde{x}_o[o] = m[o]$ and $\tilde{x}_L[o] = \tilde{m}[o]$. In the next rounds coding occurs as follows

$$\tilde{x}_i[r] = \begin{cases} m[r] + \tilde{m}[r-L], & \text{if } i = o, \\ \tilde{y}_i[r-1] - \tilde{x}_i[r-2], & \text{if } o < i < L, \\ \tilde{m}[r] + m[r-L], & \text{if } i = L, \end{cases} \quad (5.45)$$

with the convention that $m[r-L]$ and $\tilde{m}[r-L]$ are o for $r < L$. Note, that it is implied by (5.45), that node o (L), which is the receiver R_1 (R_2), has properly decoded source symbol $\tilde{m}[r-L]$ ($m[r-L]$) before starting round r . We will need to verify that the receivers are actually able to decode. Using induction over the rounds, however, we can easily verify that

$$\tilde{x}_i[r] = m[r-i] + \tilde{m}[r-L+i], \quad (5.46)$$

as also reflected in Figure 5.14.

The decoding procedure for $\tilde{m}[r-L]$ by node o at the end of round $r-1$ is

$$\tilde{m}[r-L] = \tilde{y}_o[r-1] - m[r-2], \quad (5.47)$$

which follows by $\tilde{y}_o[r-1] - m[r-2] = \tilde{x}_1[r-1] - m[r-2] = m[r-2] + \tilde{m}[r-L] - m[r-2] = \tilde{m}[r-L]$. In similar fashion it follows that the decoding procedure for $m[r-L]$ by node L at the end of round $r-1$ is

$$m[r-L] = \tilde{y}_L[r-1] - \tilde{m}[r-2]. \quad (5.48)$$

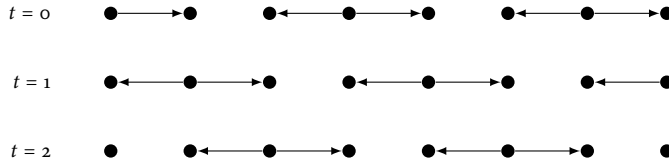


Figure 5.15: Transmission schedule for one round in the achievable scheme for the line network under B/P.

In each round one symbol for each session is transmitted and successfully decoded some rounds later. The number of time slots per session is 2. Hence, the throughput for both sessions equals $1/2$. For each session we have $|S_k - D_k| = L$, hence the transport capacity is lower bounded by L . \square

The following lemma establishes the lower bound of Theorem 5.2.

Lemma 5.22. *The transport capacity $C_{\text{B/P}}^{\text{line}}(L)$ of the $L + 1$ node line network under the B/P model satisfies*

$$C_{\text{B/P}}^{\text{line}}(L) \geq \frac{2}{3}L.$$

Proof. We consider the same multiple unicast configuration as used in the proof of Lemma 5.21, *i.e.*, according to (5.43), with two sessions that have sources and receivers at the endpoints of the network. Many elements, in particular notation, of the proof are the same as the proof of Lemma 5.21. The scheme operates in rounds of *three* time slots. Again operation is such that each node is transmitting exactly once in each round, *i.e.*,

$$x_i[t] = \begin{cases} \tilde{x}_i[\lfloor t/3 \rfloor], & \text{if } t \equiv i \pmod{3}, \\ \sigma, & \text{otherwise,} \end{cases} \quad (5.49)$$

where $\tilde{x}_i[r]$ is the symbol transmitted by node i in round r . The scheduling is illustrated in Figure 5.15. As a consequence of (5.49) each node that is not at the border of the network receives two symbols in each round. Let $\tilde{y}_i[r]$ denote the sum (over \mathbb{F}_q) of the received symbols. Now, we proceed along

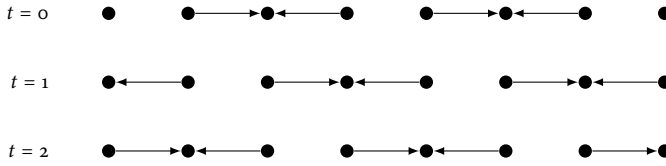


Figure 5.16: Transmission schedule for one round in the achievable scheme for the line network under P/M.

the lines of the proof of Lemma 5.21: coding is according to (5.45) and relations (5.46), (5.47) and (5.48) hold. Hence, the two sessions achieve throughput $\frac{1}{3}$ symbols per time slot over distance L , leading to a lower bound of $\frac{2}{3}L$ symbols×hops per time slot on the transport capacity. \square

The scheme given for the proof of Lemma 5.22 is essentially the same as used for the proof of Lemma 5.21. The main difference is in the scheduling of the transmissions. The next lemma provides the lower bound required for Theorem 5.3. Again the scheme is essentially the same as above.

Lemma 5.23. *The transport capacity $C_{P/M}^{\text{line}}(L)$ of the $L + 1$ node line network under the P/M model satisfies*

$$C_{P/M}^{\text{line}}(L) \geq \frac{2}{3}L.$$

Proof. We continue with the configuration and notation used in the proof of Lemmas 5.21 and 5.22. Rounds consist of three time slots, with node i transmitting the symbol $\tilde{x}_i[r]$ in round r . More precisely, we have

$$x_i[t] = \begin{cases} \tilde{x}_i[\lfloor t/3 \rfloor], & \text{if } (i - t) \equiv 0 \pmod{3} \text{ and } i > 0, \\ \tilde{x}_i[\lfloor t/3 \rfloor], & \text{if } (i - t) \equiv 1 \pmod{3} \text{ and } i < L, \\ \sigma, & \text{otherwise.} \end{cases} \quad (5.50)$$

Note that this means that nodes $1, \dots, L - 1$ transmit the same symbol twice in each round. Nodes 0 and L transmit only once. Let $a_i[t]$ denote the neighbour that i is transmitting to in time slot t . We need to define $a_i[t]$ only for

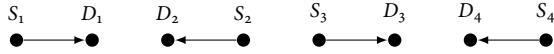


Figure 5.17: Configuration of unicast sessions, that is used to achieve $\lceil L/2 \rceil$ symbols \times hops per time slot under P/P.

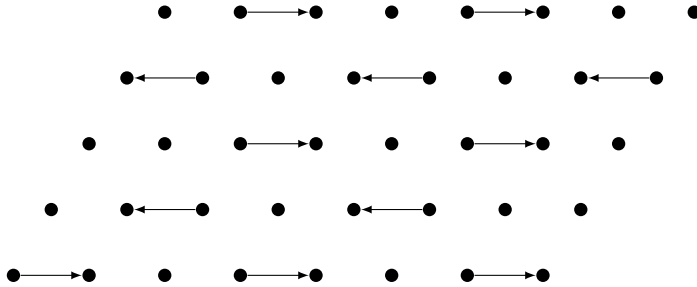


Figure 5.18: Configuration of unicast sessions on the hexagonal lattice, used to achieve $LM/3 + o(LM)$ symbols \times hops per time slot under P/P.

those time slots in which a node is transmitting. We use

$$a_i[t] = \begin{cases} i - 1, & \text{if } (i - t) \equiv 0 \pmod{3}, \\ i + 1, & \text{if } (i - t) \equiv 1 \pmod{3}, \end{cases} \quad (5.51)$$

leading to the transmission schedule depicted in Figure 5.16. Now we perform coding and decoding according to (5.45)–(5.48). Since rounds consist of three time slots, we achieve $\frac{2}{3}L$ symbols×hops per time slot. \square

Lemma 5.24. *The transport capacity $C_{P/P}^{\text{line}}(L)$ of the $L + 1$ node line network under the P/P model satisfies*

$$C_{P/P}^{\text{line}}(L) \geq \left\lfloor \frac{1}{2}L \right\rfloor.$$

Proof. Let unicast sessions be given as depicted in Figure 5.17. The number of sessions equals $\lceil L/2 \rceil$. The sources of all sessions can transmit simultaneously without causing interference. Therefore, the number of symbols×hops per time slot that is achieved equals the number of sessions, $\lceil L/2 \rceil$. No (de)coding is required since all sinks receive uncoded information directly from their source. \square

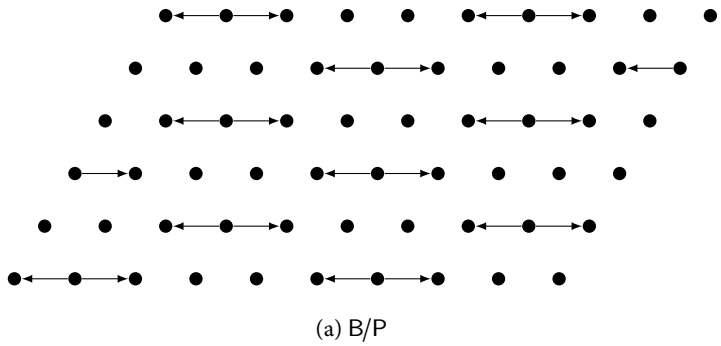
5.6.2 Hexagonal Lattice

In this section we give constructive schemes on the hexagonal lattice, providing proofs for the achievable part of Theorems 5.5–5.8. The next lemma provides the lower bound required for Theorem 5.5.

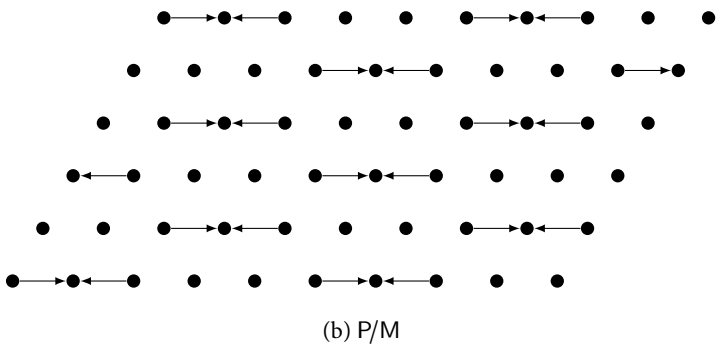
Lemma 5.25. *The transport capacity $C_{P/P}^{\text{hex}}(L, M)$ of the $(L + 1) \times (M + 1)$ node hexagonal network under the P/P model satisfies*

$$C_{P/P}^{\text{hex}}(L, M) \geq \frac{1}{3}LM + o(LM).$$

Proof. Let unicast sessions be given as depicted in Figure 5.18. The number of sessions equals $LM/3 + o(LM)$. The sources of all sessions can transmit simultaneously without causing interference at the destinations. Therefore,



(a) B/P



(b) P/M

Figure 5.19: A valid scheduling of transmissions under the B/P and P/M models.

the number of symbols×hops per time slot that is achieved equals the number of sessions, $LM/3 + o(LM)$. No (de)coding is required since all sinks receive uncoded information directly from their source. \square

The next lemma provides the lower bound required for Theorem 5.7.

Lemma 5.26. *The transport capacity $C_{\text{B/P}}^{\text{hex}}(L, M)$ of the $(L+1) \times (M+1)$ node hexagonal network under the B/P model is at least*

$$C_{\text{B/P}}^{\text{hex}}(L, M) \geq \frac{2}{5}L(M+1).$$

Proof. Consider $2(M+1)$ unicast sessions with sources and sinks at the left and right borders of the network, i.e., $S_k = (o, k)$, $D_k = (L, k)$ for $k = o, \dots, M$ and $S_{\bar{k}} = (L, \bar{k})$, $D_{\bar{k}} = (o, \bar{k})$ for $\bar{k} = M+1, \dots, 2M+1$. Consider a scheduling of transmissions as depicted in Figure 5.19a. By using 5 time slots and shifting this pattern of scheduled transmissions around, each node is transmitting to its left and right neighbour exactly once in each round. Now, using the scheme given in the proof of Lemma 5.22, we achieve a throughput of $1/5$ for each session. In total there are $2(M+1)$ sessions over distance L . \square

The next lemma provides the lower bound required for Theorem 5.6.

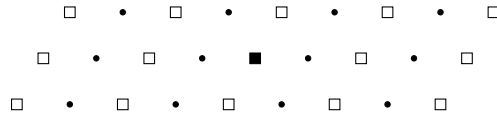
Lemma 5.27. *The transport capacity $C_{\text{P/M}}^{\text{hex}}(L, M)$ of the $(L+1) \times (M+1)$ node hexagonal network under the P/M model satisfies*

$$C_{\text{P/M}}^{\text{hex}}(L, M) \geq \frac{2}{5}L(M+1).$$

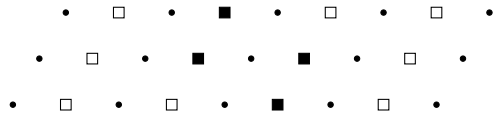
Proof. The proof is along the lines of the proof of Lemma 5.26, but with a scheduling as depicted in Figure 5.19b and the line network coding scheme from Lemma 5.23. \square

Note that in the previous two lemmas we can also achieve $\frac{2}{5}(L+1)M$ by considering sessions from top to bottom and vice versa. Both lead to $\frac{2}{5}LM + o(LM)$ symbols×hops per time slot as given in the statement of Theorems 5.6 and 5.7.

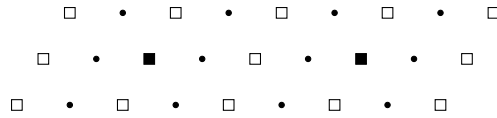
Finally we present an achievable scheme for the B/M model, providing a proof for the lower bound of Theorem 5.8. The achievable scheme for the



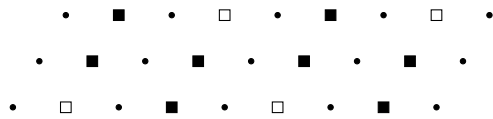
(a) $t = 0$



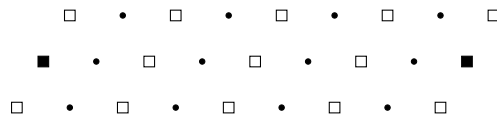
(b) $t = 1$



(c) $t = 2$



(d) $t = 3$



(e) $t = 4$

Figure 5.20: Illustrating even-odd scheduling and simple retransmissions over \mathbb{F}_2 under B/M. Nodes that are transmitting are depicted by square vertices. Filled vertices are transmitting a symbol, other vertices transmit zero.

B/M model is constructed based on a simple transmission scheme, consisting of the following elements:

Even-odd scheduling: Transmissions are scheduled in such a way that node (u_1, u_2) transmits in time slot t iff $u_1 \equiv t \pmod{2}$.

Simple retransmissions: All symbols are from \mathbb{F}_2 . Nodes retransmit what they have received in the previous time slot. Since we operate under B/M this is the sum of what has been transmitted by its neighbours.

Even-odd scheduling and simple retransmissions are illustrated in Figure 5.20 for the special case of $L = 8$ and $M = 2$. In the figure one can observe that a symbol that is initially transmitted by one node will be retransmitted four time slots later by exactly two other nodes. This is made precise in the following lemma which we will prove in Appendix 5.A.

Lemma 5.28. *Assume even-odd scheduling and simple retransmissions over \mathbb{F}_2 on the $(L + 1) \times (M + 1)$ hexagonal network, where $M = 2^\kappa - 2$, $\kappa \geq 2$ and $L \geq 2^{\kappa+1}$. Let $2^\kappa \leq u_1 \leq L - 2^\kappa$, even, and $0 \leq u_2 \leq M$. Suppose that in time slot $t = 0$ node (u_1, u_2) transmits a symbol m and all other nodes transmit 0. Then, at time $t = 2^\kappa$, nodes $(u_1 - 2^\kappa, u_2)$ and $(u_1 + 2^\kappa, u_2)$ transmit m and all other nodes transmit 0.*

Note that the height of the network, *i.e.*, the value of M , is critical. The result does not hold for arbitrary values of M . Using the even-odd scheduling, the simple retransmission scheme and the above result we are now ready to prove the lower bound of Theorem 5.8.

Lemma 5.29. *Assume $q = 2$. The transport capacity $C_{B/M}^{\text{hex}}(L, M)$ of the $(L + 1) \times (M + 1)$ node hexagonal network under the B/M model satisfies*

$$C_{B/M}^{\text{hex}}(L, M) \geq LM + o(LM).$$

Proof. Assume for the moment that

$$M = 2^\kappa - 2, \quad \text{and} \quad L = (a + 2) \cdot 2^\kappa - 2, \quad (5.52)$$

for integers $\kappa \geq 2$ and $a \geq 1$. The network is operated in rounds of 2^κ time slots. In the first time slot of a round each node transmits according to a coding

scheme that will be specified below. In the remaining time slots operation of the network is restricted to even-odd scheduling and simple retransmissions. The symbols that are received in the final time slot of a round are stored, the other symbols are discarded. From Lemma 5.28 and linearity of the coding operations it follows that employing even-odd scheduling and simple retransmissions decomposes the network into independent line networks that are operated in rounds of 2^κ time slots. More precisely, for each $0 \leq c_1 \leq 2^{\kappa-1} - 1$ and $0 \leq c_2 \leq 2^\kappa - 2$ we have an ‘induced line network’ consisting of the points

$$(2^\kappa + 2c_1, c_2), (2 \cdot 2^\kappa + 2c_1, c_2), (3 \cdot 2^\kappa + 2c_1, c_2), \dots, (a \cdot 2^\kappa + 2c_1, c_2). \quad (5.53)$$

The choice of L in (5.52) comes from the fact that for point $(a \cdot 2^\kappa + 2^\kappa - 2, u_2)$ of the line network with $c_1 = 2^{\kappa-1} - 1$ and $c_2 = u_2$, we need

$$a \cdot 2^\kappa + 2^\kappa - 2 \leq L - 2^\kappa \quad (5.54)$$

in order to apply Lemma 5.28.

There are $2^{\kappa-1}(2^\kappa - 1)$ induced line networks, each of size a . Note, that these line networks do not have any half-duplex constraints. This means that for each induced line network, the achievable strategy used in Lemma 5.21 can be extended to a strategy in which all transmissions are scheduled simultaneously. For each ‘induced line network’ this leads to 2 sessions, each operating at throughput 1 symbol per round, transmitting over a distance of $a - 1$ ‘induced hops’. Hence, each induced line network supports $2(a - 1)$ symbols×‘induced hops’ per round. Since the length of an induced hop is 2^κ , and the length of a round is 2^κ time slots, it follows that the capacity of the hexagonal network is lower bounded by

$$2(a - 1)2^{\kappa-1} (2^\kappa - 1) 2^\kappa 2^{-\kappa} = (a - 1)2^\kappa (2^\kappa - 1) \quad (5.55)$$

symbols×hops per time slot.

Finally, we relax constraint (5.52) and consider the case of arbitrary (large) L and M . The scheme that was developed above, will be applied to disjoint subsets of the network of size $(L' + 1) \times (M' + 1)$, where

$$M' = 2^\kappa - 2, \text{ and } L' = (a + 2) \cdot 2^\kappa - 2, \quad (5.56)$$

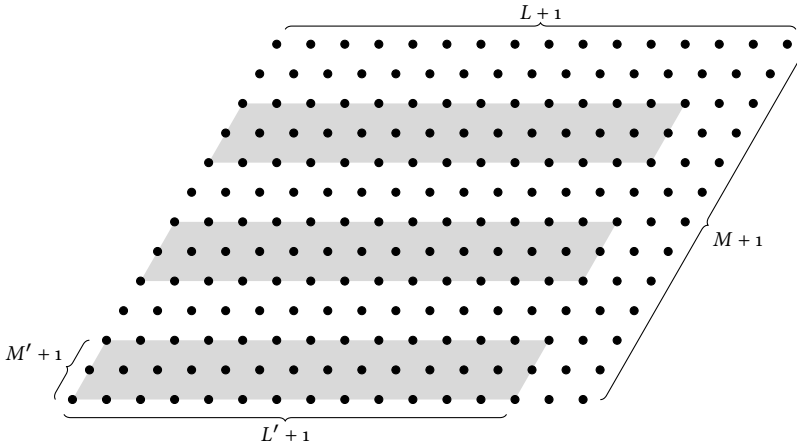


Figure 5.21: Subsets of size $(L' + 1) \times (M' + 1)$.

with

$$\kappa = \lfloor \log_2 \log_2 (M + 1) \rfloor, \quad (5.57)$$

and

$$a = \max \{ a' \in \mathbb{N} \mid (a' + 2)2^\kappa - 2 \leq L \} = \left\lfloor \frac{L + 2}{2^\kappa} \right\rfloor - 2. \quad (5.58)$$

These subsets are chosen in such a way that they are separated by one horizontal line of nodes that remain silent and are not used. The idea is depicted in Figure 5.21. Note that the condition $M \geq 15$ ensures $\kappa \geq 2$. We observe that the number of subsets created equals

$$b = \left\lfloor \frac{M + 1}{2^\kappa} \right\rfloor. \quad (5.59)$$

In each subset of size $(L' + 1) \times (M' + 1)$ the number of symbols×hops per time slot that is achieved is given by (5.55). Hence, combining (5.55), (5.57), (5.58) and (5.59), the number of symbols×hops per time slot that is achieved

in the whole network of size $(L + 1) \times (M + 1)$ equals

$$\begin{aligned}
 b(a-1)2^\kappa(2^\kappa-1) &= \left\lfloor \frac{M+1}{2^\kappa} \right\rfloor \left(\left\lfloor \frac{L+2}{2^\kappa} \right\rfloor - 3 \right) 2^\kappa (2^\kappa - 1) \\
 &\geq \left(\frac{M+1}{2^\kappa} - 1 \right) \left(\frac{L+2}{2^\kappa} - 4 \right) 2^\kappa (2^\kappa - 1) \\
 &= (M+1-2^\kappa)(L+2-2^{\kappa+2})(1-2^{-\kappa}) \\
 &\geq (M+1-\log_2(1+M))(L+2 \\
 &\quad - 4\log_2(1+M)) \left(1 - \frac{1}{\frac{1}{2}\log_2(1+M)} \right) \\
 &= LM + o(LM). \quad \square
 \end{aligned}$$

5.7 Extension to Gaussian Models

The main results of this work are Theorems 5.1–5.4 and 5.5–5.8 from Section ???. These results give bounds on the capacity of networks with a deterministic communication model, as defined in Section 2.2. Our main results can be used to infer results for networks with more intricate communication models by a two-step procedure. In the first step, the more intricate communication model is reduced to one of the four deterministic models. This step will typically involve suitable error-correcting codes. In the second step, using the reduced network model, the results of this chapter can be directly applied. In this section, we give an outline of this procedure for a simple Gaussian model with local interference.

5.7.1 Gaussian Model

We propose to consider a particularly simple Gaussian model with local interference only, as follows. Consider a set of nodes V , each $v \in V$ with a neighborhood N_v . The signal received by $v \in V$ is given by

$$Y_v = \tilde{Z}_v + \sum_{u \in N_v \setminus \{v\}} \frac{1}{d_{uv}^{\alpha/2}} X_u, \quad (5.60)$$

where \tilde{Z}_v is i.i.d. Gaussian noise of zero mean and unit variance, α is the path loss exponent, and d_{uv} denotes the distance between nodes u and v .

The transmitted signals X_u are assumed to be individually power-constrained with power P . In the remainder we will consider a line network in which all distances between neighbours are equal, and thus, we will set $d_{uv} = 1$, without loss of generality. For the $L + 1$ node Gaussian line network (5.60) reduces to

$$Y_i = \begin{cases} \tilde{Z}_0 + X_1, & \text{if } i = 0 \\ \tilde{Z}_i + X_{i-1} + X_{i+1}, & \text{if } 0 < i < L \\ \tilde{Z}_L + X_{L-1}, & \text{if } i = L. \end{cases} \quad (5.61)$$

5.7.2 P/P Model

In this section we will outline how the Gaussian line network can be reduced to the P/P model. In the first step of the procedure we need to find suitable error correcting codes that turn the network into a reliable point-to-point link. Obviously, standard error correcting codes can be used. It remains to determine the maximum rate that can be achieved on each link. Since, under the P/P model, all interference is avoided, this maximum rate is simply the standard AWGN capacity. The second step of the procedure involves application of Theorem 5.1. Note that Theorem 5.1 is based on the assumption that the link capacity is one. Taking into account that in the reduced Gaussian model the link capacity is

$$\frac{1}{2} \log_q (1 + P) \quad (5.62)$$

q -ary symbols per time slot, it follows from Theorem 5.1 that the resulting transport capacity is

$$C_{P/P}^{\text{line}}(L, P) = \left\lceil \frac{1}{2}L \right\rceil \frac{1}{2} \log_q (1 + P) \quad (5.63)$$

q -ary symbols \times hops per time slot.

5.7.3 B/M Model

The reduction of the Gaussian model to a P/P model involves only the use of standard error correcting codes. More interestingly, exploiting recent advances, we can also reduce the Gaussian network to the B/M model. In particular, consider the single multiple-access channel to node i , with $0 < i < L$,

as in (5.61). Transmitters $i - 1$ and $i + 1$ both have a q -ary message. Now suppose that the receiver attempts to decode the sum of both q -ary messages. This problem has been studied in [64], where it was shown that the maximum achievable rate R for which the sum can be reliably decoded satisfies

$$\frac{1}{2} \log_q \left(\frac{1}{2} + P \right) \leq R \leq \frac{1}{2} \log_q (1 + P). \quad (5.64)$$

We note that this involves the use of lattice codes in a particular fashion, but we refer the reader to [64] for further details. Using this formula and Theorem 5.4, we can infer that

$$C_{B/M}^{\text{line}}(L, P) \geq \frac{L}{2} \log_q \left(\frac{1}{2} + P \right). \quad (5.65)$$

q -ary symbols×hops per time slot can be achieved.

Note, that

$$\lim_{L \rightarrow \infty} \lim_{P \rightarrow \infty} \frac{C_{B/M}^{\text{line}}(L, P)}{C_{P/P}^{\text{line}}(L, P)} \geq \lim_{L \rightarrow \infty} \frac{L}{\lceil \frac{1}{2}L \rceil} = 2. \quad (5.66)$$

Hence the multiplicative improvement obtained by moving from the P/P to the B/M model is the same in the Gaussian line network as in the deterministic network, for which this result was presented in Figure 5.1. The results presented in this section provide a lower bound on the improvements in transport capacity that can be obtained by exploiting broadcast and interference in our Gaussian network, compared to reducing the network to point-to-point links. The reduction to the B/M deterministic model, using lattice codes, provides an achievable strategy that is not necessarily optimal. The interesting point is that these lattice codes provide a means of exploiting interference that could be implemented in practice.

5.8 Discussion

Capacity bounds have been compared for four different deterministic models of wireless networks, representing four different ways of handling broadcast and superposition in the physical layer. These deterministic models have been

inspired by recent studies on decoding functions of messages over a multiple access channel. One of the conclusion is that exploiting superposition and broadcast can lead to an increase in transport capacity of the hexagonal lattice of at least 150% and at most 500%.

We have presented a simple coding scheme for the hexagonal lattice under the B/M model. The proof techniques that have been introduced might be generalized to improve upper and lower bounds and to find more general coding schemes, both for the line and lattice networks and other network topologies. Of particular interest, would be to extend the results to random topologies.

We have made a connection between our deterministic models and Gaussian wireless networks. It will be of interest to extend these results to Gaussian models with more realistic interference models. Moreover, in order to apply these results in practice, decentralized coding and scheduling algorithms will need to be developed.

5.A Proof of Lemma 5.28

Part of the proof of Lemma 5.28 consists of a reduction to counting paths in a rectangular lattice. Therefore we start this appendix with a definition of this problem and a result concerning the number of such paths. Let $D_t, D_b, H > 0$ and $V > 0$ be integers. Consider the rectangular lattice and two of its diagonals; one diagonal through the points $\{(D_t + i, V + i)\}_{i \in \mathbb{Z}}$, the other through the points $\{(H + i, D_b + i)\}_{i \in \mathbb{Z}}$. The problem that we are concerned with is that of counting monotonic paths from $(0, 0)$ to (H, V) in the rectangular lattice that do not cross the diagonals. Monotonic paths are those paths that only move up or right in each step. In the remainder of this appendix, unless specified otherwise, all paths under consideration are monotonic. A subset of the rectangular lattice, the diagonals, and a valid path are depicted in Figure 5.22.

The following lemma gives this number under the assumption that no monotonic path can cross both diagonals. We follow the convention that $\binom{n}{k} = 0$, if $k < 0$.

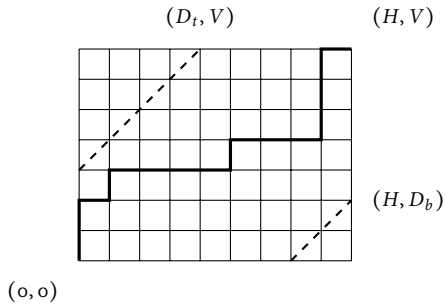


Figure 5.22: A subset of the rectangular lattice, diagonals crossing (D_t, V) and (H, D_b) and a path from $(0, 0)$ to (H, V) . In this figure: $H = 9$, $V = 7$, $D_t = 4$, $D_b = 2$.

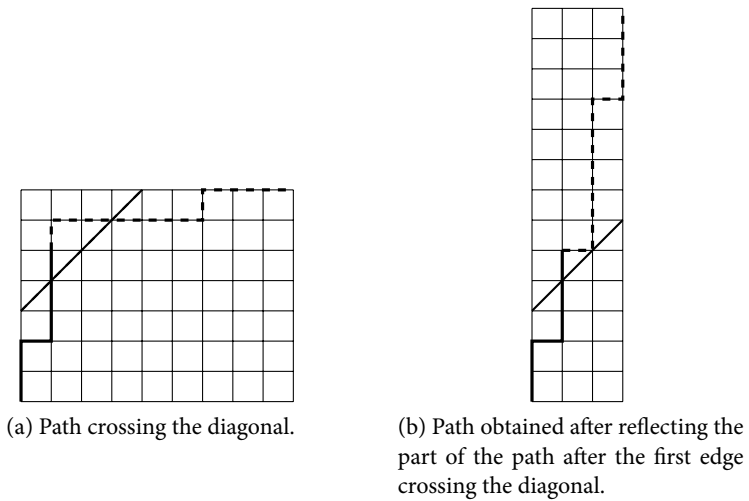


Figure 5.23: Reflection principle. There is a one-to-one correspondence between the set of diagonal-crossing paths in Figure 5.23a and the set of paths in Figure 5.23b.

Lemma 5.30. *Let $D_t, D_b, H > 0$ and $V > 0$ be integers. Consider the two-dimensional rectangular grid and two of its diagonals crossing (D_t, V) and (H, D_b) . Assume $D_t \leq H - D_b$ and $D_b \leq V - D_t$. Then the number of monotonic paths in the grid from $(0, 0)$ to (H, V) that do not cross the diagonals is*

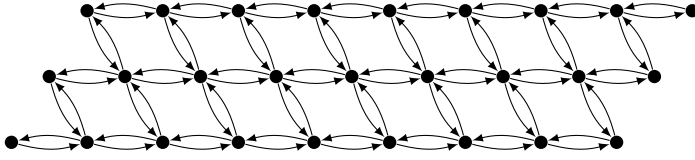
$$\binom{H+V}{H} - \binom{H+V}{D_t-1} - \binom{H+V}{D_b-1}. \quad (5.67)$$

Proof. Note that all paths are of length $H + V$. Moreover, any path needs H steps to the right and V steps up. Therefore, the total number paths equals $\binom{H+V}{H}$. The two other terms in (5.67) correspond to the number of paths crossing the top and bottom diagonal respectively. The assumption that $D_t \leq H - D_b$ and $D_b < V - D_t$ ensures that there are no paths that cross both diagonals. The number of paths crossing the top diagonal can be found using a reflection principle, a technique that is widely used in the area of combinatorics, cf. [74]. There is a one-to-one correspondence between the set of paths from $(0, 0)$ to (H, V) that cross the top diagonal and the total number of paths from $(0, 0)$ to $(D_t - 1, H + V - D_t + 1)$. The mapping giving the correspondence consists of reflecting (replacing a move right, by a move up, and vice versa) the part of the path after the first edge crossing the diagonal. This reflection principle is illustrated in Figure 5.23. Now it directly follows that the number of paths that cross the top diagonal is $\binom{H+V}{D_t-1}$. In the same way it follows that the number of paths crossing the bottom diagonal is $\binom{H+V}{D_b-1}$. \square

Note, that the problem of counting paths in the rectangular lattice with two diagonals is very similar to counting Dyck paths, cf. [74]. The differences with counting Dyck paths are that instead of one diagonal we have two diagonals. Dyck paths, moreover, would start and end at the diagonal. Various generalizations have been considered in literature [74], but we are not aware of results related to our counting problem.

Next we present a standard result on congruence relations for binomial coefficients.

Theorem 5.31 (Lucas [59]). *Let c be a prime number and let a and b , $a \geq b$, be positive integers written in base c , i.e., let $a = \sum_{i=0}^s a_i c^i$ and $b = \sum_{i=0}^t b_i c^i$ with*

Figure 5.24: Graph (V, E') .

$0 \leq a_i < c$, $0 \leq b_i < c$, $a_s \neq 0$, $b_t \neq 0$ and $s \geq t$. Then

$$\binom{a}{b} \equiv \prod_{i=0}^t \binom{a_i}{b_i} \pmod{c}. \quad (5.68)$$

We will be using the following corollary to Lucas' Theorem.

Corollary 5.32. Let κ and b be positive integers, $b < 2^\kappa$. Then $\binom{2^\kappa}{b} \equiv 0 \pmod{2}$.

Proof. Since $0 < b < 2^\kappa$, we have $b = \sum_{i=0}^t b_i 2^i$, where $0 < t < \kappa$ and $b_t = 1$. From Theorem 5.31 we have

$$\binom{2^\kappa}{b} \equiv \prod_{i=0}^t \binom{0}{b_i} \pmod{2} \equiv 0 \pmod{2}. \quad (5.69)$$

□

We make the following observation on even-odd scheduling together with simple retransmissions. Suppose that a node (u_1, u_2) is transmitting. Then, the following nodes are receiving from (u_1, u_2) :

$$(u_1 - 1, u_2 + 1), \quad (u_1 - 1, u_2), \quad (u_1 + 1, u_2), \quad (u_1 + 1, u_2 - 1).$$

Therefore, we associate with a hexagonal network (V, E) that is operated in this fashion, a graph (V, E') , where

$$E' = \left\{ ((u_1, u_2), (v_1, v_2)) \in V \times V \mid (v_1, v_2) \in \left\{ (u_1 + 1, u_2), (u_1 + 1, u_2 - 1), (u_1 - 1, u_2), (u_1 - 1, u_2 + 1) \right\} \right\}. \quad (5.70)$$

The graph (V, E') is depicted in Figure 5.24 for $L = 8$ and $M = 2$. One can easily verify the following lemma, which is therefore given without a proof.

Lemma 5.33. *Assume even-odd scheduling and simple retransmissions over \mathbb{F}_2 on a hexagonal network (V, E) . Suppose that in time slot $t = 0$ node (u_1, u_2) transmits a symbol m and all other nodes transmit 0. Then at time t node (v_1, v_2) transmits symbol m iff in the graph (V, E') the number of paths from (u_1, u_2) to (v_1, v_2) of length t is odd. Nodes not transmitting the symbol m are transmitting zero.*

Note that these paths need not be simple, *i.e.*, they can use the same vertices and edges multiple times. This implies that paths can contain cycles. In order to simplify the discussion we introduce some notation. There are four types of edges in the graph (V, E') , these types will be denoted as

$$l: \text{ for edges of type } \left((u_1, u_2), (u_1 - 1, u_2) \right), \quad (5.71)$$

$$r: \text{ for edges of type } \left((u_1, u_2), (u_1 + 1, u_2) \right), \quad (5.72)$$

$$u: \text{ for edges of type } \left((u_1, u_2), (u_1 - 1, u_2 + 1) \right), \quad (5.73)$$

$$d: \text{ for edges of type } \left((u_1, u_2), (u_1 + 1, u_2 - 1) \right), \quad (5.74)$$

where the l(ef), r(ight), u(p) and d(own) denote the movement made from the perspective of (u_1, u_2) . Note that movements u and d are also affecting the value of the first coordinate. Hence, naming these up-left and down-right would have been more accurate. Given the starting vertex of a path, it can be represented in terms of a sequence from $\{l, r, u, d\}^*$, representing the moves taken from the starting vertex. The superscript $*$ is used to denote the union of the k -ary Cartesian products, $k \in \mathbb{N}$. Since we will consider sets of paths starting from the same vertex, we will represent paths only by the sequence of moves. Let $P(s)$ be the subsequence, restricted to u and d movements, of a sequence $s \in \{l, r, u, d\}^*$. For $s = l u l u d r l u d$, for instance, we have $P(s) = u u d u d$. Finally, let $l(s)$, $r(s)$, $u(s)$ and $d(s)$ be the number of occurrences of respectively l , r , u and d in s .

The proof of Lemma 5.28, the aim of this appendix, is a direct consequence of Lemma 5.33 and the following Lemma 5.34.

Lemma 5.34. *Given (V, E') of size $(L+1) \times (M+1)$, where $M = 2^\kappa - 2$, $\kappa \geq 2$ and $L \geq 2^{\kappa+1}$. Let $(u_1, u_2) \in V$, $(v_1, v_2) \in V$, where $2^\kappa \leq u_1 \leq L - 2^\kappa$. Let A be the number of paths of length 2^κ from (u_1, u_2) to (v_1, v_2) . We have*

$$A \equiv \begin{cases} 1 \pmod{2}, & \text{if } |v_1 - u_1| = 2^\kappa \text{ and } v_2 = u_2, \\ 0 \pmod{2}, & \text{otherwise.} \end{cases} \quad (5.75)$$

Proof. Let $n = 2^\kappa$. W.l.o.g. consider $v_1 - u_1 \geq 0$. Moreover, we consider $v_1 - u_1$ even, since, if $v_1 - u_1$ is odd there are no paths of length n from (u_1, u_2) to (v_1, v_2) . Let \mathcal{A} be the set of all paths of length n from (u_1, u_2) to (v_1, v_2) . We partition \mathcal{A} into sets of paths that have the same $\{u, d\}^*$ subsequence, i.e., for $p \in \{u, d\}^*$ let

$$\mathcal{A}_p = \{s \in \mathcal{A} \mid P(s) = p\}. \quad (5.76)$$

Note that there are many p for which \mathcal{A}_p is empty, since not all p can lead to a valid path from (u_1, u_2) to (v_1, v_2) . The sequence $u u \cdots u$ of length n , for instance, is not a valid path in (V, E) , since it would ‘cross the boundary’ of the graph. Also, there are p that can not lead to a path that ends in (v_1, v_2) . More precisely, we have the following basic constraints. First, we need

$$u(s) - d(s) = u_2 - v_2. \quad (5.77)$$

Moreover, we need $(r(s) + d(s)) - (l(s) + u(s)) = v_1 - u_1$. Combined with $l(s) + r(s) + u(s) + d(s) = n$ this leads to

$$l(s) + u(s) = \frac{n - v_1 + u_1}{2}, \quad (5.78)$$

$$r(s) + d(s) = \frac{n + v_1 - u_1}{2}. \quad (5.79)$$

Since we consider $v_1 - u_1$ even, $(n - v_1 + u_1)/2$ and $(n + v_1 - u_1)/2$ are integers.

Let $A_p = |\mathcal{A}_p|$. Now,

$$A = \sum_{k=0}^n \sum_{p \in \{u, d\}^k} A_p = A_\emptyset + \sum_{k=1}^{n-1} \sum_{p \in \{u, d\}^k} A_p + \sum_{p \in \{u, d\}^n} A_p. \quad (5.80)$$

The following claims, which will be proved in the remainder, prove the lemma:

1. $A_{\emptyset} \equiv \begin{cases} 1 \pmod{2}, & \text{if } |v_1 - u_1| = 2^k \text{ and } v_2 = u_2, \\ 0 \pmod{2}, & \text{otherwise,} \end{cases}$
2. $A_p \equiv 0 \pmod{2}$ for $1 \leq |p| \leq n - 1$,
3. $\sum_{p \in \{u,d\}^n} A_p \equiv 0 \pmod{2}$.

For Claim 1 note that if $u_2 \neq v_2$ we have $A_{\emptyset} = 0$ because constraint (5.77) is not satisfied. For $u_2 = v_2$ we need to show that $A_{\emptyset} \equiv 1 \pmod{2}$ iff $v_1 - u_1 = n$. Note that $A_{\emptyset} = \binom{n}{l(s)}$. From $u(s) = 0$ and (5.78) it follows that $l(s) = (n - v_1 + u_1)/2$. Hence, if $v_1 - u_1 < n$ then $0 < l(s) < n$, and Corollary 5.32 gives $\binom{n}{l(s)} \equiv 0 \pmod{2}$. If $v_1 - u_1 = n$, then $l(s) = 0$ and $\binom{n}{l(s)} = 1$.

For Claim 2 we show that $A_p \equiv 0 \pmod{2}$ by giving an explicit construction of the sequences in \mathcal{A}_p . The construction is in two phases. We start from a length n sequence with undefined entries. In the first phase, the sequence p is embedded in this length n sequence. In the second phase the remaining undefined entries are filled with l and r moves. There are $\binom{n}{|p|}$ ways to perform the first phase. By Corollary 5.32, since $1 \leq |p| \leq n - 1$, we have $\binom{n}{|p|} \equiv 0 \pmod{2}$. The number of ways to perform the second phase is independent of the result of the first phase. A_p is, therefore, a multiple of $\binom{n}{|p|}$, proving Claim 2.

For the proof of Claim 3 first note that

$$\sum_{p \in \{u,d\}^n} A_p = \left| \left\{ s \in \mathcal{A} \mid l(s) = r(s) = 0 \right\} \right|, \quad (5.81)$$

i.e., we are counting the paths of length n from (u_1, u_2) to (v_1, v_2) that have only u and d moves. The constraints (5.77)–(5.79) reduce to

$$u(s) = \frac{n - v_1 + u_1}{2}, \quad (5.82)$$

$$d(s) = \frac{n + v_1 - u_1}{2}. \quad (5.83)$$

The problem of counting the paths that satisfy these constraints is tackled by reducing it to counting monotonic paths in the rectangular lattice, for which a

result was presented in Lemma 5.30. In the rectangular lattice consider monotonic paths from $(0, 0)$ to $((n - v_1 + u_1)/2, (n + v_1 - u_1)/2)$. Note that length of these paths is always n . By associating a u move in (V, E') to a move up in the rectangular lattice and a d move in (V, E') with a right move in the rectangular lattice, we see that there is a one-to-one correspondence between paths of u and d moves in (V, E') and monotonic paths from $(0, 0)$ to $(n - v_1 + u_1)/2 \times (n + v_1 - u_1)/2$ in the rectangular lattice.

In addition to the constraints on $u(s)$ and $d(s)$, the top and bottom borders of (V, E') impose constraints on the sequences corresponding to valid paths. Starting with the constraint imposed by the top border, note that a path starting from (u_1, u_2) can start with at most $n - 2 - u_2$ consecutive u moves. Also, after each d move, an additional u move is allowed. Therefore, the constraint imposed by the top border of (V, E') corresponds to a diagonal crossing $(0, n - 2 - u_2)$ in the rectangular lattice. A path in the lattice corresponding to a valid path in (V, E') can not cross this diagonal. In similar fashion it follows that the bottom border of (V, E') imposes a constraint in the form of a diagonal crossing $(u_2, 0)$ in the rectangular lattice. Note that the diagonal crossing in $(u_2, 0)$ also crosses in $((n + v_1 - u_1)/2, (n + v_1 - u_1)/2 - u_2)$. The diagonal crossing in $(0, n - 2 - u_2)$ also crosses in $((n - v_1 + u_1)/2, (n - v_1 + u_1)/2 - (n - 2 - u_2))$. In terms of Lemma 5.30 we have reduced our problem to counting monotonic paths from $(0, 0)$ to $((n - v_1 + u_1)/2, (n + v_1 - u_1)/2)$ in the rectangular lattice, not crossing the diagonals $((n - v_1 + u_1)/2, (n - v_1 + u_1)/2 - (n - 2 - u_2))$ and $((n + v_1 - u_1)/2, (n + v_1 - u_1)/2 - u_2)$. From Lemma 5.30 we obtain

$$\begin{aligned} \sum_{p \in \{u, d\}^n} A_p &= \binom{n}{\frac{n-v_1+u_1}{2}} \\ &\quad - \binom{n}{\frac{n-v_1+u_1}{2} - (n-2-u_2) - 1} \\ &\quad - \binom{n}{\frac{n+v_1-u_1}{2} - u_2 - 1}. \end{aligned} \quad (5.84)$$

Observe that the first term is always even. The second term is odd iff

$$(n - v_1 + u_1)/2 - (n - 2 - u_2) - 1 = 0 \implies u_2 = \frac{n + v_1 - u_1}{2} - 1. \quad (5.85)$$

The third term is odd iff

$$(n + v_1 - u_1)/2 - u_2 - 1 = 0 \implies u_2 = \frac{n + v_1 - u_1}{2} - 1. \quad (5.86)$$

From (5.85) and (5.86) it follows that the sum of the second and third term in (5.84) is always even. \square

Chapter 6

Outlook

The ideas put forward in the seminal work [2] have led to a surge of follow-up work in the area of network coding. Many different potential benefits of network coding have been identified in recent literature — some of these have been mentioned in Chapter 1, and many more exist [1, 24]. Despite the significant body of literature, most known results (including parts of this thesis) are of a theoretical nature. It is important to also develop methods that allow to implement these new ideas in technology. This chapter gives some suggestions on how to bring the results that have been reported in this thesis to practice.

A big part of this thesis has focussed on two specific benefits: 1) reduction of energy consumption and 2) increase of transport capacity. For wireless networks it has been characterized how large these benefits are if broadcast and interference are exploited in combination with the use of network coding. The results that have been obtained are based on coding and scheduling strategies that are carefully constructed using knowledge of the whole network and assuming synchronization between nodes. One of the challenges that will need to be addressed in future work is to develop coding and scheduling algorithms that allow to obtain the reported benefits in practice. This means that the coding and scheduling strategies will need to be constructed by nodes in a decentralized fashion, *i.e.*, without a priori knowledge of the complete network topology.

If network coding is not used, the coding problem reduces to a routing

problem, *i.e.*, the problem reduces to finding paths in the network. As explained in Chapter 4, in the case of multiple unicast with the aim of minimizing energy consumption, the paths between various source–destination pairs can be constructed independently of each other. Many algorithms have been developed that allow to find paths in networks in a decentralized fashion — the Dijkstra algorithm is a notable example. If network coding is employed paths can no longer be constructed independently for each session. The network configurations that have been introduced in Chapter 4 might lead the reader to think that also for the case of network coding, paths can be found independently. Indeed, it is the case that for these configurations, symbols travel only along the shortest paths. However, there are examples [19] of configurations in which these paths can not be constructed independently. The construction of optimal paths is an open problem. In fact it is not even known if the notion of “transmitting along paths” is always useful when network coding is used. Consider for example the strategy used to prove Lemma 5.29. Using this strategy each symbol is transmitted by different nodes in a large area of the network and it is not possible to identify paths along which symbols are transmitted. Of course the above scheme was used to achieve high transport capacity. If similar examples exist for the case that energy consumption is minimized is unknown.

The class of decode-and-recombine strategies, as defined in Section 1.4, was introduced as part of a complete wireless network protocol stack (COPE) in [46]. The construction of paths is done independently for each session. Even though this is not optimal, the performance of COPE in terms of energy consumption reduction seems promising. However, based on [57] and the results from Chapter 4 of this thesis it is clear that significantly more energy can be saved by considering strategies other than decode-and-recombine. The most important contribution of [46] is that it demonstrates that network coding can significantly improve performance in real networks. Interestingly, however, there is a large gap between the theoretical body of work and COPE.

The design of network codes in a decentralized fashion has been the topic of studies by many researchers in the field. However, very few results have been established. All known results deal with the case of multicast traffic. Note that for multicast problems on directed graphs it is possible to separate the path finding and coding problems. The only general solution that is avail-

able to the code design problem is to use random coding. Indeed, the random coding approach seems very promising and lends itself very well for implementation in practical algorithms. It is not clear if random coding can also be used for multiple unicast problems. Initial explorations performed during the studies that led to this thesis did not lead to positive results.

In addition to developing decentralizing coding algorithms, another challenge is to extend the results from the simple model used in this thesis, to a more complete model. One can think of more complete network models, *i.e.*, models that include packet losses or errors and delays. We have started in Chapter 4 to analyze the energy benefit of network coding based on a more complete energy consumption model. This model can be extended further by taking, for instance, also processing and packet length overhead into account. Also note that all results obtained in this thesis are based on a model with persistent sources. This means that at all times, for all connections, there are always packets to transmit. A consequence of this is that coding can always be performed in the most energy-efficient way. In the case of non-persistent sources the energy consumption might be affected because it is not always possible to transmit optimally coded packets. In this context it is interesting to analyze the tradeoff between energy consumption and delay; indeed if it is not possible to transmit an optimally coded packet one could wait for a useful packet to arrive before transmitting anything. This would reduce energy consumption at the expense of a larger delay. Preliminary results are provided in [33].

Regarding the results from Chapter 5 we can say that these have been obtained for two specific configurations: the line network and the hexagonal lattice. It is important to develop an understanding of the behaviour on other configurations. More important than considering other lattices is to consider configurations with random node placements. From a practical point of view it would be of interest to also develop general coding strategies, that might not be optimal, but that work for arbitrary configurations. Another practical issue that need to be addressed in this context is to develop practical codes that can be used to perform computation coding. Finally synchronization between nodes is of utmost importance and means to achieve synchronization will need to be developed.

Bibliography

- [1] [Online]. Available: https://hermes.lnt.e-technik.tu-muenchen.de/DokuWiki/doku.php?id=network_coding:bibliography_for_network_coding
- [2] R. Ahlswede, N. Cai, S.-Y. R. Li, and R. W. Yeung, "Network information flow," *IEEE Trans. Inf. Theory*, vol. 46, no. 4, pp. 1204–1216, 2000.
- [3] M. Amin Rahimian, A. Ayremlou, and F. Marvasti, "A general analog network coding for wireless systems with fading and noisy channels," 2010, arxiv, 1009.3797.
- [4] A. Avestimehr, S. Diggavi, and D. Tse, "A deterministic approach to wireless relay networks," in *Proceedings of Allerton Conference on Communication, Control, and Computing*, 2007.
- [5] —, "Wireless network information flow," in *Proceedings of Allerton Conference on Communication, Control, and Computing*, 2007.
- [6] B. Bollobás, *Modern graph theory*. Springer Verlag, 1998.
- [7] N. Cai and R. Yeung, "Secure network coding," in *Proceedings. 2002 IEEE International Symposium on Information Theory*, 2002, p. 323.
- [8] J. Chang and L. Tassiulas, "Energy conserving routing in wireless ad hoc networks," in *Proceedings of the Fifth Annual ACM/IEEE International Conference on Mobile Computing and Network (MobiCom)*, Dallas, TX, Aug. 1998.

- [9] S. Chen and K. Nahrstedt, "An overview of quality-of-service routing for the next generation high-speed networks: Problems and solutions," *IEEE Network, Special Issue on Transmission and Distribution of Digital Video*, pp. 64–79, Nov./Dec. 1998.
- [10] Y. Chen, E. G. Sirer, and S. B. Wicker, "On selection of optimal transmission power for ad hoc networks," in *Proceedings of the Thirty-Sixth Hawaii International Conference on System Sciences (HICSS-36)*, 2003.
- [11] P. Chou, Y. Wu, and K. Jain, "Practical network coding," in *Proceedings of the Annual Allerton Conference on Communication Control and Computing*, vol. 41, no. 1, 2003, pp. 40–49.
- [12] W. J. Cook, W. H. Cunningham, W. R. Pulleyblank, and A. Schrijver, *Combinatorial Optimization*. John Wiley & Sons, Inc, 1998.
- [13] —, *Combinatorial Optimization*. John Wiley & Sons, Inc, 1998.
- [14] T. Cover and J. Thomas, *Elements of information theory*. Wiley, 2006.
- [15] A. Dimakis, V. Prabhakaran, and K. Ramchandran, "Decentralized erasure codes for distributed networked storage," *IEEE/ACM Transactions on Networking (TON)*, vol. 14, no. SI, p. 2816, 2006.
- [16] R. Dougherty, C. Freiling, and K. Zeger, "Insufficiency of linear coding in network information flow," *IEEE Trans. Inf. Theory*, vol. 51, no. 8, pp. 2745–2759, 2005.
- [17] O. Dousse, M. Franceschetti, N. Macris, R. Meester, and P. Thiran, "Percolation in the signal to interference ratio graph," *J. Appl. Probab*, vol. 43, no. 2, pp. 552–562, 2006.
- [18] J. Ebrahimi and C. Fragouli, "Combinatorial Algorithms for Wireless Information Flow," *Arxiv preprint arXiv:0909.4808*, 2009.
- [19] M. Effros, T. Ho, and S. Kim, "A tiling approach to network code design for wireless networks," in *Information Theory Workshop, 2006. ITW '06 Punta del Este. IEEE*, 2006, pp. 62–66.

-
- [20] M. Effros, R. Koetter, and M. Médard, “Breaking network logjams,” *Scientific American Magazine*, vol. 296, no. 6, pp. 78–85, 2007.
- [21] S. El Rouayheb and E. Soljanin, “On wiretap networks II,” in *IEEE International Symposium on Information Theory, 2007. ISIT 2007*, 2007, pp. 551–555.
- [22] L. Feeney and M. Nilsson, “Investigating the energy consumption of a wireless network interface in an ad hoc networking environment,” in *IEEE INFOCOM*, vol. 3, 2001, pp. 1548–1557.
- [23] S. Fong and R. Yeung, “Variable-rate linear network coding,” in *IEEE Information Theory Workshop, 2006. ITW’06 Chengdu*, 2006, pp. 409–412.
- [24] C. Fragouli and E. Soljanin, “Network coding applications,” *Foundations and Trends® in Networking*, vol. 2, no. 2, pp. 135–269, 2007.
- [25] —, “Network coding fundamentals,” *Foundations and Trends® in Networking*, vol. 2, no. 1, pp. 1–133, 2007.
- [26] C. Fragouli, J. Widmer, and J.-Y. Le Boudec, “Efficient broadcasting using network coding,” *IEEE/ACM Trans. Netw.*, vol. 16, no. 2, pp. 450–463, 2008.
- [27] C. Fragouli and E. Soljanin, “Information flow decomposition for network coding,” *IEEE Trans. Inf. Theory*, vol. 52, no. 3, pp. 829–848, 2006.
- [28] A. Gamal, J. Mammen, B. Prabhakar, and D. Shah, “Throughput-delay trade-off in energy constrained wireless networks,” in *Information Theory, 2004. ISIT 2004. Proceedings. International Symposium on*, 2004, p. 439.
- [29] C. Gkantsidis and P. Rodriguez, “Network coding for large scale content distribution,” in *Proceedings IEEE INFOCOM 2005. 24th Annual Joint Conference of the IEEE Computer and Communications Societies*, vol. 4, 2005.

- [30] A. Goel and S. Khanna, "On the network coding advantage for wireless multicast in euclidean space," in *Proceedings of the 7th international conference on Information processing in sensor networks*, 2008, pp. 64–69.
- [31] M. Goemans, S. Iwata, and R. Zenklusen, "An Algorithmic Framework for Wireless Information Flow," in *Proceedings of Allerton Conference on Communication, Control, and Computing*, 2009.
- [32] A. Goldsmith and S. Wicker, "Design challenges for energy-constrained ad hoc wireless networks," *IEEE Trans. Wireless Commun.*, vol. 9, no. 4, pp. 8–27, 2002.
- [33] J. Goseling, R. J. Boucherie, and J. C. W. van Ommeren, "Energy consumption in coded queues for wireless information exchange," in *Proceedings of the 2009 Workshop on Network Coding, Theory, and Applications*, 2009.
- [34] J. Goseling and S. N. Diggavi, "Scaling laws for energy-constrained wireless networks," EPFL, Tech. Rep. LICOS-REPORT-2005-002, 2005.
- [35] P. Gupta and P. R. Kumar, "The capacity of wireless networks," *IEEE Trans. Inf. Theory*, vol. 46, no. 2, pp. 388–404, 2000.
- [36] Y. Hao, D. Goeckel, Z. Ding, D. Towsley, and K. Leung, "Achievable rates of physical layer network coding schemes on the exchange channel," in *Military Communications Conference, (MILCOM-07)*, 2007.
- [37] S. Haykin, "Cognitive radio: brain-empowered wireless communications," *IEEE J. Sel. Areas Commun.*, vol. 23, no. 2, pp. 201–220, 2005.
- [38] T. Ho and D. Lun, *Network coding: an introduction*. Cambridge Univ Pr, 2008.
- [39] T. Ho, M. Médard, R. Koetter, D. Karger, M. Effros, J. Shi, and B. Leong, "A random linear network coding approach to multicast," *IEEE Trans. Inf. Theory*, vol. 52, no. 10, pp. 4413–4430, 2006.
- [40] S. Jaggi, P. Sanders, P. Chou, M. Effros, S. Egner, K. Jain, and L. Tolhuizen, "Polynomial time algorithms for multicast network code construction," *IEEE Trans. Inf. Theory*, vol. 51, no. 6, pp. 1973–1982, 2005.

-
- [41] —, “Polynomial time algorithms for multicast network code construction,” *IEEE Trans. Inf. Theory*, vol. 51, no. 6, pp. 1973–1982, 2005.
- [42] K. Jain, J. Padhye, V. Padmanabhan, and L. Qiu, “Impact of interference on multi-hop wireless network performance,” *Wireless networks*, vol. 11, no. 4, pp. 471–487, 2005.
- [43] C. Jones, K. Sivalingam, P. Agarwal, and J. Chen, “A survey of energy efficient network protocols for wireless and mobile networks,” *ACM/Kluwer Wireless Networks*, vol. 7, no. 4, pp. 343–358, 2001.
- [44] R. M. Karp, “Reducibility among combinatorial problems,” in *Complexity of Computer Computations*, R. E. Miller and J. W. Thatcher, Eds., 1972, pp. 85–103.
- [45] S. Katti and D. Katabi, “Embracing wireless interference: Analog network coding,” in *Proc. of the 2007 Conference on Applications, Technologies, Architectures, and Protocols for computer communications*, 2007, pp. 397–408.
- [46] S. Katti, H. Rahul, W. Hu, D. Katabi, M. Médard, and J. Crowcroft, “XORs in the air: practical wireless network coding,” in *Proc. of ACM SIGCOMM*, 2006, pp. 243–254.
- [47] A. Keshavarz-Haddad and R. Riedi, “Bounds on the Benefit of Network Coding: Throughput and Energy Saving in Wireless Networks,” in *Proc. of IEEE INFOCOM*, 2008, pp. 376–384.
- [48] S. Kim, M. Effros, and T. Ho, “On low-power multiple unicast network coding over a wireless triangular grid,” in *Forty-Fifth Annual Allerton Conference on Communication, Control and Computing*, 2007.
- [49] R. Koetter and M. Médard, “An algebraic approach to network coding,” *IEEE/ACM Trans. Netw.*, vol. 11, no. 5, pp. 782–795, 2003.
- [50] G. Kramer, M. Gastpar, and P. Gupta, “Cooperative strategies and capacity theorems for relay networks,” *IEEE Trans. Inf. Theory*, vol. 51, no. 9, pp. 3037–3063, 2005.

- [51] G. Kramer and S. A. Savari, "Edge-cut bounds on network coding rates," *Journal of Network and Systems Management*, vol. 14, no. 1, pp. 49–67, 2006.
- [52] S. Li, R. Yeung, and N. Cai, "Linear network coding," *IEEE Trans. Inf. Theory*, vol. 49, no. 2, pp. 371–381, 2003.
- [53] Z. Li and B. Li, "Network coding in undirected networks," in *Proc. of the 38th Annual Conf. on Information Sciences and Systems (CISS)*, 2004.
- [54] —, "Network coding: The case for multiple unicast sessions," in *Allerton Conference on Communications*, 2004.
- [55] X. Lin, N. Shroff, and R. Srikant, "A tutorial on cross-layer optimization in wireless networks," *IEEE J. Sel. Areas Commun.*, vol. 24, no. 8, pp. 1452–1463, 2006.
- [56] C.-H. Liu, F. Xue, and J. G. Andrews, "Network coding with two-way relaying: Achievable rate regions and diversity-multiplexing tradeoffs," 2009, arxiv, 0902.2260.
- [57] J. Liu, D. Goeckel, and D. Towsley, "Bounds on the gain of network coding and broadcasting in wireless networks," in *Proc. of IEEE INFOCOM*, 2007, pp. 6–12.
- [58] K. Lu, S. Fu, Y. Qian, and H.-H. Chen, "On capacity of random wireless networks with physical-layer network coding," *IEEE J. Sel. A. Commun.*, vol. 27, no. 5, pp. 763–772, 2009.
- [59] E. Lucas, "Théorie des fonctions numériques simplement périodiques," *American Journal of Mathematics*, vol. 1, no. 2, pp. 184–196, 1878.
- [60] D. S. Lun, N. Ratnakar, M. Médard, R. Koetter, D. Karger, T. Ho, E. Ahmed, and F. Zhao, "Minimum-cost multicast over coded packet networks," *IEEE Trans. Inf. Theory*, vol. 52, no. 6, pp. 2608–2623, 2006.
- [61] W. Nam, S.-Y. Chung, and Y. H. Lee, "Nested lattice codes for gaussian relay networks with interference," 2009, arxiv, 0902.2436.

- [62] K. Narayanan, M. Wilson, and A. Sprintson, "Joint physical layer coding and network coding for bi-directional relaying" in *45th Annual Allerton Conference*, 2007.
- [63] B. Nazer and M. Gastpar, "Computing over multiple-access channels with connections to wireless network coding," in *Proc. of the 2006 International Symposium on Information Theory (ISIT 2006)*, 2006, pp. 1354 – 1358.
- [64] —, "Computation over multiple-access channels," *IEEE Trans. Inf. Theory*, vol. 53, no. 10, pp. 3498–3516, 2007.
- [65] —, "Reliable computation over multiple-access channels," in *43rd Annual Allerton Conference September, 2005.*, Monticello, IL, September 2005.
- [66] A. Ozgür, O. Lévêque, and D. Tse, "Exact capacity scaling of extended wireless networks," in *Proceedings of the IEEE International Symposium on Information Theory, Nice, France, 2007*.
- [67] A. Ozgur, O. Leveque, and D. Tse, "Hierarchical cooperation achieves optimal capacity scaling in ad hoc networks," *IEEE Trans. Inf. Theory*, vol. 53, no. 10, pp. 3549 –3572, oct. 2007.
- [68] R. Ramanathan and R. Rosales-Hain, "Topology control of multi-hop wireless networks using transmit power adjustment," in *Proceedings of IEEE INFOCOM*, Tel Aviv, Israel, Mar. 2000.
- [69] V. Rodoplu and T. H. Meng, "Minimum energy mobile wireless networks," *IEEE J. Sel. Areas Commun.*, vol. 17, no. 8, pp. 1333–1344, 1999.
- [70] H. Saffar and P. Mitran, "Capacity bounds and lattice coding for the star relay network," 2010, arxiv, 1001.3708.
- [71] N. Sai Shankar, C. Cordeiro, and K. Challapali, "Spectrum agile radios: Utilization and sensing architectures," in *First IEEE International Symposium on New Frontiers in Dynamic Spectrum Access Networks (DySPAN)*, 2005, pp. 160–169.

- [72] C. U. Saraydar, N. B. Mandayam, and D. J. Goodman, "Efficient power control via pricing in wireless data networks," *IEEE Trans. Commun.*, vol. 50, pp. 291–303, 2002.
- [73] D. Silva, F. Kschischang, and R. Koetter, "A rank-metric approach to error control in random network coding," *IEEE Transactions on Information Theory*, vol. 54, no. 9, pp. 3951–3967, 2008.
- [74] R. P. Stanley, *Enumerative combinatorics, Volume 2*. Cambridge University Press, 1999.
- [75] J. K. Sundararajan, D. Shah, and M. Médard, "Feedback-based online network coding," 2009, arxiv, 0904.1730.
- [76] S. Tang, O. Shagdar, H. Yomo, M. Shirazi, R. Suzuki, and S. Obana, "Layer-2 retransmission and combining for network coding-based forwarding in wireless networks," in *11th IEEE Singapore International Conference on Communication Systems, 2008. ICCS 2008*, 2008, pp. 1597–1602.
- [77] Texas Instruments, "CC2520, 2.4 GHz IEEE 802.15.4/ZigBee RF transceiver," datasheet.
- [78] J. Widmer and J.-Y. Le Boudec, "Network coding for efficient communication in extreme networks," in *Applications, Technologies, Architectures, and Protocols for Computer Communication*. ACM Press New York, NY, USA, 2005, pp. 284–291.
- [79] J. Wieselthier, G. Nguyen, and A. Ephremides, "On the construction of energy-efficient broadcast and multicast trees in wireless networks," in *IEEE INFOCOM*, 2000, pp. 585–594.
- [80] P. Winter, "Steiner problem in networks: a survey," *Networks*, vol. 17, no. 2, pp. 129–167, 1987.
- [81] Y. Wu, P. A. Chou, and S.-Y. Kung, "Information exchange in wireless networks with network coding and physical-layer broadcast," in *Proc. 39th Annual Conference on Information Sciences and Systems (CISS)*, 2005.

-
- [82] L. L. Xie and P. R. Kumar, "A network information theory for wireless communication: Scaling laws and optimal operation," *IEEE Trans. Inf. Theory*, vol. 50, no. 5, pp. 748–767, 2004.
- [83] S. Yazdi and S. Savari, "A Max-Flow/Min-Cut Algorithm for a Class of Wireless Networks," in *ACM-SIAM Symposium on Discrete Algorithms (SODA 2010)*, Austin, Texas, 2010.
- [84] R. W. Yeung and N. Cai, "Network coding theory," *Foundations and Trends® in Communications and Information Theory*, vol. 2, no. 4 and 5, pp. 241–381, 2006.
- [85] R. Yeung and N. Cai, "Network error correction, part I: Basic concepts and upper bounds," *Communications in Information and Systems*, vol. 6, no. 1, pp. 19–36, 2006.
- [86] R. Yeung and Z. Zhang, "Distributed source coding for satellite communications," *IEEE Trans. Inf. Theory*, vol. 45, no. 4, pp. 1111–1120, 1999.
- [87] S. Zhang, S. Liew, and P. Lam, "Hot topic: physical-layer network coding," in *Proc. of the 12th Annual International Conference on Mobile Computing and Networking*, 2006, pp. 358–365.
- [88] S. Zhang, S. Liew, and L. Lu, "Physical layer network coding schemes over finite and infinite fields," in *Proc. IEEE Globecom 2008*, 2008.
- [89] H. Zimmermann, "OSI reference model—The ISO model of architecture for open systems interconnection," *IEEE Transactions on communications*, vol. 28, no. 4, pp. 425–432, 1980.

Summary

Network Coding: Exploiting Broadcast and Superposition in Wireless Networks

In this thesis we investigate improvements in efficiency of wireless communication networks, based on methods that are fundamentally different from the principles that form the basis of state-of-the-art technology. The first difference is that broadcast and superposition are exploited instead of reducing the wireless medium to a network of point-to-point links. The second difference is that the problem of transporting information through the network is not treated as a flow problem. Instead we allow for network coding to be used.

First, we consider multicast network coding in settings where the multicast configuration changes over time. We show that for certain problem classes a universal network code can be constructed. One application is to efficiently tradeoff throughput against cost.

Next, we deal with increasing energy efficiency by means of network coding in the presence of broadcast. It is demonstrated that for multiple unicast traffic in networks with nodes arranged on two and three dimensional rectangular lattices, network coding can reduce energy consumption by factors of four and six, respectively, compared to routing.

Finally, we consider the use of superposition by allowing nodes to decode sums of messages. We introduce different deterministic models of wireless networks, representing various ways of handling broadcast and superposition. We provide lower and upper bounds on the transport capacity under these models. For networks with nodes arranged on a hexagonal lattice it is found that the capacity under a model exploiting both broadcast and superposition is at least 2.5 times, and no more than six times, the transport capacity under a model of point-to-point links.

Jasper Goseling

Samenvatting

Netwerkcodering: Benutten van Broadcast en Superpositie in Draadloze Netwerken

In dit proefschrift onderzoeken we de efficiëntieverbetering van draadloze communicatienetwerken, gebaseerd op methodes die fundamenteel verschillen van principes die in huidige technologie gebruikt worden. Het eerste verschil is dat broadcast en superpositie benut worden in plaats van het draadloze medium te reduceren tot een netwerk van punt-naar-punt verbindingen. Het tweede verschil is dat transport van data door het netwerk niet wordt behandeld als stroomprobleem, maar dat we gebruik van netwerkcodering.

Als eerste beschouwen we multicast-netwerkcodering in situaties waarin de multicast-configuratie verandert met de tijd. We laten zien dat voor bepaalde klassen van problemen een universele netwerkcode kan worden geconstrueerd. Een applicatie is het efficiënt uitwisselen van datasnelheid tegen kosten.

Vervolgens, beschouwen we verbeterde energie-efficiëntie door gebruik te maken van netwerkcodering en broadcast. We laten zien dat voor meerdere unicast-verbindingen in netwerken van nodes die geplaatst zijn op twee- en driedimensionale rechthoekige lattices, netwerkcodering het energieverbruik kan reduceren met een factor van respectievelijk 4 en 6 vergeleken met routeren.

Als laatste beschouwen we het gebruik van superpositie door middel van het decoderen van sommaties van verschillende boodschappen. We introduceren meerdere deterministische modellen van draadloze netwerken, die verschillende manieren van het omgaan met broadcast en superpositie representeren. We geven onder- en bovengrenzen aan de transportcapaciteit onder deze modellen. Voor netwerken met nodes geplaatst op het hexagonale lattice vinden we dat de capaciteit onder een model dat zowel broadcast als superpositie benut, tussen de 2, 5 en 6 maal zo groot is als de capaciteit van een model met punt-naar-punt verbindingen.

Jasper Goseling

Curriculum Vitae

Ir. Jasper Goseling

Date of birth: 29 October, 1978
Place of birth: Enschede, The Netherlands
Nationality: Dutch

Professional Experience

- 2008 University of Twente, The Netherlands
Stochastic Operations Research Group,
Faculty of Electrical Engineering, Mathematics and Computer Science
– Researcher. (12.08 – present)

- 2007 Delft University of Technology, The Netherlands
Wireless and Mobile Communications Group,
Faculty Electrical Engineering, Mathematics and Computer Science
– Research assistant. (06.07 – 05.10)

- 2007 Twente Institute for Wireless and Mobile Communications
Enschede, The Netherlands.
– Researcher. (05.07 – 11.08)

- 2005 Ecole Polytechnique Fédérale de Lausanne, Switzerland
School of Computer and Communication Sciences,
– Research assistant. (09.05 – 04.07)

- 2002 Philips Research Eindhoven, The Netherlands.
Processing and Architectures for Content Management group.
- Scientist, continuation of Master’s work. (10.03 – 03.04)
 - Master’s project on protection of biometric templates. (01.03 – 08.03)
 - Internship on estimation and detection problems related to physical identifiers. (08.02 – 12.02)
- 2001 3T B.V., Enschede, The Netherlands
- Software engineer for embedded systems. (01.01 – 04.01)

Education

- 2003 M.Sc. in Electrical Engineering (with honors), University of Twente, The Netherlands.
- Thesis: “Biometric Template Protection”.
- 2002 First years examination in Cognitive Artificial Intelligence (with honors), University of Utrecht, The Netherlands.

Activities

Organization of the Twente Symposium on Industrial Engineering, 2009. Organization of the 31st Symposium on Information Theory in the Benelux, May 2010. Reviews for IEEE Transactions on Information Theory, IEEE Transactions on Networking, IEEE Communication Letters, IEEE Wireless Magazine and various international symposia.

Awards

- 2008 Stichting Gauss, Best Young Researcher Paper Award for “Energy Benefit of Network Coding for Multiple Unicast in Wireless Networks” at 29th Symposium on Information Theory in the Benelux.

Patents

- Pim Tuyls, Ton Akkermans and Jasper Goseling, “Secure Protection of Biometric Templates”, WO Patent WO/2007/036822, 2007.
- Pim Tuyls and Jasper Goseling, “Key Generation Using Biometric Data and Secret Extraction Codes”, WO Patent WO/2006/070322, 2006.
- Pim Tuyls, Jasper Goseling, Boris Skoric and Geert-Jan Schrijen, “Method and Device for Key Generation and Proving Authenticity”, WO Patent WO/2006/067739, 2006.
- Stan Baggen, Jasper Goseling and Ton Akkermans, “Method and device for verifying the identity of an object”, WO Patent WO/2004/104908, 2004.

Publications

- Jasper Goseling, Michael Gastpar and Jos H. Weber, “Line and Lattice Networks under Various Deterministic Interference Models”, *submitted to IEEE Transactions on Information Theory, Special Issue on Interference Networks*, April 2010.
- Jasper Goseling and Jos H. Weber, “On the Energy Savings of Network Coding in Wireless Networks”, in *Proceedings of the 31st Symposium on Information Theory in the Benelux*, Rotterdam, The Netherlands, 2010.
- Jan-Willem van Bloem, Richard Boucherie, Jasper Goseling, Maurits de Graaf, Geert Heijenck, Jan-Kees van Ommeren and Roel Schiphorst, “Effective Scheduling for Coded Distributed Storage in Wireless Sensor Networks”, in *Proceedings of the 31st Symposium on Information Theory in the Benelux*, Rotterdam, The Netherlands, 2010.
- Jasper Goseling, Ryutaroh Matsumoto, Tomohiko Uyematsu, and Jos H. Weber, “Lower Bounds on the Maximum Energy Benefit of Network Coding for Wireless Multiple Unicast”, *EURASIP Journal on Wireless Communications and Networking*, vol. 2010, Article ID 605421, 13 pages, 2010. (Special Issue on Wireless Network Coding)

- Jasper Goseling, Richard Boucherie, Sonia Heemstra de Groot, Jan-Kees van Ommeren and Jos H. Weber, “Energy Savings in Wireless Networks through Network Coding”, in *Workshop on the Pervasive Application of Wireless Technologies*, 2009.
- Jan-Willem van Bloem, Richard Boucherie, Jasper Goseling, Geert Heijenk, Jan-Kees van Ommeren and Roel Schiphorst, “Distributed Storage in Wireless Sensor Networks with Network Coding”, in *Workshop on the Pervasive Application of Wireless Technologies*, 2009.
- Jasper Goseling, Richard Boucherie and Jan-Kees van Ommeren, “Energy Consumption in Coded Queues for Wireless Information Exchange”, *Proceedings of the 2009 Workshop on Network Coding, Theory, and Applications, NetCod ’09*, 2009.
- Jasper Goseling, Michael Gastpar and Jos H. Weber, “Transport Capacity of Wireless Networks: Benefits from Multi-access Computation Coding”, in *Proceedings of the 30th Symposium on Information Theory in the Benelux*, 2009.
- Jasper Goseling, Ryutaroh Matsumoto, Tomohiko Uyematsu, and Jos H. Weber, “On the Energy Benefit of Network Coding for Wireless Multiple Unicast”, in *Proc. of 2009 IEEE Int. Symp. Information Theory*, pp. 2567–2571, Seoul, Korea, 2009.
- Jasper Goseling, Christina Fragouli and Suhas N. Diggavi, “Network Coding for Undirected Information Exchange”, *IEEE Communication Letters*, vol. 13, no. 1, pp. 25–27, 2009.
- Jasper Goseling and Jos H. Weber, “Multi-rate Network Coding for Minimum-Cost Multicasting”, in *Proc. 2008 IEEE Int. Symp. Information Theory*, pp. 36–40, Toronto, Canada, 2008.
- Jasper Goseling and Jos H. Weber, “Energy Benefit of Network Coding for Multiple Unicast in Wireless Networks”, in *29th Symposium on Information Theory in the Benelux*, Leuven, Belgium, 2008. (Stichting Gauss, best young researcher paper award.)

- Jasper Goseling and Suhas N. Diggavi, “Scaling Laws for Energy-constrained Wireless Networks”, *EPFL Technical Report*, LICOS-REPORT-2005-002, 2005.
- Pim Tuyls, Evgeny Verbitskiy, Jasper Goseling and Dee Denteneer, “Privacy Protecting Biometric Authentication Systems: An Overview”, *Eusipco*, Vienna, 2004.
- Pim Tuyls and Jasper Goseling, “Capacity and Examples of Template-Protecting Biometric Authentication Systems”, in *Biometric Authentication: ECCV 2004, International Workshop BioAW 2004, Prague, Czech Republic*, LNCS, vol. 3087/2004, pp. 158–170, Springer, 2004.
- Jasper Goseling and Pim Tuyls, “Information-Theoretic Approach to Privacy Protection of Biometric Templates”, in *Proceedings 2004 IEEE Int. Symp. Information Theory*, Chicago, IL USA, 2004.
- Frans Willems, Ton Kalker, Jasper Goseling and Jean-Paul Linnartz, “On the Capacity of a Biometrical Identification System”, in *Proc. 2003 IEEE Int. Symp. Information Theory*, pp 82, Yokohama, Japan, 2003.
- Jasper Goseling, Stan Baggen and Ton Akkermans, “Optimal Verification Using Partially Known Biometrics”, *24th Symposium on Information Theory in the Benelux*, Veldhoven, The Netherlands, pp. 117-124, 2003.